



Norwegian University of
Science and Technology

Thruster-Assisted Position Mooring of C/S Inocean Cat I Drillship

Jon Bjørnø

Marine Technology

Submission date: July 2016

Supervisor: Roger Skjetne, IMT

Co-supervisor: Andreas Dahl, IMT
Hans-Martin Heyn, IMT

Norwegian University of Science and Technology
Department of Marine Technology



MSC THESIS DESCRIPTION SHEET

Name of the candidate: Jon Bjørnø
Field of study: Marine control engineering
Thesis title (Norwegian): Thruster-assistert forankring av C/S Inocean Cat I Drillship
Thesis title (English): Thruster-assisted position mooring of C/S Inocean Cat I Drillship

Background

Stationkeeping operations for offshore vessels (drillrigs, drillships, construction and intervention vessels, PSVs, etc.) are essential for offshore field development and oil and gas production. There has been much attention in the research community on stationkeeping operations, especially by Dynamic Positioning (DP) and Thruster-Assisted Position Mooring (TAPM) of turret-anchored offshore vessels. In TAPM the mean environmental loads shall be balanced by the mooring lines, while the thrusters are used for automatic heading control to keep the heading pointed against incoming waves. In addition, the thrusters are used to generate extra surge/sway damping and to aid the mooring lines in case of extreme loads.

In this project the focus is on developing the model ship “C/S Inocean Cat I Drillship” (hereafter abbreviated CSAD), including its TAPM control system. This is a 1:90 scaled model of an Arctic drillship design by Inocean, having a rotatable turret, 6 azimuth thrusters (3 fore and 3 aft) for DP and thruster assist, and both DP and TAPM control modes.

Work description

1. Perform a background and literature review to provide information and relevant references on:
 - MC-Lab and C/S Inocean Cat I Drillship design and model.
 - Conventional TAPM control functions, modes, and control algorithms.
 - Hybrid control techniques for switching between different control modes.

Write a list with abbreviations and definitions of terms, explaining relevant concepts related to the background study and project assignment.

2. Manufacturing and assembly, considering:
 - Follow up the manufacturing process of the CSAD hull.
 - Acquisition of instrumentation, batteries, thrusters, and control system hardware.
 - Mounting of batteries.
 - Mounting of thrusters and mooring lines in the hull.
 - Fitting of electronics in a watertight container.
 - Lid to shield the equipment inside the hull.
3. Control system design:
 - Make drawings that describe:
 - Control system hardware architecture.
 - Power system single line diagram, detailing circuits and power flow, voltage levels, and converters.
 - Communication signal/network information flow.
 - cRIO software topology, incl. fitting navigation, guidance, and control modules in the topology.
 - Implementation of necessary control functions:
 - *Direct Thruster Control* from joystick and keyboard (in collaboration with P. Frederich).
 - *Direct Motion Control* (with thrust allocation) from joystick, both body-relative and basin-relative modes (in collaboration with P. Frederich).
 - Automatic TAPM/DP control functions.
 - Necessary HMI functions and layout.

4. Study theory on TAPM control modes, such as heading control, surge/sway damping, and setpoint chasing:
 - Explain all important terms related to the TAPM control algorithm.
 - Develop a suitable TAPM control design model for CSAD, implement relevant TAPM control algorithms, and simulate the resulting responses.
 - Present the effectiveness of the different parts of the TAPM control algorithm for normal vessel loading.
5. Consider TAPM for extreme loads.
 - Develop a TAPM control algorithm customized for extreme loads.
 - Propose a hybrid setup for smooth switching between the “nominal” control algorithm and the algorithm for extreme loads.
 - Simulate and verify the algorithm for transition from normal to extreme and back to normal loads.
6. Implement the control algorithms for CSAD, test in MC-Lab, and discuss the results.

Guidelines

The scope of work may prove to be larger than initially anticipated. By the approval from the supervisor, described topics may be deleted or reduced in extent without consequences with regard to grading. The candidate shall present personal contribution to the resolution of problems within the scope of work. Theories and conclusions should be based on mathematical derivations and logic reasoning identifying the various steps in the deduction.

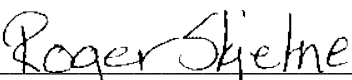
The report shall be organized in a logical structure to give a clear exposition of background, results, assessments, and conclusions. The text should be brief and to the point, with a clear language. The report shall be written in English (preferably US) and contain the following elements: Title page, abstract, acknowledgements, thesis specification, list of symbols and acronyms, table of contents, introduction and background, problem formulations, scope, and delimitations, main body with derivations/developments and results, conclusions with recommendations for further work, references, and optional appendices. All figures, tables, and equations shall be numerated. The original contribution of the candidate and material taken from other sources shall be clearly identified. Work from other sources shall be properly acknowledged using quotations and a Harvard citation style (e.g. *natbib* Latex package). The work is expected to be conducted in an honest and ethical manner, without any sort of plagiarism and misconduct. Such practice is taken very seriously by the university and will have consequences. NTNU can use the results freely in research and teaching by proper referencing, unless otherwise agreed upon.

The thesis shall be submitted with a printed and electronic copy to the main supervisor, each copy signed by the candidate. The final revised version of this thesis description must be included. The report must be submitted according to NTNU procedures. Computer code, pictures, videos, data series, and a PDF version of the report shall be included electronically with all submitted versions.

Start date: 15 January, 2016 **Due date:** As specified by the administration.

Supervisor: Roger Skjetne
Co-advisor(s): Hans-Martin Heyn and Andreas Dahl

Trondheim, 13.03.2016



Roger Skjetne (supervisor)

Preface

This master thesis is a continuation of the master project delivered in December 2015, and is carried out during the spring 2016. The work has been done as a part of the study program Marine Technology at NTNU, with the use of their laboratory facilities at Marine Cybernetics Laboratory (MC lab). The thesis presents a literature review on thruster-assisted position mooring, construction process of the C/S Inocean Cat I Drillship, and a verification of different controllers implemented on the model.

The assignment has been challenging and interesting to work with, but sometimes very frustrating due to all the delays. It has also been a rewarding period, seeing the vessel fully functional with the controllers at the end. I have gained much knowledge during this thesis, both regarding thruster-assisted position mooring and how to construct a fully functional experimental model.

The readers should preferably have knowledge of basic hydrodynamics, marine cybernetics and control theory.

Trondheim, 2016-07-08

A handwritten signature in blue ink, reading "Jon Bjørnø". The signature is fluid and cursive, with the first name "Jon" and the last name "Bjørnø" clearly distinguishable.

Jon Bjørnø

Acknowledgment

I have had much help during this thesis, and I would like to acknowledge them for their contributions.

I would first like to thank my supervisor, Professor Roger Skjetne, for his guidance and for providing the resources I needed to build the model.

The help I have gotten from my co-advisors, Andreas Reason Dahl and Hans-Martin Heyn, has been to great use and providing me with both knowledge and support during the work with this thesis. I would especially thank Andreas Reason Dahl for offering his time when I needed, and for following up during the spring.

Thank you to Torgeir Wahl for helping me with the electronics, acquisition of parts and facilitating equipment in the Marine Cybernetics Laboratory. Without him the building process would have taken longer time.

Finally, I would like to thank Kristine Bøyum Riste for support and encouragement, and a thanks to my fellow students for a great final year.

J.B.

Abstract

This thesis presents the development of a new research foundation into the Marine Cybernetic Laboratory, the *C/S Inocean Cat I Drillship*. This is a 1:90 scaled model of an Arctic drillship design by Inocean for Statoil.

The *C/S Inocean Cat I Drillship* model is equipped with six Aero-naut Precision Schottel azimuth thrusters which are driven by six O.S. OMA-2820-950 motors and six Dynamixel MX-106R servo motors. To control the model a real time controller, CompactRIO, from National Instruments is used. The system is powered by six 12 V 12 Ah lead batteries. To make the hull durable and lightweight, it is constructed by carbon fiber and a casted frame stiffens the hull. The model has a detachable lid made of Plexiglass, that secures the equipment inside from water.

In order to design a thruster-assisted position mooring control system, a 6 DOF mathematical model of the scale model is needed. Equations for hydrodynamic modeling of marine vessels and mooring lines are presented, and combined to get the system equations. In addition, a 3 DOF mathematical model has been derived to verify other experiments.

The scaled model is tested in the MC Lab, where real scaled conditions can be applied. The experiments show great results for the different controllers, and the vessel manages the different conditions.

Comparison between the simulation model and the scale model is performed for all cases. The results yield that the simulation model needs further development to be more similar to the scale model, but it gives a good indication on the behavior of the vessel.

The complete *C/S Inocean Cat I Drillship* is a fully functional vessel, and a stable research foundation to be used in further experiments in the MC Lab.

Sammendrag

Denne avhandlingen presenterer utviklingen av en ny forskningsplattform i marine cybernetics laboratoriet, C/S Inocean Cat I Drillship. Dette er en 1:90 skala modell av et arktisk boreskip, utformet av Inocean på oppdrag for Statoil.

Modellen C/S Inocean Cat I Drillship er utstyrt med seks Aero-Naut Precision Schottel azimuth thrustere, som drives av seks O.S. OMA-2820-950 motorer og seks Dynamixel MX-106R servomotorer. En sanntids kontroller, CompactRIO, fra National Instruments blir brukt for å kontrollere modellen. Systemet er drevet av seks 12 V 12 Ah blybatterier. For å gjøre skroget holdbart og lett, er det konstruert av karbonfiber og en støpt ramme som stiver av skroget. Modellen har et avtakbart lokk laget av pleksiglass, som beskytter det elektriske utstyret fra vann.

For å kunne utforme et thruster-assistert forankring kontrollsystem, er en matematisk modell av skalamodellen med 6 frihetsgrader nødvendig. Ligninger for hydrodynamisk modellering av marine fartøy og forankringsliner er presentert, og er kombinert for å få systemlikningene. I tillegg, har en matematisk modell med 3 frihetsgrader blitt utledet for å støtte andre eksperimenter.

Den skalerte modellen er testet i MC Lab, hvor ekte skalerte forhold kan bli anvendt. Forsøkene viser gode resultater for de forskjellige kontrollerene, og fartøyet håndterer forskjellig ytre belastning fra bølger. En sammenligning mellom simuleringsmodellen og skala-modell er gjort for alle forsøkene. Resultatene viser at simuleringsmodellen må videreutvikles for å samsvare mer med skalamodellen, men den gir en god indikasjon på oppførselen til fartøyet.

C/S Inocean Cat I Drillship er et fullt funksjonelt fartøy, og en stabil forskningsplattform som skal brukes i videre eksperimenter i MC Lab.

Contents

MSc Thesis Description	i
Preface	v
Acknowledgment	vii
Abstract	ix
Sammendrag	xi
Nomenclature	xxiii
Terms and Concepts	xxvii
1 Introduction	1
1.1 Motivation	1
1.2 Background	2
1.2.1 Arctic Oil and Gas Extraction	2
1.2.2 Dynamic Positioning and Stationkeeping	2
1.2.3 Thruster-Assisted Position Mooring	3
1.2.4 C/S Inocean Cat I Drillship	5
1.3 Objectives of the Thesis	10
1.4 Contributions of the Thesis	11
1.5 Outline of the Thesis	12
1.5.1 Structure	12
1.5.2 Notation	13
2 Requirements Specification	15
2.1 Experimental Platform Purpose	15
2.2 Key Features	16
2.2.1 Functional	16
2.2.2 Physical	16
2.3 Measurements	17
2.3.1 Position	17
2.3.2 Acceleration	17
2.3.3 Mooring Line Tension	17
2.4 Actuators	17

2.5	Human-Machine Interface	18
2.5.1	Basic Control Functions	18
2.5.2	Graphical Interface	18
2.5.3	Gamepad	18
2.5.4	Logging	18
2.6	Practical Considerations	19
3	Construction and Equipping	21
3.1	Body	21
3.1.1	Hull	22
3.1.2	Lid	23
3.2	Turret and Mooring Lines	25
3.3	Thrusters	26
3.3.1	Rudder Propeller	26
3.3.2	Motor and Servo	27
3.4	Embedded System	28
3.4.1	National Instruments CompactRIO	28
3.4.2	Electronic Speed Controllers	29
3.4.3	Sixaxis Gamepad Controller	29
3.4.4	Raspberry Pi 2	29
3.4.5	Wi-Fi Bridge	29
3.4.6	Watertight Container with Equipment	30
3.5	Inertial Measurement System	30
3.6	Power	31
3.6.1	Batteries	31
3.6.2	Power Panel	32
3.6.3	Distribution	32
3.7	Qualisys Reflectors	37
3.8	Summary	38
4	Control System Design	41
4.1	System Diagrams	41
4.1.1	Communication	41
4.1.2	CompactRIO Software Topology	46
4.2	Low Level Control	48
4.2.1	ESC Calibration	48
4.2.2	Servo Calibration	48
4.2.3	Control Input to Actuator Signals	50
4.3	Necessary Control Functions	51
4.3.1	Individual Actuator Control	51

4.3.2	Generalized Force Control	51
4.3.3	Automatic Control	53
4.4	Human-Machine Interface Functions and Layout	54
5	Mathematical Modeling	57
5.1	Dynamics	57
5.1.1	Kinematics	57
5.1.2	Kinetics	59
5.2	System Identification 6 DOF Model	61
5.2.1	Vessel Model	61
5.2.2	Mooring Model	61
5.3	System Identification 3 DOF Model	62
5.3.1	Drag Coefficients	63
6	Observer and Controller Design	67
6.1	Observer Design	67
6.1.1	Nonlinear Passive Observer	67
6.2	Controller Design	70
6.2.1	Heading Control	70
6.2.2	Surge/Sway Damping and Restoring	70
6.2.3	Setpoint Chasing by Lowpass Filtering	70
6.2.4	Hybrid Control Concept	72
6.2.5	Additional Hybrid Switching Setup	74
7	Experiment Setup	77
7.1	Mooring	78
7.2	Waves	78
8	Results	81
8.1	Observer Verification	81
8.1.1	Simulation	81
8.1.2	Experiment	82
8.2	Simulation	82
8.2.1	Heading Controller	82
8.2.2	Surge/Sway Damping and Restoring Controller	84
8.2.3	Hybrid Control with Setpoint Chasing	86
8.2.4	Additional Hybrid Switching Setup	91
8.3	Experiment	92
8.3.1	Heading Controller	92
8.3.2	Surge/Sway Damping and Restoring Controller	93

8.3.3	Hybrid Control with Setpoint Chasing	95
9	Discussion	101
9.1	Heading Controller	101
9.2	Surge/Sway Damping and Restoring Controller	102
9.3	Hybrid Controller with Setpoint Chasing	102
9.4	Additional Hybrid Switching Setup	103
9.5	Simulation Uncertainties	103
9.6	Experiment Uncertainties	104
10	Concluding Remarks	105
10.1	Conclusion	105
10.2	Further Work	107
	Bibliography	108
A	Instruction Manuals for C/S Inocean Cat I Drillship	111
A.1	OCA-150 Manual	112
A.2	Operating Manual	116
A.2.1	Controller Implementation	116
A.2.2	Ship Launching Procedure - Before Sailing	117
A.2.3	Known Errors	117
A.2.4	Ship Docking Procedure - After Sailing	118
B	Content in Attached Zip-file	119

Figures

1.1	Cat I Arctic Drilling Unit [Courtesy: Jorde (2014)].	6
1.2	Regular wave test of the Cat I model from Inocean [Courtesy: Jorde (2014)].	7
1.3	MC Lab axes with positive direction based on maneuvering type coordinates with Z positive downwards [Adapted from: NTNU (2015b)].	9
3.1	CSAD hull construction stages.	23
3.2	CSAD lid with noise reduction mat.	24
3.3	The inside of the hull with noise reduction mat.	24
3.4	CSAD turret (upside down).	25
3.5	The thrusters at their respective places [Courtesy: Frederich (2016)].	26
3.6	The aero-naut precision schottel thruster with fitting ring and belt-driven swivels.	27
3.7	Mounted servos and motors with brackets and Divinycell.	27
3.8	Example of a NI cRIO chassis with modules [Courtesy: National Instruments (2015)].	28
3.9	CSAD aft with (from the left) batteries, Wi-Fi bridge, watertight container and actuators.	30
3.10	The approximate mounting place for the brackets containing the batteries.	32
3.11	How the batteries are mounted in the brackets with straps.	32
3.12	CSAD power system, bow.	33
3.13	CSAD power system, midship.	34
3.14	CSAD power system, aft.	35
3.15	Single line diagram of the power system.	36
3.16	The reflector spheroid for the Qualisys system.	37
3.17	The finished model vessel.	38
4.1	The communication signal/network information flow, bow.	42
4.2	The communication signal/network information flow, midship.	43
4.3	The communication signal/network information flow, aft.	44
4.4	Example of PWM signal with frequency = 50 Hz and duty cycle = 0.2.	45
4.5	Software topology for the CompactRIO.	46
4.6	The switching logic between the different controllers.	47

4.7	A line segment (AB) drawn so that it forms right angles with a line (CD).	49
4.8	Definition of the different control reference frames. [Adapted from: Skjetne (2014)]	52
4.9	The current HMI for the basic DP controller.	55
4.10	The current HMI for the the generalized force controller.	55
5.1	Definition of the different reference frames [Adapted from: Skjetne (2014)].	58
5.2	The towing setup for CSAD.	63
5.3	Drag forces acting on the hull in surge.	64
5.4	Drag forces acting on the hull in sway.	64
5.5	Drag forces acting on the hull in yaw.	65
6.1	A block diagram of the setpoint generator.	71
6.2	Explanation of the safety circle [Adapted from: Skjetne (2014)].	73
7.1	The experiment setup, with wave direction in an angle to the bow.	77
7.2	One of the mooring lines that are used in the experiments.	78
8.1	Observer verification in simulations.	81
8.2	Observer verification in experiment.	82
8.3	Results from heading controller simulations, with wave height $H_s = 4$ meters.	83
8.4	Results from heading controller simulations, with wave height $H_s = 9$ m.	84
8.5	Results from surge/sway damping and restoring controller simulations, with wave height $H_s = 4$ meters.	85
8.6	Results from surge/sway damping and restoring controller simulations, with wave height $H_s = 9$ meters.	86
8.7	Results from hybrid controller with setpoint chasing simulation, with wave height $H_s = 0.5$ meters.	87
8.8	Results from hybrid controller with setpoint chasing simulation, with wave height $H_s = 2.5$ meters.	88
8.9	Results from hybrid controller with setpoint chasing simulation, with wave height $H_s = 4$ meters.	89
8.10	Results from hybrid controller with setpoint chasing simulation, with wave height $H_s = 9$ meters.	90
8.11	Results from the additional hybrid switching setup simulations, with wave heights $H_s = 2.5$ m, $H_s = 4$ m and $H_s = 9$ m.	91
8.12	The converted wave frequency with corresponding wave height.	91
8.13	Results from heading controller experiments, with wave height $H_s = 4$ meters.	92
8.14	Results from heading controller experiments, with wave height $H_s = 9$ meters.	93
8.15	Results from surge/sway damping and restoring controller experiments, with wave height $H_s = 4$ meters.	94

8.16 Results from surge/sway damping and restoring controller experiments, with wave height $H_s = 9$ meters.	95
8.17 Results from hybrid controller with setpoint chasing experiments, with wave height $H_s = 0.5$ meters.	96
8.18 Results from hybrid controller with setpoint chasing experiments with wave height $H_s = 2.5$ meters.	97
8.19 Results from hybrid controller with setpoint chasing experiments, with wave height $H_s = 4$ meters.	98
8.20 Results from hybrid controller with setpoint chasing experiments, with wave height $H_s = 9$ m.	99
A.1 Error code 56 in the startup phase.	118

Tables

1.1	Statoil’s Cat I Arctic Drillship specifications.	7
1.2	Statoil’s Cat I Arctic Drillship dimensions.	7
3.1	C/S Inocean Cat I Drillship dimensions.	21
3.2	Scaled thruster location [Courtesy: Frederich (2016)].	26
3.3	Power consumption calculations	31
4.1	Generic control modes.	46
4.2	Current calibration of ECSs.	48
4.3	Defined neutral angles for the thruster.	49
4.4	Signed number representations conversion.	49
5.1	Froude scaling table.	62
5.2	CSAD rigid body and added mass parameters.	62
5.3	Drag coefficients in surge, sway and yaw based on test result.	65
5.4	Drag coefficients in surge, sway and yaw with coupling terms.	66
6.1	Set of control laws [Adapted from: Nguyen and Sørensen (2009b)].	72
6.2	Switching sequence [Adapted from: Nguyen and Sørensen (2009b)].	72
7.1	Scaled waves in the experiment.	79
7.2	Definition of sea states according to Price and Bishop (1974).	79

Nomenclature

Abbreviations

AMOS	Centre for Autonomous Marine Operations and Systems
ALS	Accidental Limit State
AWACS 2	Active Wave Absorption Control System
CAD	Computer-Aided Design
CO	Center of Origin
COT	Center of Turret
CS	Cybership
CSEI	Cybership Enterprise I
CSII	Cybership II
CSIII	Cybership III
CSAD	Cybership Inocean Cat I Drillship
cRIO	NI CompactRIO
DC	Direct Current
DP	Dynamic Positioning
DOF	Degrees of Freedom
DNV	Det Norske Veritas
ESC	Electronic Speed Controller
FEM	Finite Element Method
FPGA	Field-Programmable Gate Array
FZP	Field Zero Point
GNSS	Global Navigation Satellite System
GPS	Global Positioning System
GUI	Graphical User Interface
HMI	Human–Machine Interaction
IMO	International Maritime Organization
IMT	Department of Marine Technology
IMU	Inertial Measurement Unit
ISSC	International Social Science Council
ITTC	International Towing Tank Conference
I/O	Inputs/Outputs
LF	Low Frequency
MARINTEK	Norsk Marinteknisk Forskningsinstitutt
MC Lab	Marine Cybernetics Laboratory
MODU	Mobile Offshore Drilling Unit
MSc	Master of Science

NED	North-East-Down
NI	National Instruments
NTNU	Norwegian University of Science and Technology
PhD	Doctor of Philosophy
PID	Proportional, Integral, Derivative
PWM	Pulse Width Modulation
QTM	Qualisys Track Manager
RAO	Response Amplitude Operator
RIO	Reconfigurable I/O modules
RPi2	Raspberry Pi 2
TAPM	Thruster Assisted Position Mooring
UUB	Uniformly Ultimeated Bounded
UGAS	Uniform Global Asymptotically Stable
UGES	Uniform Global Exponentially Stable
WF	Wave Frequency

Greek Letters

Λ	First order diagonal and non-negative filter gain matrix
η	Position vector of vessel
η_{xy}	Position vector of vessel in x- and y-direction
η_d	Desired position vector
η_0	Equilibrium position vector
\mathbf{v}	Velocity vector of vessel
\mathbf{v}_c	Current velocity
\mathbf{v}_r	Relative velocity
$\boldsymbol{\tau}_{\text{moor}}$	Mooring system forces and moments
$\boldsymbol{\tau}_{\text{wind}}$	Wind forces
$\boldsymbol{\tau}_{\text{wave}}$	Wave forces
$\boldsymbol{\tau}_{\text{wave2}}$	Second-order wave forces
$\boldsymbol{\tau}_{\text{env}}$	Environmental forces
$\boldsymbol{\tau}_{\text{thr}}$	Thruster forces
$\boldsymbol{\tau}_H$	Horizontal component of the mooring line tension
$\boldsymbol{\tau}_{\text{pid}}$	Thrust forces given from the PID-controller
$\boldsymbol{\tau}_{\text{pid}}^{\psi}$	Thrust forces given from the heading PID-controller
$\boldsymbol{\tau}_d^{xy}$	Thrust forces given from the surge/sway D-controller
ξ	Wave frequency motion vector, and the integrated error between desired position and position
β	Mooring line orientation vector
Ω	Dominating wave response frequencies matrix

Γ	Damping ratios matrix
ψ_d	Desired heading angle
ψ	Yaw angle of vessel
β_w	Wave direction
β_c	Current direction
∇	Displacement of vessel
Δ	Mass of the vessel

Roman Letters

{B}	Body-fixed frame
{Basin}	Basin-fixed frame
b	Bias force
C_{RB}	Coriolis force matrix
C_A	Centripetal force matrix
D	Damping force matrix
D_{lin}	Linearized damping force matrix
D_{mo}	Linearized mooring damping matrix
d_{mo}	Mooring damping matrix
D_{NL}	Non-linear damping matrix
{D}	Reference-parallel frame
{E}	Earth-fixed frame
G_{mo}	Linearized mooring stiffness matrix
g_{mo}	Mooring stiffness matrix
H_s	Significant wave height
J(η)	Transformation matrix from NED to Body 6 DOF
K_{1,2,3,4}	Observer gain matrices
K_{p,i,d}	Controller gain matrices
L_p	Coefficient matrix with line breakage information
M_{RB}	Mass matrix of the vessel
M_A	Added mass matrix of the vessel
M	Mass + added mass matrix of the vessel
R(ψ)	Rotation matrix from NED to Body
{T}	Turret-fixed frame
T(β)	Mooring line configuration matrix
T_s	Cutoff time constant for setpoint chasing algorithm
{User}	User-fixed frame
w_b	White noise bias
\bar{x}	Longitudinal position of spread mooring point in x-direction
x	Longitudinal position of vessel in surge

\bar{y}	Longitudinal position of spread mooring point in y-direction
y	Longitudinal position of vessel in sway
z	Longitudinal position of vessel in heave

Terms and Concepts

- **Dynamic positioning system** is a computer-controlled system to automatically maintain a vessel's position and heading by using its own propellers and thrusters.
- **Dynamic positioning** is an operation to automatically maintain a vessel's position and heading.
- **Thruster-assisted position mooring** is a positioning activity that uses a combination of mooring lines and dynamic positioning to maintain the vessel's position inside a safety circle to avoid mooring line breakage.
- **Catenary equation** is an equation that can describe the shape of the mooring lines under influence of gravity and supported at its end points, i.e. the anchor and mounting point on the vessel.
- **Equilibrium position** is the natural position where the mooring lines and the environmental loads balance each other with zero thrust.
- **Heading control** is a controller that regulates the vessel's heading to a desired heading that minimizes the environmental loads on the vessel and the mooring lines. A more advanced version of this is weather-vaning where it automatically estimates the heading that gives the minimum environmental impact on the system.
- **Damping control** is a negative feedback from the vessel's velocity in surge and sway to damp out oscillatory motions.
- **Setpoint chasing** automatically generates new setpoints to the TAPM vessel in varying environmental conditions. This is to find the optimal equilibrium position where the environmental loads and mooring loads are zero.
- **Field Zero Point** is the local position in NED used by the DP or TAPM system. This is typically chosen to be the center of the mooring line configuration and the COT and FZP coincide when no environmental loads or thruster force act on the vessel.

Chapter 1

Introduction

1.1 Motivation

Stationkeeping, i.e. maintaining a vessel's position fixed, is challenging in the ice and harsh weather of the Arctic. The capability is nevertheless essential for oil and gas exploration and, as melting sea ice is making the Arctic more accessible, the topic sees increased relevance. Dynamic position (DP) and thruster-assisted position mooring (TAPM) of turret-anchored vessel are possible concepts for arctic deepwater offshore operations.

The challenging ice and weather conditions in the Arctic make the control task more complicated, compared to a normal DP operation. The control system experiences new challenges due to the harsher conditions. These are related to how the controller can position and dampen the motion of the vessel, by minimizing the use of thrusters. In addition, the controller needs to minimize the risk of line break in the mooring lines. If line breakage occurs, this needs to be detected and handled.

1.2 Background

The main focus for this thesis is the building of the C/S Inocean Cat I Drillship model and test TAPM control algorithms on the vessel. Relevant background information on this topic is presented here, in addition to a brief introduction to the Marine Cybernetic Laboratory.

1.2.1 Arctic Oil and Gas Extraction

The Arctic oil and gas extraction is more technically challenging compared to other environments. However, relatively high oil prices in the period 2010-2014 and technological developments have allowed exploration. During 2014 the oil prices plummeted, and the profit margin of Arctic oil and gas extraction vanished. In the research community, there is still great interest in further development in the Arctic. This research, development and innovation will enable safe operations in the Arctic, with minimum environmental impact.

1.2.2 Dynamic Positioning and Stationkeeping

To get a clearer understanding on some basic definitions in a marine control system, a set of definitions are presented in this section.

1.2.2.1 Principles

Dynamic Positioning: The International Maritime Organization (IMO, 1994) gives the following definition to a DP vessel:

"Dynamically positioned vessel (DP-vessel) means a unit or a vessel which automatically maintains its position (fixed position or predetermined track) exclusively by means of thruster force."

and they define the DP-system as:

"Dynamic positioning system (DP-system) means the complete installation necessary for dynamic positioning a vessel comprising of the following sub-systems:

- *power system,*
- *thruster system, and*
- *DP-control system".*

Seakeeping: Fossen (2011, Sec. 1.2.2) defines seakeeping as:

"Seakeeping [...] is the study of motion when there is wave excitation and the craft keeps its heading ψ and its speed U constant (which includes the case zero speed)."

1.2.3 Thruster-Assisted Position Mooring

This section will give an overview of what TAPM is, a little bit of the historic background and presents some control strategies.

1.2.3.1 Principle

A TAPM-system consists of two parts, a conventional mooring system and a DP-system. The mooring lines have a fixed position at the turret and seabed, which allows for the vessel to rotate freely about the turret. The DP part of the system allows the vessel to use its thrusters to assist the mooring system. This will allow the system to withstand harsher weather and faults that can occur during operations. The DP part also gives the ability to reduce the loads on the mooring lines by reducing the vessel motions and offset from desired position, which also reduces the probability of loss of mooring lines.

This configuration gives the ability for the vessel to weather-vane, which means that the vessel can keep the position aligned with the environmental forces and the turret is the connection point for transfer of loads between the vessel and the mooring lines.

TAPM can also be referred to as thruster-assisted mooring (TF), position mooring (POSMOOR) or thruster-assisted mooring system (TAMS). In the ISO document (ISO, 2013) thrusters-assisted mooring is defined as:

"A stationkeeping system consisting of mooring lines and thrusters. The thrusters contribute to control the structure's heading and to reduce mooring line forces and reduce structure offset."

1.2.3.2 Historical Development

The first vessel that introduced the TAPM system was Petrojarl in 1986 with its weather-vaning system (Aalbers et al., 1995). From this year on, all vessels were constructed with the turret inside 1/3 from the bow, and the placement of the accommodation could either be in behind the turret in the aft or fore in the front. Both solutions have their advantages and disadvantages, and the most marked disadvantage was when the accommodation block was placed in the front. This

lead to a large wind area that could deteriorate the weather-vaning ability of the vessel, which then required an active heading controller.

Aalbers et al. (1995) stated that the mooring line tension is strongly dependent on how the water depth, turret location and mooring line configuration are. Due to the combination of the two mooring principles, thrusters to reduce loads on the mooring lines and a fluid swivel to allow continuous fluid flow during weather-vaning, more advanced control techniques were needed. This led to the development of more advanced TAPM controllers.

From 2007 until now, there has been more and more focus on the exploitation of oil and gas in deep water (>500 m), and further north than before. This has made fixed platforms on the seabed impractical, at least for the first case. Instead, semi-submersibles and vessels with positioning systems have been widely used. The TAPM system is an economical solution for station keeping in deep water and in ice, due to longer operational periods before the operation has to be shut down. As mentioned before, the TAPM system is required in harsh environmental conditions to avoid loss of mooring lines. This focus has temporarily calmed down, due to low oil prices.

Wassink and List (2013) performed an analysis on development of solutions for Arctic offshore drilling. The results of this analysis shows that the drillship with a TAPM solution is the best alternative when drilling in the Arctic. All alternatives have their specialties, and in two out of three categories the drillship with a TAPM solution wins.

1.2.3.3 Control Strategies

There have been numerous different control strategies for TAPM systems during the years, and the following controllers are mostly basic controllers with some more advanced in the end.

Heading Control: The first heading control was proposed by Strand et al. (1998) and Sørensen et al. (1999). It consists of a PID-controller to control the heading automatically to the desired heading against the environmental loads. Later an automatic weathervaning system was proposed by Fossen (2001) and Kjerstad and Breivik (2010) to automatically sense and control the vessel against the environmental forces.

Surge-Sway Damping Control: The surge-sway damping control is designed to dampen unwanted large oscillatory motion in surge and sway, and to reduce the stress on the mooring system. This damping control was proposed by Strand et al. (1998) and Sørensen et al. (1999).

Roll-Pitch Damping Control: Due to undesired oscillatory motion in roll-pitch caused by the thruster usage in combination with the mooring lines, a roll-pitch damping control was proposed by Sørensen and Strand (2000). This was to reduce roll-pitch motion of an semisubmersibles due to low waterplane area.

Line Break Detection and Compensation: The line break detection algorithm was proposed by Strand et al. (1998) to detect and compensate the loss of one or more mooring lines. This is done by using feedforward to the thrusters to compensate the loss of mooring force. Later work on diagnosis and fault-tolerant control is done by Nguyen et al. (2007).

Setpoint Chasing: In addition to the basic control functions, there are now more advanced methods for controlling the vessel. Setpoint chasing for TAPM vessels was proposed by Nguyen and Sørensen (2009a) to automatically find and control the vessel to the equilibrium position where the environmental loads are counteracted by the mooring forces. Sørensen et al. (2001) also discussed the topic on setpoint chasing for drilling and well-intervention operations to minimize the riser angle. This will then minimize the thruster usage. Different methods have been proposed for setpoint chasing; finite element method (FEM)-based (Sørensen et al., 2001), reliability-based (Berntsen et al., 2006; Leira et al., 2008) and setpoint calculation by lowpass filter (Nguyen and Sørensen, 2009a).

1.2.4 C/S Inocean Cat I Drillship

In 2015 it was decided that a cybership should be built to conduct research in the TAPM field. This cybership is based on Statoil's Cat I Arctic Drillship and could be used in the MC Lab. This section presents background information on the Statoil's Cat I Arctic Drillship and the laboratory that the model will be used in. The requirements and building of C/S Inocean Cat I Drillship is covered in Chapter 2 and 3.

1.2.4.1 Statoil's Cat I Arctic Drillship

In 2013 Inocean won a contract from Statoil to design an arctic drillship, and the result from this can be seen in Figure 1.1. This is a DP and turret moored mobile offshore drilling unit (MODU) with specifications as listed in Table 1.1. The vessel is also fully winterized with enclosed drilling areas. This enclosing can be seen in Figure 1.1.

Statoil (2012) presents Cat I as:



Figure 1.1: Cat I Arctic Drilling Unit [Courtesy: Jorde (2014)].

"New arctic drilling unit. Cat I will be a tailor-made floating drilling concept, able to operate across our Arctic acreage. Statoil has on-going R&D activities to qualify drilling and critical support technologies. Going forward we will invite the supplier industry, as we have done on the other category concepts on the NCS, to work with us on arctic drilling solutions."

The main philosophy for the vessel design is (Jorde, 2014):

- *The drillship is designed with similar safety level as on conventional drillships.*
- *Minimal Environmental footprint, mainly to be achieved with low fuel consumption.*
- *Enclose drilling areas to utilize proven drilling technology and limit harsh environment exposure.*
- *The enclosed area is designed as "outdoor areas" to limit cost impacts.*
- *Design a hull that is optimized for forward operation in open seas with a conventional bow – and for aftwards operation in ice with an ice optimized stern.*
- *Locate the turret amidships will improve drilling operability in open and harsh environment.*

There have been several tests on the model to decide what parameters the hull should have and to test out different bilge keels. The following test is just some of them, and Figure 1.2 shows the model in one of the wave tests.

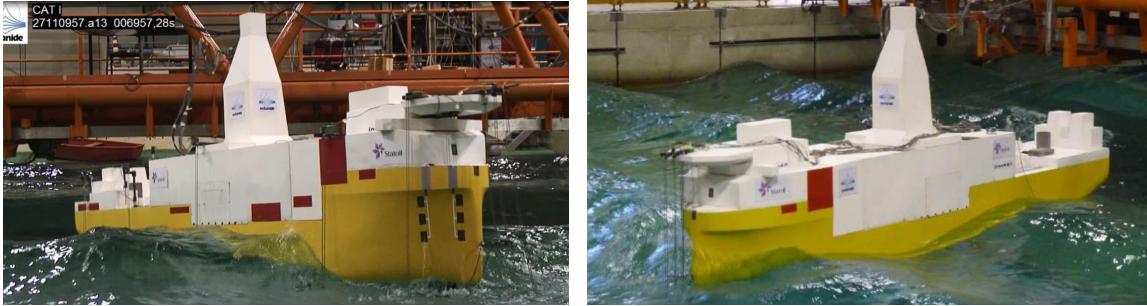


Figure 1.2: Regular wave test of the Cat I model from Inoceen [Courtesy: Jorde (2014)].

- Regular wave tests from 0° to 90° heading to verify the response amplitude operator (RAO) and drift forces.
- Irregular Accidental Limit State (ALS) test (10,000 years) from 0° to 30° heading to obtain the slamming values and assess the green sea on deck.
- Transit test to obtain the vessel resistance.

Table 1.1: Statoil's Cat I Arctic Drillship specifications.

Specification:	
Ice breaking capability:	1.2 meter level ice
Det Norske Veritas (DNV) class:	1A1 ICE10
Minimum design temperature:	-30°C
Variable deck load:	16,000 tonns
Payload:	22,400 tonns
Drilling depth:	100 - 1500 meters
Open water well depth:	8500 meters
Arctic well depth:	5000 meters
Maximum drilling endurance:	120 days

Table 1.2: Statoil's Cat I Arctic Drillship dimensions.

Description	Data
Length over all (L_{oa})	232 [m]
Breadth (B)	40 [m]
Depth moulded (D)	19 [m]
Draft design (T)	12 [m]

Cat I Arctic drillship has several drilling features, Table 1.1 lists the main features. The vessel data is shown in Table 1.2.

1.2.4.2 Marine Cybernetic Laboratory

The Marine Cybernetics Laboratory (MC Lab) has a small wave basin, located next to the large towing tank at MARINTEK. This small basin was previously used to store vessels made of paraffin wax (NTNU, 2015b). This laboratory is mainly used for testing the motion control systems for marine vessels, due to its advanced instrumentation package. It is also used to test more specialized hydrodynamic tests as well, due to the towing carriage, which has capability for very precise movement of the vessels in 6 degrees of freedom (DOF).

The laboratory today, have a fleet of model vessels, and the vessels Cybership II and Cybership III (Nilsen, 2003) have been used in mooring experiments before. For more information about these vessels and the other vessels, see NTNU (2015a). The newest addition to this fleet is C/S Inocean Cat I drillship (CSAD). This vessel is a 1:90 scaled model of an Arctic drillship, designed by Inocean, with both DP and TAPM functions. With a rotating turret and six azimuth thrusters (three fore and three aft), for DP and thruster assist, gives this vessel a wide range of applications. More information about CSAD will be presented in Chapter 3 and 4.

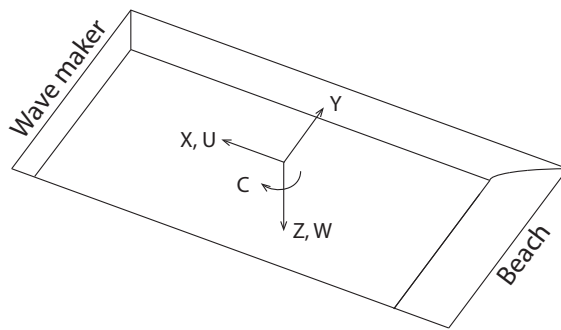
The MC Lab is primarily used by MSc students and PhD candidates, but it is also used by external users. The laboratory is operated by the Department of Marine Technology and MARINTEK.

To emulate a full scale global navigation satellite system (GNSS) system the MC Lab is fitted with a real-time positioning system, both over and under the water surface. The Qualisys motion capture system consist of Oqus cameras and the Qualisys Track Manager (QTM) software. The vessels that are being tested must be fitted with a minimum of three/four silver spheres, to obtain accurate 6 DOF position data by triangulation within 1 mm precision.

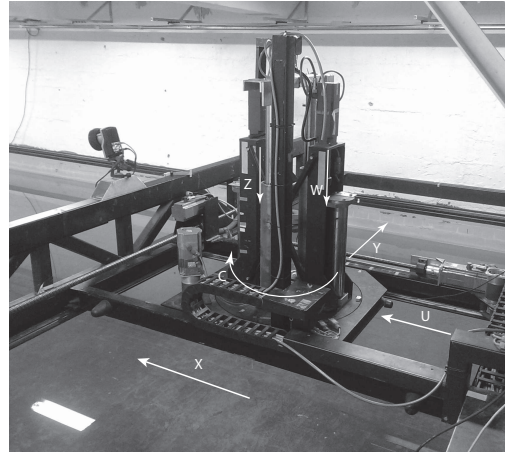
The wave maker is a single paddle wave making machine with a width of 6 meter and it is equipped with an Active Wave Absorption Control System (AWACS 2). The machine can produce both regular and irregular waves because of the DHI Wave Synthesizer the system has. The capacity of the wave maker is presented in the following list (NTNU, 2015b):

- Regular waves $H < 0.25$, $T = 0.3 - 3$ s.
- Irregular waves $H_s < 0.15$ m, $T = 0.6 - 1.5$ s.
- Available Spectrum: JONSWAP, Pierson-Moskowitz, Bretschneider, ISSC, ITTC.
- Wave controller update rate = 10 Hz.
- No. wave gauge on paddle = 4.
- Stroke length on actuator = 590 mm.
- Speed limit = 1.2 m/s.

The towing carriage can be used in two modes, either computer controlled or manual mode. The computer controlled mode is operated through special applications for LabVIEW, to setup regular or irregular movement on the different axes. The manual mode is operated from the console at the towing carriage. Figure 1.3 shows the setup for the different axes of the basin and on the towing carriage.



(a) Basin



(b) Towing carriage

Figure 1.3: MC Lab axes with positive direction based on maneuvering type coordinates with Z positive downwards [Adapted from: NTNU (2015b)].

1.3 Objectives of the Thesis

The superior objective of this thesis is to develop a new research foundation into the Marine Cybernetics Laboratory, the C/S Inocean Cat I Drillship, and all experiments are done in here. To achieve the main objective, several partial objectives are defined:

1. Find background and do a literature review on thruster-assisted position mooring and appropriate controllers.
2. Find background on the NTNU Marine Cybernetics laboratory.
3. Build the C/S Inocean Cat I Drillship model.
4. Implement the software on the C/S Inocean Cat I Drillship.
5. Derive a mathematical model of C/S Inocean Cat I Drillship.
6. Simulate the different thruster-assisted position mooring control algorithms on the mathematical model.
7. Implement the control algorithms on the C/S Inocean Cat I Drillship and test the different control laws in the Marine Cybernetics laboratory.

1.4 Contributions of the Thesis

This thesis brings a new research foundation into the Marine Cybernetics Laboratory, and the cybership fleet. Hence, this contributes with:

1. A new vessel into the cybership fleet in the Marine Cybernetics Laboratory at NTNU.
2. Mathematical model of a TAPM vessel, both full scale and model scale.
3. Controller design and validation by simulation and laboratory experiments.
4. Validation of mathematical model by simulations and laboratory experiments.
5. A collection of literature on TAPM, from early days and up until now.

It is reasonable to believe that this thesis and its contents can inspire and help in future master and PhD research at NTNU. In addition, this research may help to new development in the area of TAPM controllers.

1.5 Outline of the Thesis

1.5.1 Structure

The thesis is build up around the development of the C/S Inocean Cat I Drillship model and relevant control algorithms. It is organized in the following way:

Chapter 1 introduces the thesis to a reader. It provides relevant background information regarding thruster-assisted position mooring and the C/S Inocean Cat I Drillship model. This chapter also provides the objectives and contribution of the thesis.

Chapter 2 addresses the main requirements and the intended use with corresponding controllers for the C/S Inocean Cat I Drillship. In addition to the requirements, instruments, and human-machine interface are presented.

Chapter 3 presents the building process of the C/S Inocean Cat I Drillship. In addition diagrams of the architecture, regarding position of thrusters and power flow is presented.

Chapter 4 presents the control system design with how the different controllers and navigation algorithms are implemented. In addition, the communication flow and the human-machine interface is presented.

Chapter 5 presents the mathematical modeling for the simulation model, where both the kinematics and kinetics are presented. The identification of the system parameters is also presented.

Chapter 6 covers the controller and observer design. Different thruster-assisted position mooring controllers are presented, and an observer that is suitable for the system is proposed.

Chapter 7 presents the experiment setup for the C/S Inocean Cat I Drillship in the MC Lab.

Chapter 8 the results from all the different controller, in both the simulations and experiments, are presented and commented.

Chapter 9 presents a discussion on the results from Chapter 8. In addition to a discussion on different issues that have occurred, are brought up.

Chapter 10 covers the concluding remarks are made and summarizing the main contributions of this master thesis. Suggestions for further work is also presented.

Appendix A presents different manuals for the C/S Inocean Cat I Drillship are provided.

Appendix B presents an overview over what the digitally attached zip-file contents are, is provided.

1.5.2 Notation

Throughout the thesis bold style font is used for vectors and matrices, while scalars are in regular style font. Text written in cursive, is a definition or a direct copy from the reference.

Chapter 2

Requirements Specification

This chapter specifies the functional and physical needs the experimental platform should satisfy, i.e. what the system should do. The specific implementation, i.e how the system meets the requirements, is given in Chapters 3 and 4. Requirements mostly specific to this vessel model are the main focus. Generally, the model will be constructed according to the established practices of MARINTEK and the MC Lab. These are not detailed here, but by NTNU (2015a).

2.1 Experimental Platform Purpose

The intended use of the vessel, is to provide experimental data to support research. TAPM is the primary research focus, and specifically control design, without preventing research on operation and other disciplines. Control design research will be able to address the interaction between anchor and thrusters, thrust allocation, observing, motion control, etc. Finally, the design must be flexible, to allow for adaption to unforeseen research needs.

2.2 Key Features

2.2.1 Functional

It should be possible to design and implement own regulators. This requires specially

- software framework that makes it possible to effectively change only the signals desired,
- preprogrammed generic software modules that can handle functions that are not of particular interest to the specific experiment.

Again, the design must be flexible, to allow for adaption to unforeseen research needs, new framework, hardware, etc.

2.2.2 Physical

The model will be a scaled version of the Statoil's Cat I Arctic Drillship, design by Inocean. The background for this is that Department of Marine Technology (IMT) and the Centre for Autonomous Marine Operations and Systems (AMOS) wished to develop and build a new model ship for use in the MC Lab. This model should be according to a drillship design, with full stationkeeping capabilities by both DP and TAPM. The vessel is intended to have a modern design, with good stationkeeping performance in both open water waves and in sea-ice.

2.2.2.1 Turret

On the vessel there must be a turret. This turret must have the ability to rotate freely, but if necessary have the possibility to command a rotation of the turret. This setup is normal on full scale vessels.

2.2.2.2 Mooring Lines

The scale model must have the ability to connect at least 4 or more mooring lines to the turret. This requirement comes from what is normal in full scale operations.

2.2.2.3 Riser

An adaptation of the turret has to be made, such that a riser has the possibility connect in the center. This is desired so that research with risers is also possible.

2.3 Measurements

Essential measurements available on the full scale TAPM vessel must be available to control the system.

2.3.1 Position

It must be possible to measure the position of the vessel in the MC Lab. Normally, DP-systems get this via GPS, but this is not possible in the MC Lab.

2.3.2 Acceleration

This is a measurement that exist and is measured by IMUs onboard the vessel. Measurements of the acceleration is also desired on the scale model.

2.3.3 Mooring Line Tension

Normally there is no measuring of line tension i full scale, but for research purposes it is desired that the scale model as the opportunity to measure this as well.

2.4 Actuators

Thrust forces must be able to produce at the same hull relative positions and angles as on the Inocean design. This yields six rotatable thrusters, with location as specified in Section 4.1. The scale model thruster forces and rotational velocities must, as a minimum, equal the capabilities of the full-scale vessel. The reason for this is that Inocean will have the ability to access the data from the experiments.

2.5 Human-Machine Interface

2.5.1 Basic Control Functions

To position the vessel before, between and after experiment, pre-implemented control functions should be available. These include (NTNU, 2015a)

- individual actuator control,
- generalized force control in the
 - vessel body frame,
 - MC Lab inertial frame, and
 - user frame, and
- position regulation, i.e. stationkeeping.

2.5.2 Graphical Interface

The graphical interface should be easily configurable, so the user can see it adapt it to their needs. In particular, these requirements could vary from experiment to experiment

- plotting,
- buttons and control parameters for online tuning.

The interface must clearly show which control mode is active.

2.5.3 Gamepad

For ease of access, all basic control functions must be available through a gamepad.

2.5.4 Logging

It must be possible and easy to customize logging for each experiment. All signals must be available for logging.

2.6 Practical Considerations

This vessel is going to have a lot of users, which requires the vessel to be easy in use. In addition, it is desired that the vessel is robust and waterproof. Such that it has the ability to get wave splashes on the deck, without worrying about the electronics onboard. If unforeseen behavior occurs for the vessel, an emergency function is desired to turn off the system.

Chapter 3

Construction and Equipping

Bjørnø (2015) a plan was proposed for the construction, equipping and assembly process. This plan has been followed with minor changes and additions. During this process, the hardware architecture of the vessel was decided. Parts that need a specific placement, such as the thrusters and the turret, were placed at these places. The other parts were placed such that easy access for maintenance and replacement is possible. The electronics were positioned at the rear section of the model to avoid most of water splash during experiments. This section will present the drawings for the power system, Section 3.6.3, signal flow, Section 4.1.1, and the software topology of the CompactRIO, Section 4.1.2. From the same figure, the placement of each part can be seen.

3.1 Body

Due to limitations in the MC Lab, see Section 1.2.4.2, a scaling of 1:90 is chosen. Table 3.1 shows the scaled data of the vessel.

Table 3.1: C/S Inocean Cat I Drillship dimensions.

Description	Data
Length over all (L_{oa})	2.578 [m]
Breadth (B)	0.440 [m]
Depth moulded (D)	0.211 [m]
Draft design (T)	0.133 [m]

3.1.1 Hull

The original vessel hull is designed by Inocean for Statoil, and now these drawings are used by MARINTEK to build a model of the same hull. The model hull is constructed in carbon fiber with brackets for the thrusters and with a deck (3-4 mm) out of acrylic fiber covering all of the bottom deck. Instead of a lowered mid-ship section, the deck is made planar.

The construction steps were

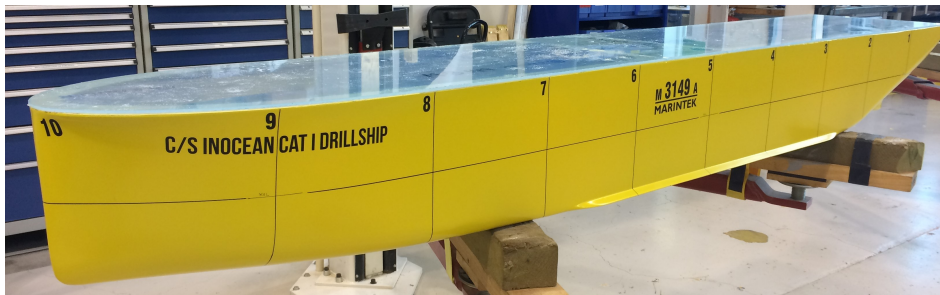
1. Making a plug using the computer-aided design (CAD) drawings. This plug is used to get the correct shape of the vessel. The it was cleaned and polished to make the plug so smooth that the mold easily can be removed afterwards.
2. Making a mold from the plug by covering the outside of the plug with a material, that is stiff enough to hold its shape during the curing process later on. This mold was also stiffened up to make sure it was stiff enough.
3. Cast the hull. This was done with carbon fiber and slowly curing epoxy, by using Vacuum assisted methods. This makes the epoxy spread evenly over the carbon fiber, which results in a strong and thin hull. Since a slowly curing epoxy has been used, the curing process took a long time. The result of this process can be seen in Figure 3.1a.
4. Paint the model with yellow paint and mark it with the correct markings, which can be seen in Figure 3.1c.



(a) After epoxy curing process.



(b) After painting, not finished yet.



(c) Complete with markings and lid.

Figure 3.1: CSAD hull construction stages.

3.1.2 Lid

When it comes to the lid, there were several factors that needed to be considered; waterproofing, easy access to parts and noise reduction. The waterproofing issue was fixed by fitting a rubber seal between the lid and the edge on the vessel, then securing the lid with several screws around the edge of the lid. The easy access factor was solved by fitting watertight hatches in both of the lid, so that the weight, batteries and other parts can be reach. For the last part, noise reduction, the lid is fitted with noise reducing mats, in addition to mats fitted inside the hull as well. See Figure 3.2 and 3.3 for the solutions.



(a) Top view.

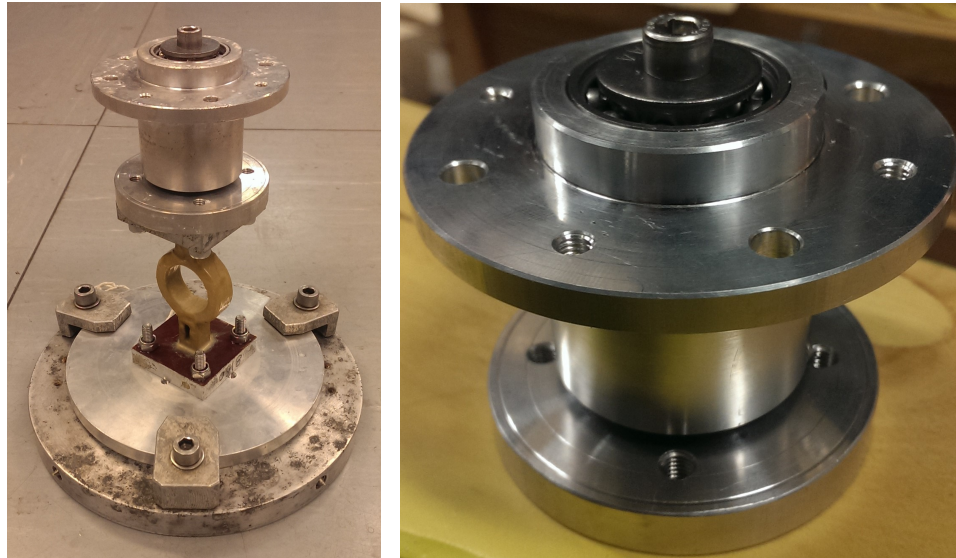


(b) Underside view.

Figure 3.2: CSAD lid with noise reduction mat.



Figure 3.3: The inside of the hull with noise reduction mat.



(a) Complete.

(b) Lower part close-up.

Figure 3.4: CSAD turret (upside down).

3.2 Turret and Mooring Lines

The mooring lines are connected to the turret by using clips. This will be a secure way to connect the mooring lines to the turret and the risk of them detaching is minimal. See Figure 3.4b for the connection setup, with maximum eight mooring connections. This is a preliminary setup, since there is no way to command rotation on the turret, it can only rotate freely.

The upper part of the turret is mounted to the cylindrical cut-out of the hull, and attached by screws. The upper and lower parts are connected with a spacer. This spacer can be a force measurement, such that total force measurements in x-, y- and z-direction can be obtained. In addition to the spacer, force measurements rings are attached to the mooring lines to measure the force on each mooring line.

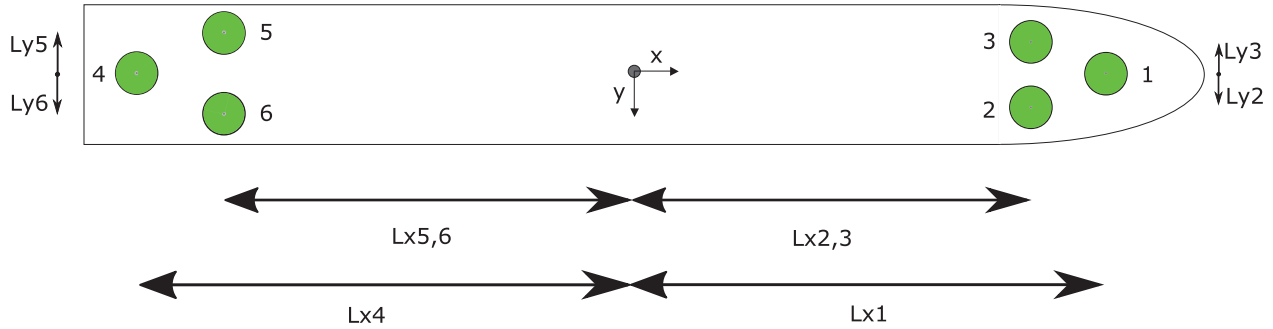


Figure 3.5: The thrusters at their respective places [Courtesy: Frederich (2016)].

Table 3.2: Scaled thruster location [Courtesy: Frederich (2016)].

Thruster	Position X [m]	Position Y [m]
Thruster 1	1.0678	0.0
Thruster 2	0.9344	0.1100
Thruster 3	0.9344	-0.1100
Thruster 4	-1.1644	0.0
Thruster 5	-0.9911	-0.1644
Thruster 6	-0.9911	0.1644

3.3 Thrusters

The thrusters are placed according to respective places at Statoil's Cat I Arctic Drillship, as given in Figure 3.5, and the scaled dimensions are given in Table 3.2. The thrusters consist of multiple parts; rudder propeller, motor and servo. These parts are more specifically described in the following subsections.

3.3.1 Rudder Propeller

The Aero-naut Precision Schottel drive is an azimuth thruster. These have a propeller that is 30 millimeters in diameter, and the thrusters come with both left and right going blades. The six thrusters that are needed, are mounted on the bottom of the hull with the fitting ring that came with the thrusters, so that they can easily be replaced if needed. The fitting ring is coated with a silicon seal to create a watertight seal that prevents the water entering the hull. The thruster hub is easily passed through the hole of the ring, and secured with clips inside. The gears for the drive belts are fitted on top. The thrusters and how they are fitted, can be seen in Figure 3.6.

A very important matter is, that the thrusters are water lubricated. Therefore, the thrusters can only be driven a light speed outside water. For more documentation, see the digital Appendix.



(a) The unmounted thruster [Courtesy: aero naut (2015)].



(b) The mounted thruster.

Figure 3.6: The aero-naut precision schottel thruster with fitting ring and belt-driven swivels.

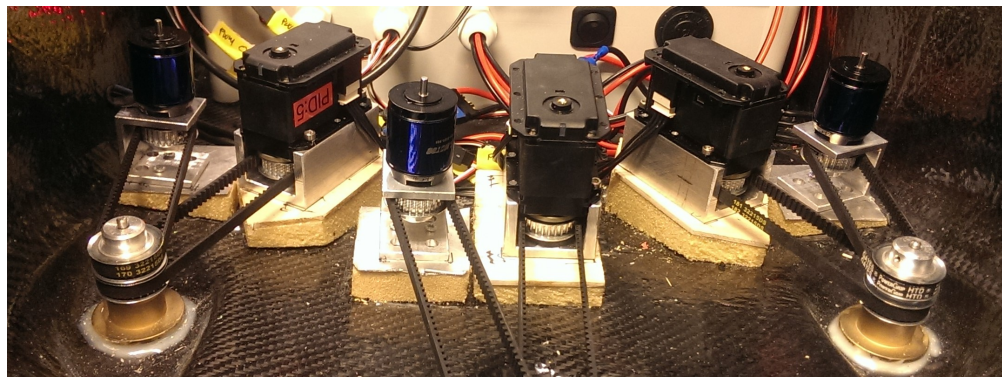


Figure 3.7: Mounted servos and motors with brackets and Divinycell.

3.3.2 Motor and Servo

Each thruster is driven by a brushless OMA-2820-950 DC motor. The DC motor requires a 12 V power supply, the power supply and how the motors operates, speed and direction, will be determined by the electronic speed controller (ESC).

Dynamixel MX-106R servo motors are fitted to control the angle of the six thrusters. The servos are fitted with a 1:1 gear, which means that a 1 degree turn on the servos results in 1 degree turn on the thrusters. The servo requires a 12 V power supply and pulse-width modulation (PWM) signal to control the position of the thrusters. For more information about PWM signal check Section 4.1.1.1, and for the servo check the digital appendix.

Mounting of the servos and motors is done by attaching them to brackets, which again are bolted onto a plate with Divinycell under it. Figure 3.7 shows how this is done. The Divinycell is necessary in order to reduce the vibrations from the hull and access for the screws.

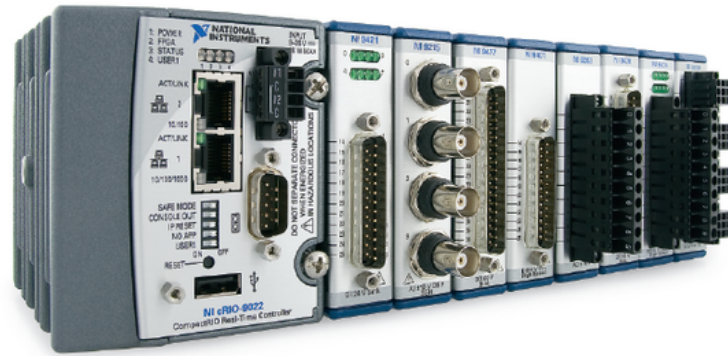


Figure 3.8: Example of a NI cRIO chassis with modules [Courtesy: National Instruments (2015)].

3.4 Embedded System

The embedded system consist of different parts to be working perfectly. These parts are described more specific in the following subsections.

3.4.1 National Instruments CompactRIO

The NI CompactRIO (cRIO) is a real-time embedded industrial controller made by National Instruments. An example of a controller can be seen in Figure 3.8. The CompactRIO is a combination of a real-time controller, reconfigurable I/O modules (RIO), field-programmable gate array (FPGA) module, and an Ethernet expansion chassis (National Instruments, 2015). The system runs real-time control systems programmed either in LabVIEW or Simulink code through the software NI VeriStand.

In this case for CSAD the cRIO is fitted with the following modules and chassis:

- The expansion chassis NI cRIO-9024
- The modules:
 - One NI 9474 Digital output
 - One NI 9215 Analog input
 - One NI-9871 Serial interface
 - Two NI 9237 Analog bridge
 - One NI 9411 Digital input
 - Two NI 9401 Bidirectional digital input

In this case a default FPGA personality is not sufficient enough due to the combination of modules in the chassis. So the FPGA personality file is made from scratch and will handle the inputs and outputs of the system.

3.4.2 Electronic Speed Controllers

O.S. OCA-150 50 A BL electronic speed controllers (ESCs) are fitted to control the DC motors driving the six thrusters. The ESC requires a 5 V power supply and a PWM signal to control the speed of the motor, in addition to the 12 V power supply required to run the motor. The PWM signal area is between 5 % and 10 % of the total signal length, where 5 % is full reverse, 7.5 % neutral and 10 % full forward. More information about PWM signals, see Section 4.1.1.1. More information on the ESC and its initialization procedure can be found in Appendix A.1.

3.4.3 Sixaxis Gamepad Controller

The Sixaxis is a widespread gamepad. It can transmit a broad range of input to the cRIO, and is suitable for human operator input. The device communicates over Bluetooth.

3.4.4 Raspberry Pi 2

To receive the signal from the Sixaxis controller the system is fitted with one Raspberry Pi 2 (RPi2). The RPi2 is a credit card-sized single-board computer including Ethernet and USB connections. In the laboratory setup, the unit is used to transmit the Sixaxis' data to the cRIO. The Sixaxis controller sends a Bluetooth signal to the RPi2, which again transfers the signal received to the cRIO by Ethernet cable.

3.4.5 Wi-Fi Bridge

The Wi-Fi bridge that is used in the CSAD, is the ASUS EA-N66. This device is use in bridge mode, not the other modes that the device is capable of, to communicate wireless with the computer that runs VeriStand. It is a very versatile device with powerful performance and exhilarating design.

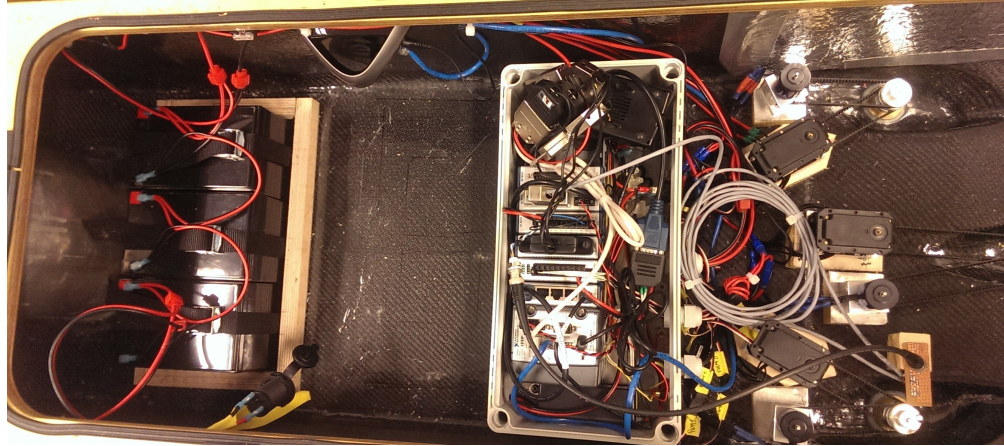


Figure 3.9: CSAD aft with (from the left) batteries, Wi-Fi bridge, watertight container and actuators..

3.4.6 Watertight Container with Equipment

Figure 3.9 shows how the electronic parts are positioned inside a watertight container. The box contains the following parts, CompactRIO, Raspberry Pi 2, the emergency switch and the power panel with an on/off switch. The watertight container is mounted to the hull using Velcro, and the cRIO parts are mounted with screws inside the box. The Wi-Fi bridge module is fitted onto the side of the vessel, with wiring going into the cRIO.

3.5 Inertial Measurement System

The vessel will be fitted with an IMU from Analog Devices, more specific the ADIS16364. The setup for the assembly is finished, but as the IMU is in use, this has not been fitted. This is an IMU that includes a triaxis gyroscope and triaxis accelerometer. The IMU can provide an accurate sensor measurement over a temperature range of -20°C to $+70^{\circ}\text{C}$. This gives a simple and cost-effective method to measure accelerations in different directions. The size of the unit is approximately 23 mm x 23 mm x 23 mm. To handle the signals from the IMU, a custom FPGA, made specific to the ADIS16364 IMU, is used to interpret the signals that the NI 9401 module receives.

3.6 Power

All vessels need a power source to operate. How this power source and the capacity was decided, are described in the following subsections.

3.6.1 Batteries

The system is powered from six 12 V 12 Ah lead batteries. Most of the equipment needs 12 V power, but there are some parts that need 5 V, such as the Raspberry Pi 2. These components are connected to either the USB outlet on the cRIO chassis or the 5 V outlet on cRIO modules.

3.6.1.1 Battery Requirements

The amount of batteries and electrical charges was found by checking the total current consumption on the desired operational time. Table 3.3 was used in this process.

Table 3.3: Power consumption calculations

Part	Units	Max ampere/unit [A]	Total ampere [A]	Voltage [V]	Power [W]	Total power [W]
Servo	7	5.2	36.4	12	62.4	436.8
Motor	6	18	108	12	216	1296
cRIO	1	5	5	12	60	60
Raspberry Pi 2	1	0.8	0.8	5	4	4
ESC	6	2	12	12	24	144
			162.2			1940.8

This shows the maximum consumptions of the different parts. In a true loading condition, it will not be the case that all of the parts will run at maximum power, thus, the batteries are not scaled for this. For 30 min - 1 hour of operating time, it is sufficient with approximately half the maximum capacity. The resulting even number of batteries and ampere hours is then 6x12 Ah batteries.

3.6.1.2 Assembly

The batteries need to be fixed at the location they are placed. To ensure this, the batteries are mounted by using a mounting bracket with straps over the batteries. This will provide a safe and durable solution, which will keep the batteries in place and avoid any damage to them. In Figure 3.11 one of the mounting bracket is shown, and Figure 3.10 shows the placement of the batteries before installing the brackets. Three batteries are contained in each of the brackets. To reduce vibration on the batteries, there are placed Divinycell foam underneath each battery.

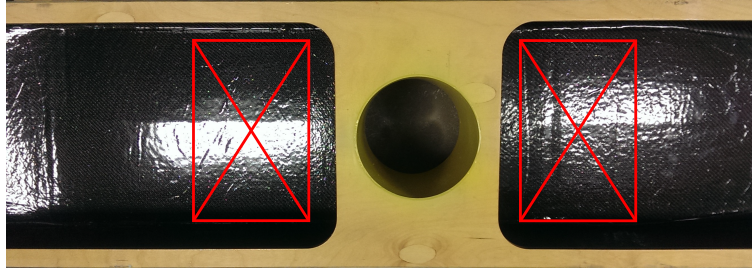


Figure 3.10: The approximate mounting place for the brackets containing the batteries.

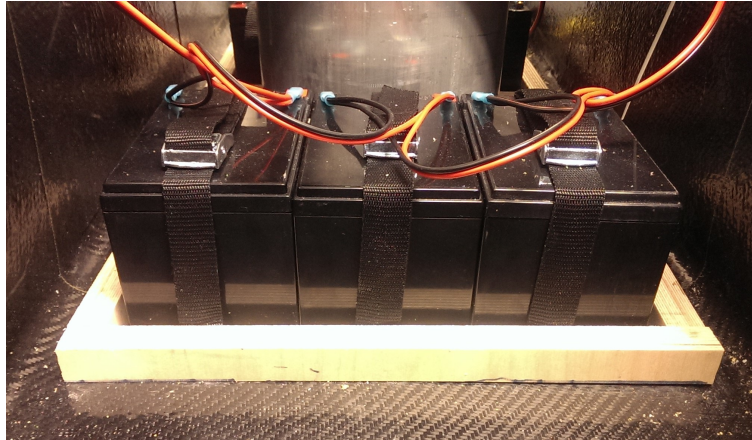


Figure 3.11: How the batteries are mounted in the brackets with straps.

3.6.2 Power Panel

In order to keep track of the power circuit the vessel is fitted with on/off switches, fuses, low voltage indicator, charging connection and a wireless emergency switch. This wireless switch uses radio frequency to control the system on and off if necessary, and it will work up to 100 meters in clear sight. This power panel has been fitted to the side of the watertight box.

3.6.3 Distribution

The power system consist of a 12 V grid. The grid is marked as a red line throughout the Figures 3.12, 3.13 and 3.14. A second grid is a 5 V grid, which powers the Raspberry Pi 2, is marked green in the same figures. In addition to this, the model is fitted with a power panel that has a 25 A fuse. This is to ensure that the system parts would not get broken if a higher current enters the grid.

Another representation of the power system can be seen in Figure 3.15, as a power single line diagram.

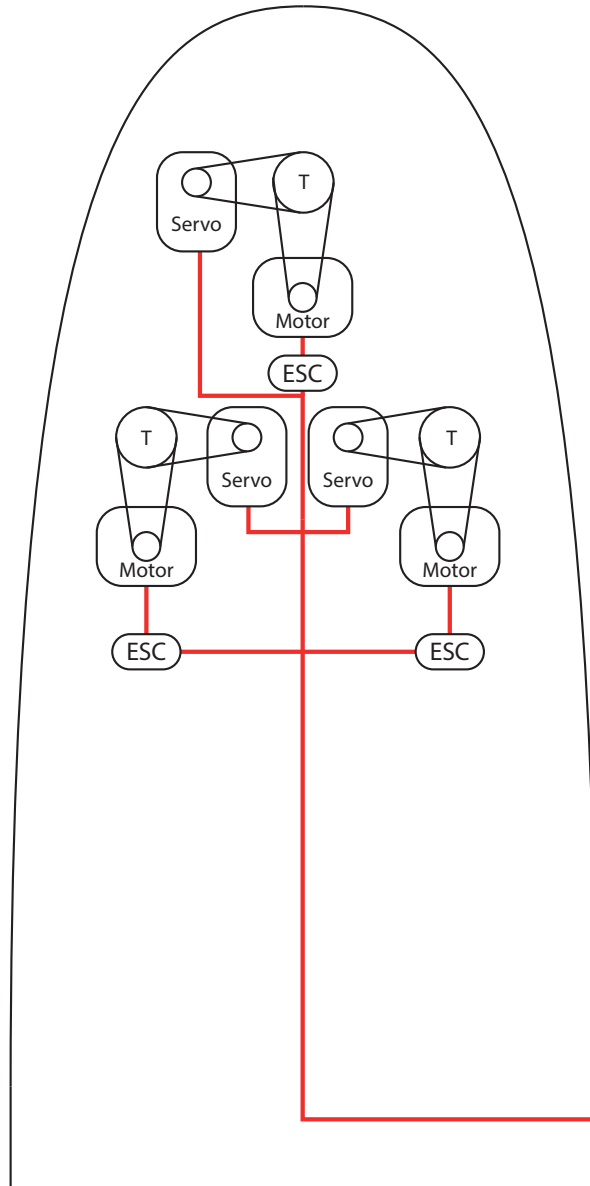


Figure 3.12: CSAD power system, bow.

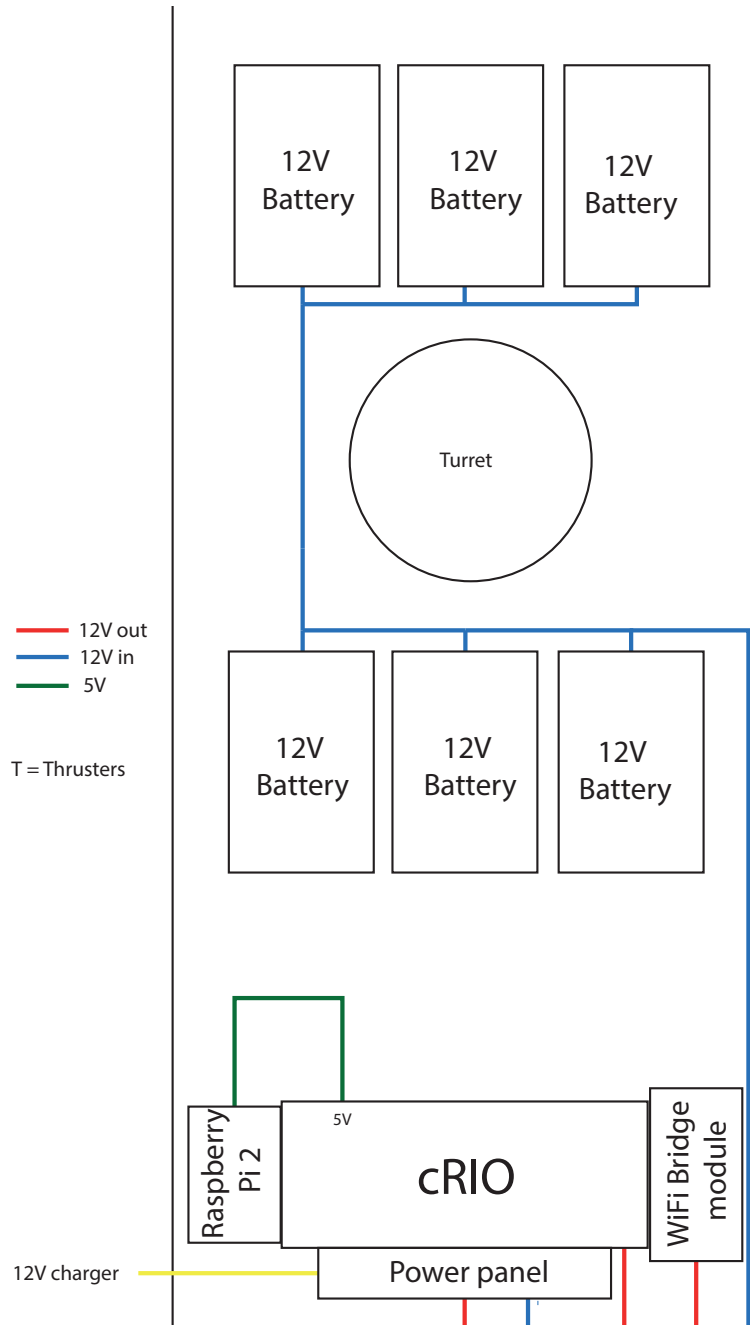


Figure 3.13: CSAD power system, midship.

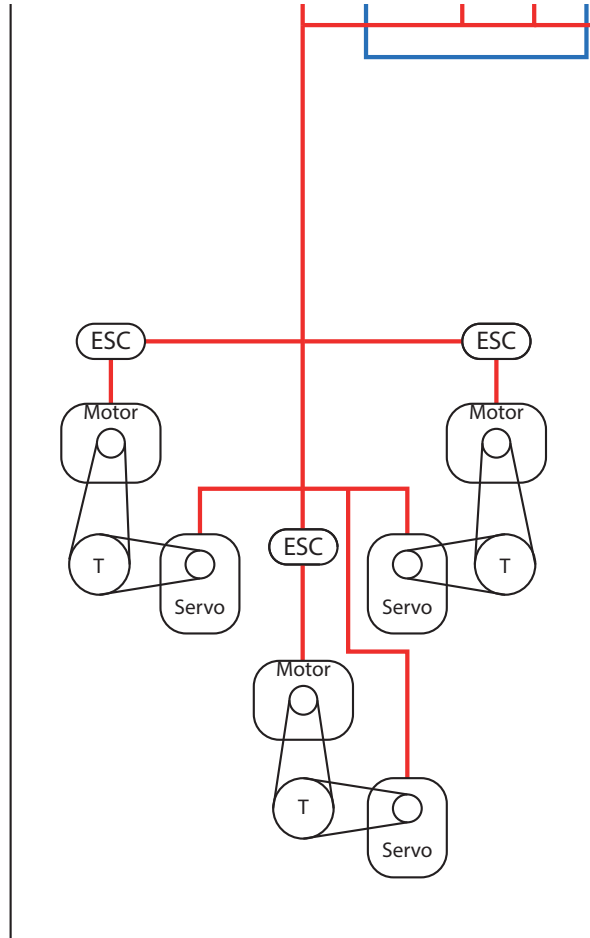


Figure 3.14: CSAD power system, aft.

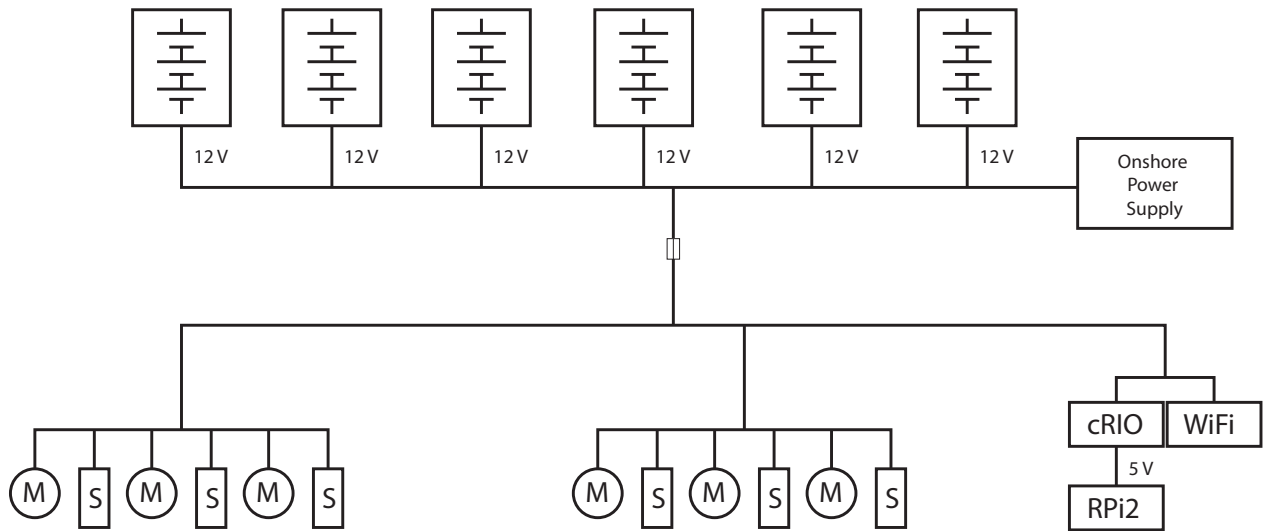
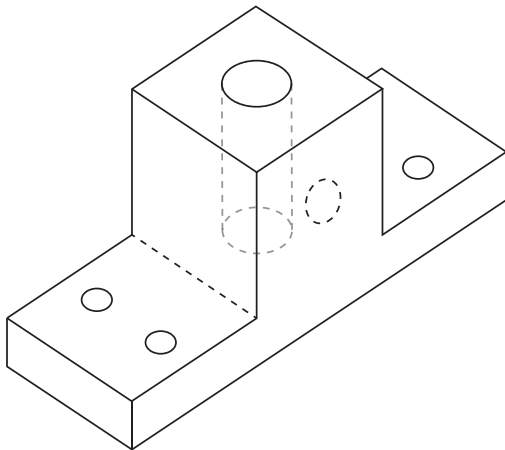


Figure 3.15: Single line diagram of the power system.



(a) Bracket design.



(b) Rod with reflector spheroid.

Figure 3.16: The reflector spheroid for the Qualisys system.

3.7 Qualisys Reflectors

To get the position of the vessel it is necessary to fit reflector spheroids on the vessel. This was done by fabricating a bracket and a rod to hold the reflector spheroids. In Figure 3.16a and 3.16b the bracket design and final result are shown. The rods are cut into different length; 10 cm, 20 cm, 30 cm and 40 cm. This is done so the Qualisys system detects the vessel faster, by creating different triangles.



(a) At land.



(b) In water.

Figure 3.17: The finished model vessel.

3.8 Summary

In Figure 3.17 the finished model vessel is shown, and all the parts that are fitted onto the exterior of the hull can be seen. The other parts inside are, as mentioned, shielded with a watertight lid. How to operate the CSAD is explained in Appendix A.2.

The following list includes which items in the requirements specification, Chapter 2, that have been fulfilled or not.

- Turret:
 - Can freely rotate, but cannot force rotation.
 - Not possible to connect a riser in the center.
 - Possible to connect a maximum of 8 mooring lines, but can be further increased.

- Measurements:
 - It is possible to measure all of the desired elements, when the IMU is put in.
- Actuators:
 - All actuators fulfill the requirements.
- Practical:
 - The hull is water proof. It will allow splashing, but not submerging the vessel under water.
 - The vessel is fitted with an emergency switch to cut the power supply the cRIO and thrusters.

To recap, some elements are still to be done, and are as following:

- Fix the turret such that it is possible to force rotation in addition to have it freely rotating.
- Make it possible to connect a riser in the center if the turret.
- Put in the IMU, when it is not used in other experiments.

Chapter 4

Control System Design

4.1 System Diagrams

In this section the communication signal/network information flow are presented. In addition to the CompactRIO software topology.

4.1.1 Communication

The communication signals and network flow for the model consist of different types of signals that are required to run the system. These signals with descriptions can be seen in Figures 4.1, 4.2 and 4.3.

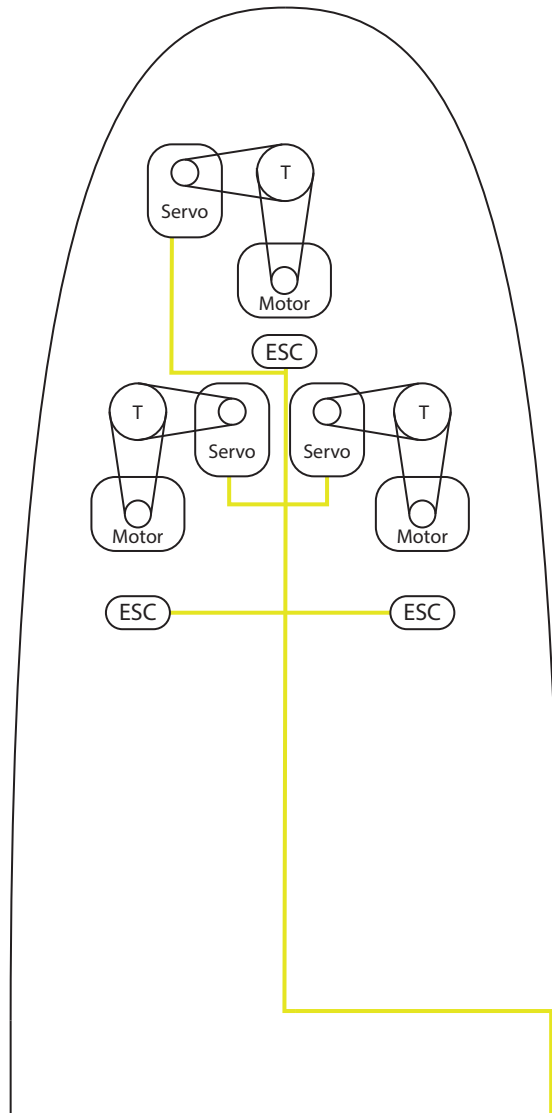


Figure 4.1: The communication signal/network information flow, bow.

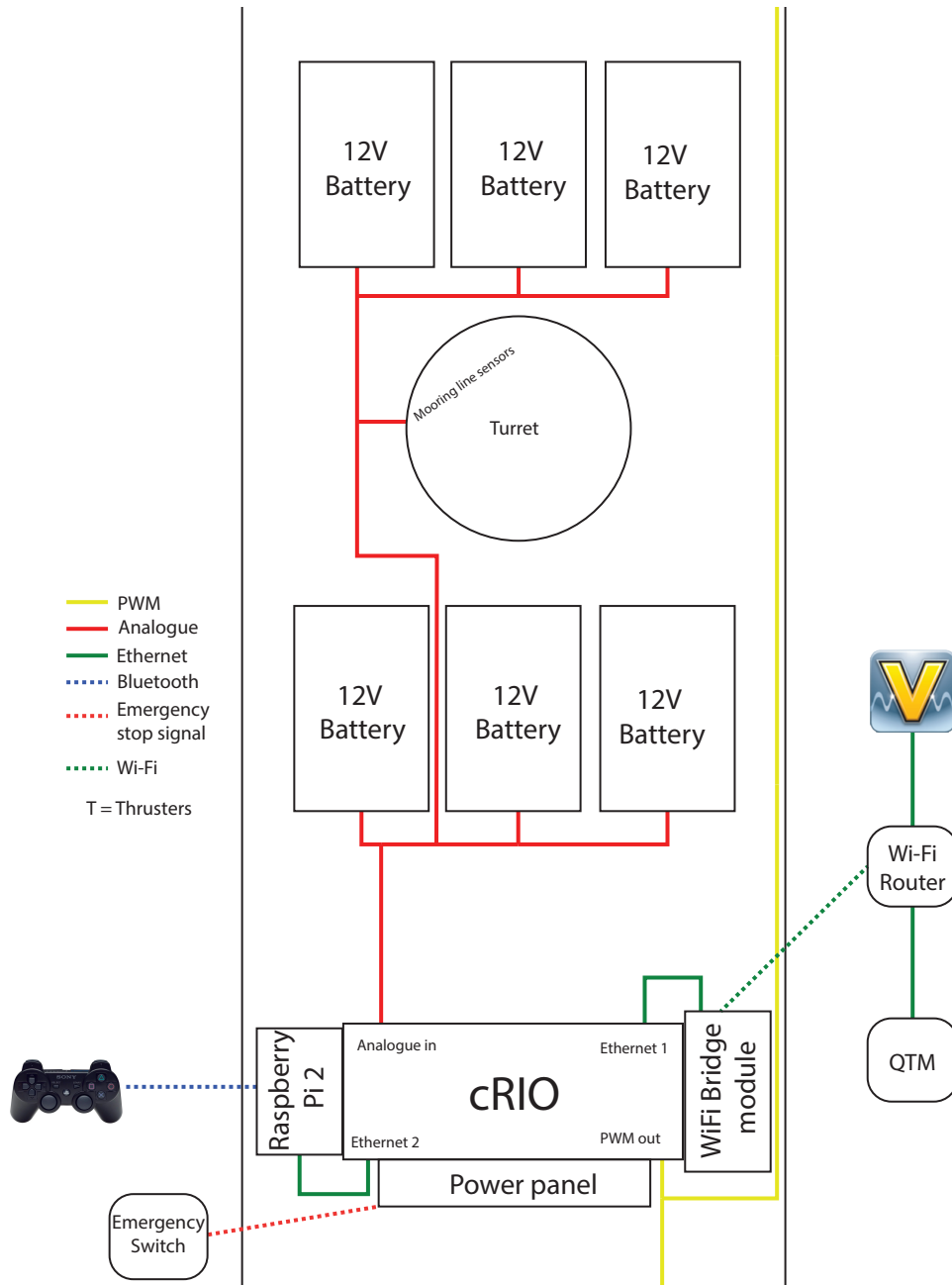


Figure 4.2: The communication signal/network information flow, midship.

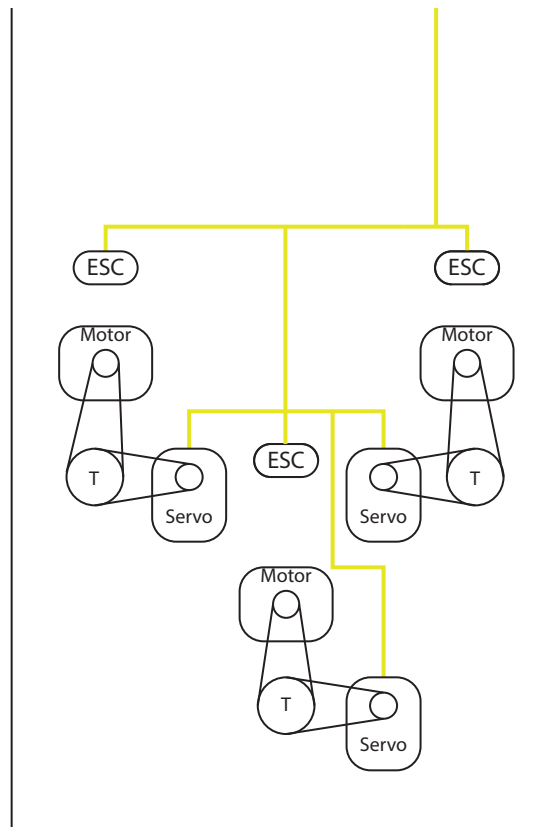


Figure 4.3: The communication signal/network information flow, aft.

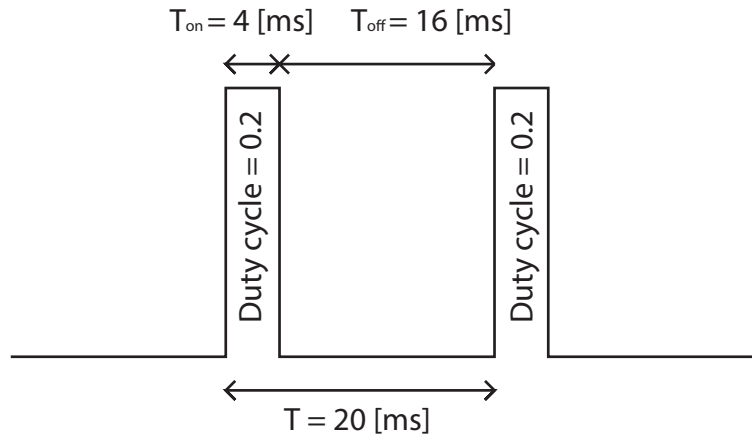


Figure 4.4: Example of PWM signal with frequency = 50 Hz and duty cycle = 0.2.

4.1.1.1 Pulse-Width Modulation

A pulse-width modulation (PWM) signal consists of a frequency cycle and a duty cycle. The frequency used in this thesis for the ESCs is set to constant 50 Hz. The only parameter controlled is the duty cycle, in the range of $[0, 1]$, in order to generate the PWM signal. The duty cycle indicates, when the signal is "on" for the period. An example of this is that if the duty cycle is 0.2 it will mean that the signal is "on" for 20 % of the period. This is illustrated in Figure 4.4. On the servo, the delivery of this PWM signal is a bit different. The PWM signal comes from the cRIO through a RS-485 protocol, which is a multi-drop protocol so that one can communicate with several units on the same line.

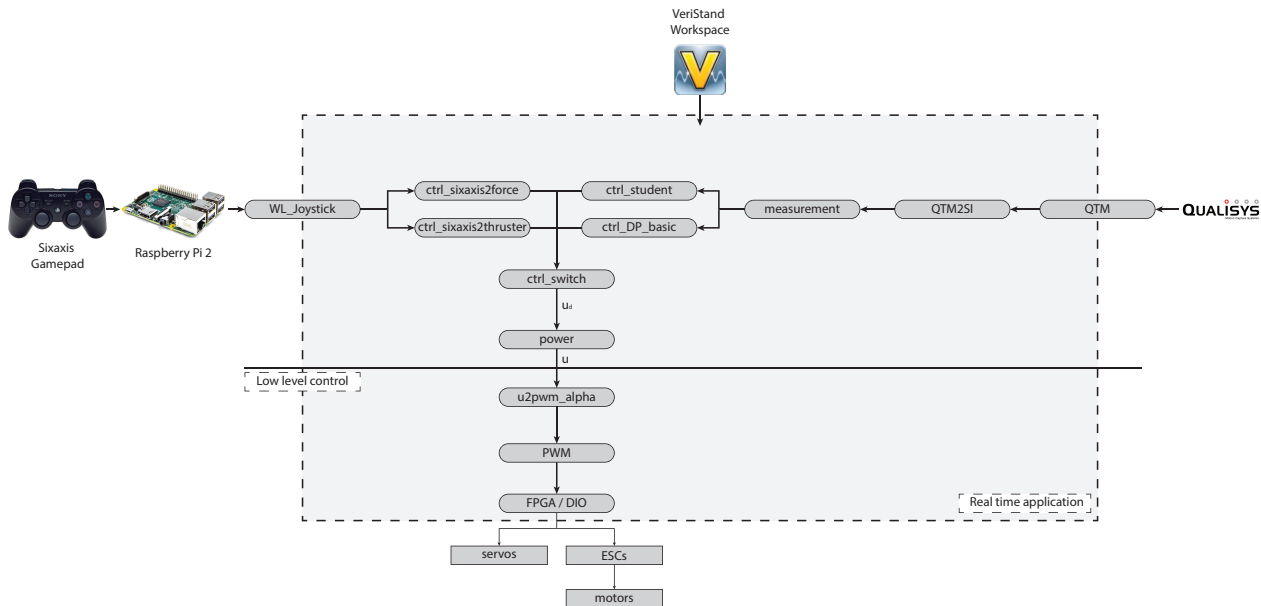






Figure 4.5: Software topology for the CompactRIO.

4.1.2 CompactRIO Software Topology

To control the vessel the CompactRIO must have a software which routes the signals to the correct destinations. Figure 4.5 contains how these signals are routed.

The switching logic between the different controllers is explained in Figure 4.6, where the symbols in the switch corresponds to the symbols on the Sixaxis controller. A more detailed view on these controllers are given in Table 4.1.

Table 4.1: Generic control modes.

Sixaxis	Control modes
	Individual actuator control Max force: up and down arrows Left joystick: front thrusters Right joystick: aft thrusters
	Generalized force control Max force: up and down arrows Left joystick: surge and sway forces L2/R2: yaw moment
	Basic dynamic positioning (DP) Setpoint: user interface Gains: user interface
	Student controller User implemented controller

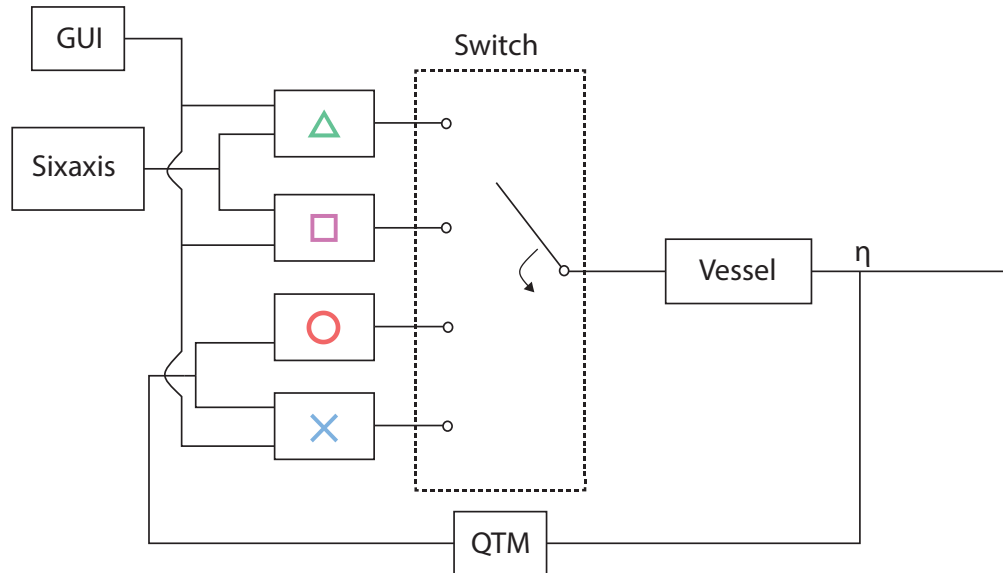


Figure 4.6: The switching logic between the different controllers.

The necessary control functions in Section 4.3 are either operated by the Sixaxis controller, with its manual control functions, or by VeriStand, with its automatic positioning system. The input from the different controllers defines how the vessel should respond to a command given by the Sixaxis controller or the automatic controller.

For implementation of navigation, guidance and control algorithms, the block called `ctrl_student` in the detailed figure of the software topology can be used. The inputs in these blocks, are 3 DOF position, quality and error in the measurement of the position. Outputs are the desired force and angle of the different thrusters. Thus, this control algorithm must contain a thrust allocation to give the optimal values to the different thrusters.

4.2 Low Level Control

The high level control signals from the controller need to be interpreted correctly, since it gives out normalized thrust and angle for each thruster, $\mathbf{u} = [u_1, \dots, u_6, \alpha_1, \dots, \alpha_6]$. A mapping from normalized to physical thrust and angle is required. The term for this is low level control, and in the following sections the various signal mappings are explained. Due to the open loop property of the control system, mapping from the desired force and angle to a PWM signal is required. This mapping must be well defined in order to give an accurate responds. How this is done and the outcome of it are explained in Frederich (2016).

4.2.1 ESC Calibration

In order to calibrate the electronic speed controller, the range where it operates must be identified. The normal range where ESCs operate is between 5 % and 10 % of the full signal, and this was also the case with these ESCs. As mentioned in Section 4.1.1.1 the signal consists of a frequency and a duty cycle. For these ESCs the frequency is set to a constant of 50 Hz, which gives a period of 20 ms. cRIO FPGA PWM output frequencies are given in terms of FPGA clock pulses, also known as ticks. Since the embedded controller frequency is 40 MHz, a 50 Hz PWM signal has a period of 4.1.

$$\frac{40 \text{ MHz}}{50 \text{ Hz}} = \frac{40 \cdot 10^6}{50} = 800\,000 \text{ tick.} \quad (4.1)$$

Table 4.2: Current calibration of ECSs.

Direction	Signal range PWM	Tick
Full reverse	5 [%]	40 000
Neutral	7.5 [%]	60 000
Full forward	10 [%]	80 000

The rotational direction for the PWM signal range were found to be as in Table 4.2. For more specific on how to calibrate the ESCs, see the manual in Appendix A.1.

4.2.2 Servo Calibration

To make sure that the thrusters are positioned in neutral position when not commanded to otherwise, it is necessary to calibrate the angle. Neutral position is when the thrusters are pointing in negative direction along the x-axis of the body-fixed coordinate system. Since all commands to the servos are in degrees it is easy to set the neutral position angle. This was done by making two straight lines on a piece of paper so that they forms a right angle, see Figure 4.7, and rotate the thrusters until they line up with the straight lines on the paper.

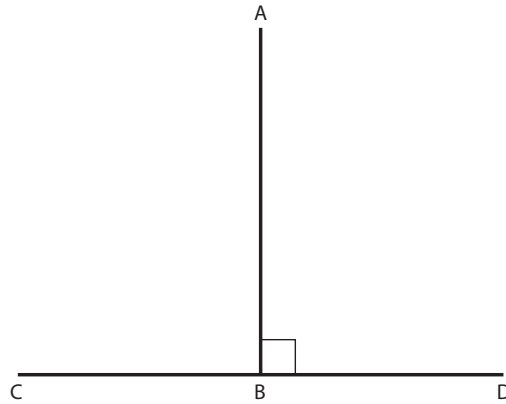


Figure 4.7: A line segment (AB) drawn so that it forms right angles with a line (CD).

Table 4.3: Defined neutral angles for the thruster.

Thruster angle	Neutral position
α_1	-165
α_2	-154
α_3	-147
α_4	-8
α_5	165
α_6	-12

From this the neutral angle of all servos were found, these values can be seen in Table 4.3. For all servos the maximum and minimum rotation angle is defined by:

$$\alpha = [\alpha_1, \alpha_2, \alpha_3, \alpha_4, \alpha_5, \alpha_6] \in [-10242, 10240]. \quad (4.2)$$

The angle measurements that are returned from the servos are given in the range from $\alpha_{\text{signed}} = [0, 32768]$, so these values have to be converted to degrees. By using signed number representation conversion the correct values in degrees are found, the minimum and maximum value range is given in Table 4.4.

Table 4.4: Signed number representations conversion.

	Value	Degree
Maximum	14335	10240
Zero	0 / 32768	0
Minimum	18433	-10242

4.2.3 Control Input to Actuator Signals

The block `u2pwm_alpha` handles the correct mapping from the control input signals to the PWM signals sent to the motors and servos. The inputs to the block consists of two vectors; the desired PWM signal from the thrust allocation and the desired thruster angle (Frederich, 2016):

$$\mathbf{PWM}_{in} = [PWM_{1in}, PWM_{2in}, PWM_{3in}, PWM_{4in}, PWM_{5in}, PWM_{6in}]. \quad (4.3)$$

$$\boldsymbol{\alpha}_{in} = [\alpha_{1in}, \alpha_{2in}, \alpha_{3in}, \alpha_{4in}, \alpha_{5in}, \alpha_{6in}] \in [-180, 180]. \quad (4.4)$$

For the PWM signals, the $PWM_{in} = 0$ is mapped so that it corresponds to the neutral signal out. Higher PWM signals are mapped in the range neutral to full forward, and lower PWM signals are mapped in the range neutral to full backwards.

Regarding the thruster angles, they are mapped so that they take the shortest route to the desired angle. An example of this: if $\alpha_{commanded} = -160^\circ$ and $\alpha_{current} = 150^\circ$, then the shortest way becomes $\alpha_{desired} = -200^\circ$, since the difference is only 50° instead of 310° . By including this, the thrusters can operate more efficiently.

Note: If one of the thrusters reach maximum angle, see (4.2), then this thruster needs to return to neutral position, see Table 4.3. If possible, if one reaches maximum rotate all thrusters back to neutral position.

4.3 Necessary Control Functions

Some of the controllers that are implemented are the basic controllers. These are controllers for manual thruster command, motion command and automatic control functions. The last one, the automatic controller, will be a controller design by the user. This controller will then perform the desired tasks set by the user. The different controllers and how the implementation of these is done can be seen in Figure 4.5.

4.3.1 Individual Actuator Control

This controller uses the input from the Sixaxis controller to directly control the individual thrust vectors

$$\mathbf{u} = [u_1, u_2, \dots, u_n]^T = \mathbf{u}_{\text{cmd}}. \quad (4.5)$$

To make it easier to control, the three thruster in the bow are mapped together like this: left joystick $\rightarrow u \rightarrow [u_1, u_2, u_3, \alpha_1, \alpha_2, \alpha_3]$. The same for the three in the aft, but with the right joystick.

4.3.2 Generalized Force Control

Generalized force control uses thrust allocation to enable the user to command motions of the fully actuated vehicle without the need to consider individual thruster settings. These motions can be commanded relative to different reference frames, body-frame, basin-frame and user-frame. These controllers are defined as in the following subsections (Skjetne, 2015).

The relationship between the different control motion frames are given in Figure 4.8. The following list explains these relationships:

- The basin-fixed frame {Basin} is located at mean sea-level with x-axis pointing longitudinal, y-axis transversal and z-axis downwards. The origin is defined as Field Zero Point (FZP) located in the center of the turret when no environmental loads act on the vessel.
- The body-fixed frame {Body} is fixed to the vessel body with the origin located in vessel origin (VO) of the hull. With x-axis positive forward, y-axis positive towards starboard and z-axis positive downwards.
- The user-fixed frame {User} is fixed to the user with the origin located in the user origin and rotated an angle ψ_{user} relative to the basin x-axis. With x-axis pointing forwards, y-axis right and z-axis downwards.

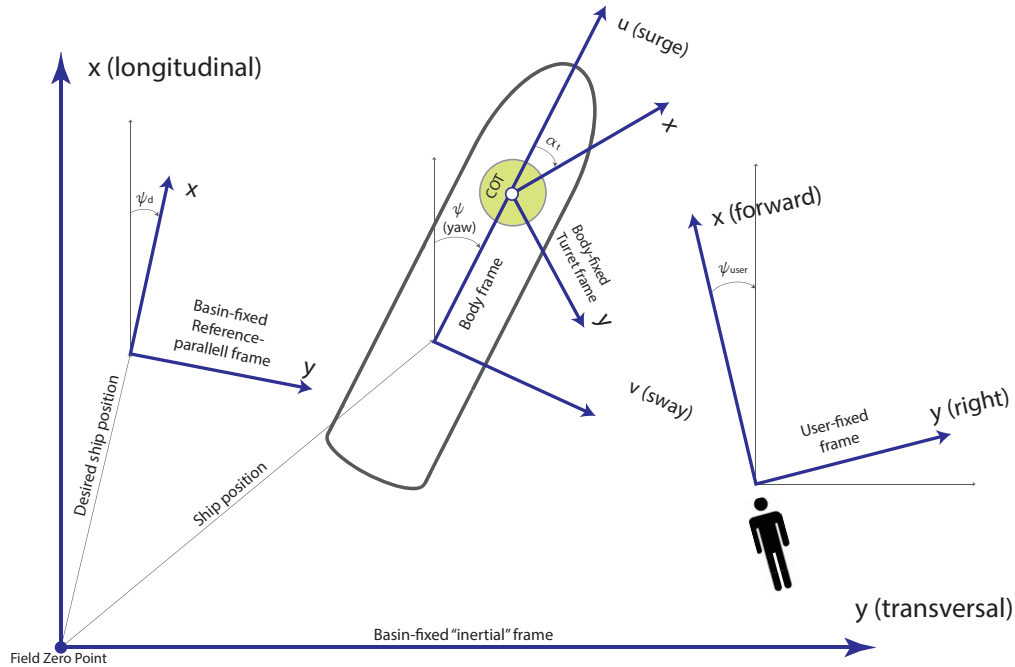


Figure 4.8: Definition of the different control reference frames. [Adapted from: Skjetne (2014)]

Thrust allocation is not covered in this thesis, for further information about this see Frederich (2016).

4.3.2.1 Body-Relative Motion

This controller uses the input from the device to command the generalized body-relative thrust vector $\boldsymbol{\tau}$

$$\boldsymbol{\tau} = [X, Y, N]^T = \boldsymbol{\tau}_{\text{cmd}}, \quad (4.6)$$

where X is the total thrust force in surge, Y in sway and N is the yaw moment. Then it uses thrust allocation to calculate the corresponding individual commanded thrust vectors

$$\mathbf{u}_{\text{cmd}} = \mathbf{B}(\boldsymbol{\alpha})^\dagger \boldsymbol{\tau}_{\text{cmd}}, \quad (4.7)$$

where $\mathbf{B}(\boldsymbol{\alpha})^\dagger$ is the pseudo inverse of the input matrix.

4.3.2.2 Basin-Relative Motion

This controller uses the input from the device to command the generalized basin-relative thrust vector $\boldsymbol{\tau}_{\text{cmd}}^{\text{Basin}}$. By knowing the orientation vector of the vessel we can use basin to Body transfor-

mation and calculate the corresponding body-fixed thrust vector

$$\boldsymbol{\tau}_{\text{cmd}}^{\text{Body}} = \mathbf{J}(\theta)^{-1} \boldsymbol{\tau}_{\text{cmd}}^{\text{Basin}}. \quad (4.8)$$

The individual commanded thrust vectors can then be obtained by use of thrust allocation.

$$\mathbf{u}_{\text{cmd}} = \mathbf{B}(\boldsymbol{\alpha})^\dagger \boldsymbol{\tau}_{\text{cmd}}^{\text{Body}} = \mathbf{B}(\boldsymbol{\alpha})^\dagger \mathbf{J}(\theta)^{-1} \boldsymbol{\tau}_{\text{cmd}}^{\text{Basin}}, \quad (4.9)$$

where $\mathbf{B}(\boldsymbol{\alpha})^\dagger$ is the pseudo inverse of the input matrix.

4.3.2.3 User-Relative Motion

The user-relative controller uses the input from the device to command the generalized user-relative thrust vector $\boldsymbol{\tau}_{\text{cmd}}^{\text{User}}$. By knowing the orientation vector of the user we can use transformation and calculate the corresponding body-fixed thrust vector as following:

$$\boldsymbol{\tau}_{\text{cmd}}^{\text{Basin}} = \mathbf{J}(\theta_{\text{User}}) \boldsymbol{\tau}_{\text{cmd}}^{\text{User}}, \quad (4.10)$$

then, by using the orientation θ of the vessel, we can use Basin-Body transformation to get the body-fixed thrust vector:

$$\boldsymbol{\tau}_{\text{cmd}}^{\text{Body}} = \mathbf{J}(\theta)^{-1} \boldsymbol{\tau}_{\text{cmd}}^{\text{Basin}} = \mathbf{J}(\theta)^{-1} \mathbf{J}(\theta_{\text{User}}) \boldsymbol{\tau}_{\text{cmd}}^{\text{User}}. \quad (4.11)$$

Finally, the thrust vector for the individual thruster can be allocated:

$$\mathbf{u}_{\text{cmd}} = \mathbf{B}(\boldsymbol{\alpha})^\dagger \boldsymbol{\tau}_{\text{cmd}}^{\text{Body}} = \mathbf{B}(\boldsymbol{\alpha})^\dagger \mathbf{J}(\theta)^{-1} \mathbf{J}(\theta_{\text{User}}) \boldsymbol{\tau}_{\text{cmd}}^{\text{User}}, \quad (4.12)$$

where $\mathbf{B}(\boldsymbol{\alpha})^\dagger$ is the pseudo inverse of the input matrix.

4.3.3 Automatic Control

The automatic control functions, that are initially implemented, are AutoPos: Automatic control of (x, y) , AutoHead: Automatic control of (ψ) . For this thesis, the automatic control functions are expanded with a setpoint chasing algorithm and other TAPM control modes that are normally used in TAPM systems.

4.4 Human-Machine Interface Functions and Layout

As presented in Section 2.5 there is need of an HMI, the following list includes the functions that are implemented to support the operator:

- Which control mode is in use and a switch to change modes
- Thrust usage and angle of the thrusters
- Voltage indicator from the batteries
- Position and heading in the basin
- A description of the wireless controller functions
- Indicators that describes what is done on the wireless controller
- Mooring line tensions
- Error messages
- Other functions that can be useful for the operator to know

The layout for these functions are easy to follow and easy to use. This layout was designed when the model was fitted with all the necessary equipment and controlled that the entire system was working together. In Figure 4.9 and 4.10, are two examples on how the Veristand HMI can look like.

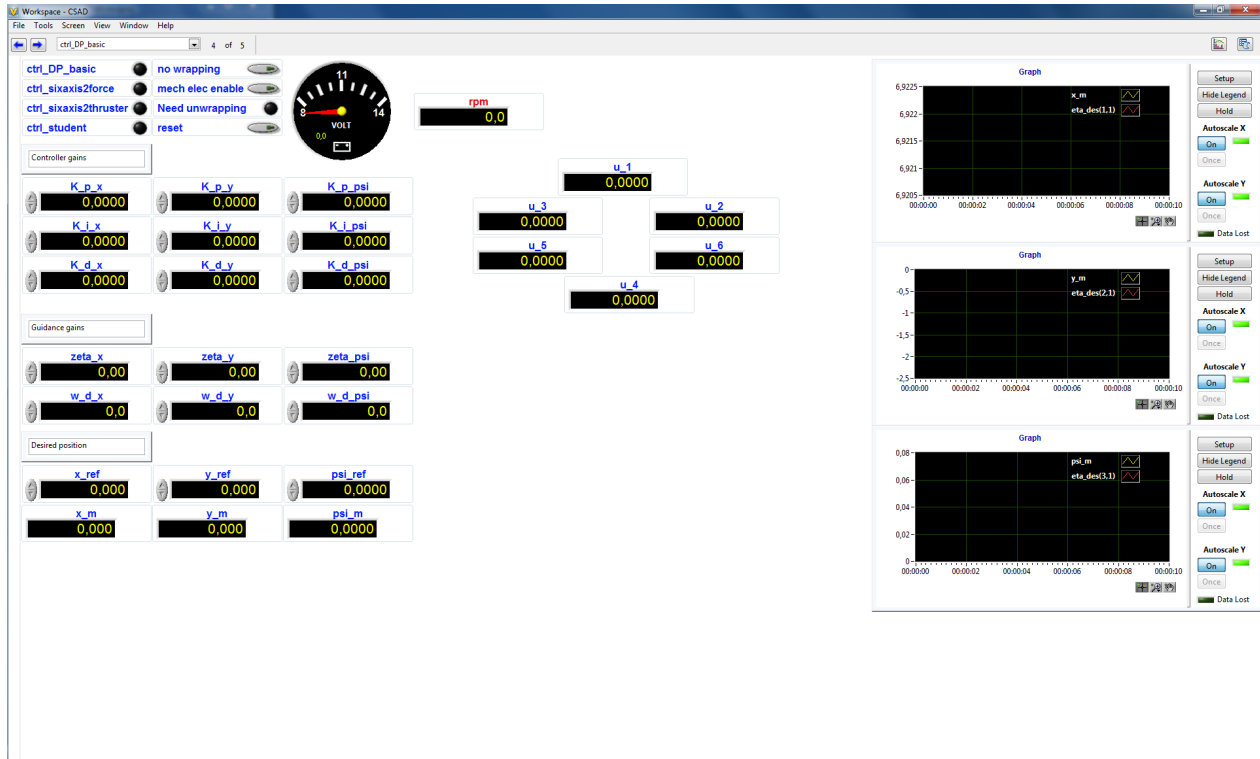


Figure 4.9: The current HMI for the basic DP controller.

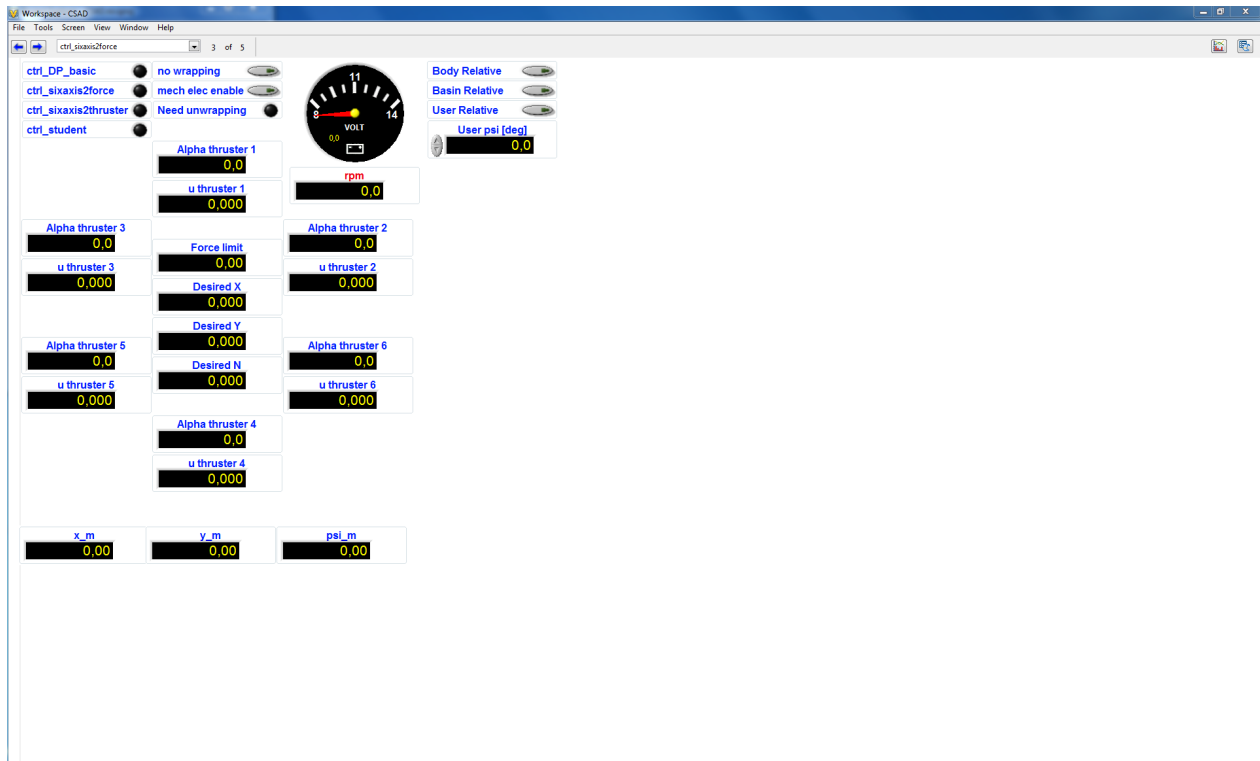


Figure 4.10: The current HMI for the the generalized force controller.

Chapter 5

Mathematical Modeling

5.1 Dynamics

By using the proposed notations and reference frames in Strand et al. (1998) the kinematics and kinetics for a TAPM vessel can be described as shown in the following subsections.

5.1.1 Kinematics

There are four different reference frames used in thruster-assisted position mooring, as illustrated in Figure 5.1.

- The earth-fixed frame {E} is located at mean sea-level with x-axis pointing north (N), y-axis east (E) and z-axis downwards (D). The origin is defined as Field Zero Point (FZP) located in the center of the turret when no environmental loads act on the vessel. The earth-fixed frame is in this thesis represented by the Basin-fixed frame.
- The reference-parallel frame {D} is the basin-fixed reference frame rotated to the desired heading angle ψ_d and origin in the desired (x_d, y_d) position. The desired position vector is the represented with $\boldsymbol{\eta}_d = [x_d, y_d, \psi_d]^\top$.
- The body-fixed frame {B} is fixed to the vessel body with the origin located in vessel origin (VO) of the hull. With x-axis positive forward, y-axis positive towards starboard and z-axis positive downwards.
- The turret-fixed frame {T} is fixed to the turret with the origin located in the center of the turret (COT) and rotated an angle α_t relative to the body x-axis.

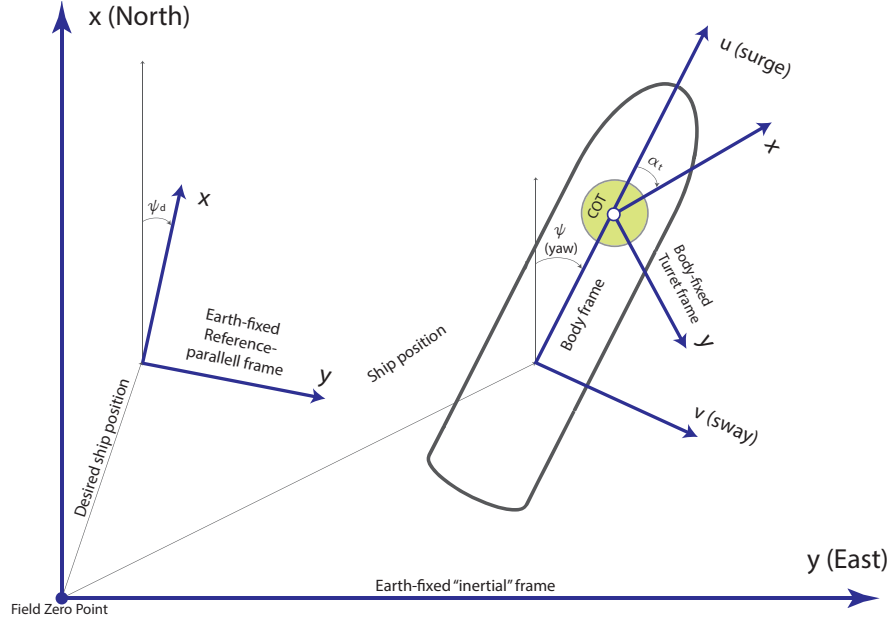


Figure 5.1: Definition of the different reference frames [Adapted from: Skjetne (2014)].

The linear and angular velocities of the vessel in body-fixed are related to the earth-fixed frame by transformation:

$$\dot{\boldsymbol{\eta}} = \mathbf{J}(\boldsymbol{\eta})\mathbf{v} \quad (5.1)$$

where earth-fixed positions and body-fixed velocities are defined by $\boldsymbol{\eta} = [x, y, z, \phi, \theta, \psi]^\top$ and $\mathbf{v} = [u, v, w, p, q, r]^\top$ respectively. The transformation matrix $\mathbf{J}(\boldsymbol{\eta})$ is given by:

$$\mathbf{J}(\boldsymbol{\eta}) = \begin{bmatrix} \mathbf{J}_1(\boldsymbol{\eta}) & \mathbf{0} \\ \mathbf{0} & \mathbf{J}_2(\boldsymbol{\eta}) \end{bmatrix}, \quad (5.2)$$

$$\mathbf{J}_1(\boldsymbol{\eta}) = \begin{bmatrix} c\psi c\theta & -s\phi + c\theta + c\phi s\theta s\phi & s\psi s\phi + c\psi c\phi s\theta \\ s\psi c\theta & c\psi c\phi + s\phi s\theta s\psi & -c\psi s\phi + s\theta s\psi c\phi \\ -s\theta & c\theta s\phi & c\theta c\phi \end{bmatrix}, \quad (5.3)$$

$$\mathbf{J}_2(\boldsymbol{\eta}) = \begin{bmatrix} 1 & s\phi t\theta & c\phi t\theta \\ 0 & c\phi & -s\phi \\ 0 & s\phi/c\theta & c\phi/c\theta \end{bmatrix}, \quad (5.4)$$

where $s = \sin$; $c = \cos$; $t = \tan$.

5.1.2 Kinetics

The motion of a marine vessel is divided into two different dynamics; the low-frequency (LF) model and the wave-frequency (WF) model. These two models are combined through superposition. The details of the full 6 DOF model can be found in Fossen (2011).

From Fossen (2011) the LF model for a moored vessel is given by:

$$\mathbf{M}_{RB}\dot{\mathbf{v}} + \mathbf{M}_A\dot{\mathbf{v}} + \mathbf{C}_{RB}(\mathbf{v})\mathbf{v} + \mathbf{C}_A(\mathbf{v}_r)\mathbf{v}_r + \mathbf{D}(\mathbf{v}_r)\mathbf{v}_r = \boldsymbol{\tau}_{env} + \boldsymbol{\tau}_{moor} + \boldsymbol{\tau}_{thr}, \quad (5.5)$$

where \mathbf{M}_{RB} is the mass matrix, \mathbf{M}_A is added mass matrix, \mathbf{C}_{RB} and \mathbf{C}_A are Coriolis and centripetal force matrices. \mathbf{v}_r is the relative speed between the vessel and the water, which means that current is taken into account. $\mathbf{D}\mathbf{v}_r$ is damping force function and $\boldsymbol{\tau}_{env} = \boldsymbol{\tau}_{wind} + \boldsymbol{\tau}_{wave2}$ are the wind loads and 2nd order wave drift loads respectively.

Since this is a low-speed control situation, we can neglect the Coriolis and centripetal terms because they are very small. Also, the non-linear parts of the damping term can be disregarded, due to the fact that they are connected to higher order velocity-terms. Since we are using a simplified model, there might be some uncertainties and other changes not accounted for. By adding a bias model and removing $\boldsymbol{\tau}_{wind}$, the uncertainties are accounted for. The influence of the wind is removed, because it is not implemented in the model. Then, end up with the following LF control model:

$$\dot{\boldsymbol{\eta}} = \mathbf{J}(\boldsymbol{\eta})\mathbf{v}, \quad (5.6)$$

$$\dot{\mathbf{b}} = -\mathbf{T}_b\mathbf{b} + w_b, \quad (5.7)$$

$$\mathbf{M}\dot{\mathbf{v}} + \mathbf{D}_{lin}\mathbf{v} = \mathbf{J}(\boldsymbol{\eta})^\top\mathbf{b} + \boldsymbol{\tau}_{moor} + \boldsymbol{\tau}_{thr}, \quad (5.8)$$

where the bias force is $\mathbf{J}(\boldsymbol{\eta})^\top\mathbf{b} \approx \mathbf{D}_{lin}\mathbf{v}_c + \boldsymbol{\tau}_{wave2}$ and $\boldsymbol{\tau}_{moor} = \mathbf{G}_{mo} + \mathbf{D}_{mo}$. Describing the restoring and damping terms respectively.

5.1.2.1 Mooring Line Forces

The simplest of the mooring models is the linear model, where the assumption is, that the mooring force has a linear relation to the horizontal displacement. The linear mooring model force is then given by:

$$\boldsymbol{\tau}_{moor} = -\mathbf{J}^\top(\boldsymbol{\eta})\mathbf{G}_{mo}(\boldsymbol{\eta} - \boldsymbol{\eta}_0) - \mathbf{D}_{mo}\mathbf{v}, \quad (5.9)$$

where $\boldsymbol{\eta} \in \mathbb{R}^6$ is the position and $\boldsymbol{\eta}_0 \in \mathbb{R}^6$ is the equilibrium position where both is in Earth-fixed frame, and $\mathbf{v} \in \mathbb{R}^6$ is the velocities in body-fixed frame. The matrices \mathbf{G}_{mo} and \mathbf{D}_{mo} are the linearized mooring stiffness and damping respectively, and it is assumed that they only act in

the horizontal plane, such that:

$$\mathbf{G}_{mo} = \left. \frac{\partial \mathbf{g}_{mo}}{\partial \boldsymbol{\eta}} \right|_{\boldsymbol{\eta}=\boldsymbol{\eta}_0}, \quad (5.10)$$

$$\mathbf{D}_{mo} = \left. \frac{\partial \mathbf{d}_{mo}}{\partial \mathbf{v}} \right|_{\mathbf{v}=\mathbf{v}_0}, \quad (5.11)$$

where \mathbf{G}_{mo} in symmetric cases is zero, but can however, due to line breakage, be non zero. \mathbf{G}_{mo} can be formulated as

$$\mathbf{G}_{mo} = \mathbf{T}(\boldsymbol{\beta})\mathbf{L}_p\boldsymbol{\tau}_H, \quad (5.12)$$

where $\boldsymbol{\tau}_H$ is the horizontal component of the tension and \mathbf{L}_p is a diagonal coefficient matrix denoting the line breakage information. The mooring line configuration matrix is given by

$$\mathbf{T}(\boldsymbol{\beta}) = \begin{bmatrix} \cos \beta_1 & \cdots & \cos \beta_n \\ \sin \beta_1 & \cdots & \sin \beta_n \\ \bar{x}_1 \sin \beta_1 - \bar{y}_1 \cos \beta_1 & \cdots & \bar{x}_n \sin \beta_n - \bar{y}_n \cos \beta_n \end{bmatrix}, \quad (5.13)$$

where $\boldsymbol{\beta}$ is the mooring line orientation vector with angles between the mooring lines and the x-axis, and $\bar{\mathbf{x}}$ and $\bar{\mathbf{y}}$ are the horizontal displacement of the mooring lines between the turret and the anchor cable.

5.1.2.2 Resulting Model

By combining the LF control model in (5.8) with the mooring line forces, we get the following LF control model:

$$\dot{\boldsymbol{\eta}} = \mathbf{J}(\boldsymbol{\eta})\mathbf{v}, \quad (5.14)$$

$$\dot{\mathbf{b}} = -\mathbf{T}_b\mathbf{b}(t) + w_b, \quad (5.15)$$

$$\mathbf{M}\dot{\mathbf{v}} = -\mathbf{D}\mathbf{v} - \mathbf{J}(\boldsymbol{\eta})^\top \mathbf{G}_{mo}\boldsymbol{\eta} + \mathbf{J}(\boldsymbol{\psi})^\top \mathbf{b}(t) + \boldsymbol{\tau}_{thr}, \quad (5.16)$$

where $\mathbf{D} = \mathbf{D}_{lin} + \mathbf{D}_{mo}$, $\mathbf{J}(\boldsymbol{\eta})^\top + \mathbf{b}(t) \approx \mathbf{D}_{lin}\mathbf{v}_c + \boldsymbol{\tau}_{wave2}$ and $\mathbf{G}_{mo} = \mathbf{T}(\boldsymbol{\beta})\mathbf{L}_p\boldsymbol{\tau}_H$.

5.2 System Identification 6 DOF Model

5.2.1 Vessel Model

In order to get the system parameters for the 6 DOF vessel mode, MSS Toolbox is used (Fossen and Perez, 2004). Before this toolbox even could be used, it was necessary to run some simulations in ShipX. The AutoCAD drawings of the Statoil's Cat I Arctic Drillship was converted to ShipX file, and then scaled down by Froude scaling in ShipX. In ShipX it was necessary to calculate the vessel response, so a test run at first showed that the prefilled wave periods gave wrong vessel response amplitude operators (RAOs). Since this was a model of a vessel, the wave periods had to be scaled as well. By setting the minimum wave period to a period that the vessel operates in, in this case 0.671 seconds, and filling in at least 10 periods in the area where it operates, the RAOs became correct. Then by using the result files from ShipX with the functions in MSS Toolbox, `veres2vessel` and `vessel2ss`, the data files for the model was complete. This then is used in the Simulink model, by using the build in Simulink block, 6 DOF DP model (zero speed model with fluid memory), from MSS Toolbox.

The entire procedure on how to go from a ShipX model to get the system parameters in MATLAB is described by Fossen (2008).

5.2.2 Mooring Model

For the mooring system, a Simulink model made by Ren (2015) is used. This model is in full scale, so it was necessary to scale it down so it would fit the CSAD model. This scaling was done by Froude scaling, which is explained in the following subsection.

5.2.2.1 Froude Scaling

Physical conditions such as wind, currents, waves, water depths among others must be reproduced realistically. To do this it is necessary to apply Froude similitude law to give realistic value in model scale, or vice versa. This means that gravity is considered to be the dominant force acting on the hull. By using the geometrical similarity requirement: $\lambda = L_F/L_M$, Table 5.1.

Table 5.1: Froude scaling table.

Physical Parameter	Unit	Multiplication factor
Length:	[m]	λ
Structural mass:	[kg]	$\lambda^3 \cdot \frac{\rho_F}{\rho_M}$
Force:	[N]	$\lambda^3 \cdot \frac{\rho_F}{\rho_M}$
Moment:	[Nm]	$\lambda^4 \cdot \frac{\rho_F}{\rho_M}$
Acceleration:	[m/s ²]	$a_F = a_M$
Time:	[s]	$\sqrt{\lambda}$
Pressure:	[Pa=N/m ²]	$\lambda \cdot \frac{\rho_F}{\rho_M}$

5.3 System Identification 3 DOF Model

Since this vessel will be used for other applications than just TAPM, a 3 DOF model is needed as well. This requires some modifications to (5.8), the resulting model then becomes:

$$\dot{\boldsymbol{\eta}} = \mathbf{R}(\psi)\mathbf{v}, \quad (5.17)$$

$$\mathbf{M}\dot{\mathbf{v}} = -\mathbf{C}(\mathbf{v})\mathbf{v} - \mathbf{D}(\mathbf{v})\mathbf{v} + \boldsymbol{\tau}_{\text{env}} + \boldsymbol{\tau}_{\text{thr}}, \quad (5.18)$$

where $\boldsymbol{\eta} = [x, y, \psi]^\top \in \mathbb{R}^3$, $\mathbf{v} = [u, v, r]^\top \in \mathbb{R}^3$ and $\boldsymbol{\tau} = [X, Y, N]^\top \in \mathbb{R}^3$. The rotation matrix $\mathbf{R}(\psi)$ is given by:

$$\mathbf{R}(\boldsymbol{\eta}) = \mathbf{R}(\psi) = \begin{bmatrix} \cos \psi & -\sin \psi & 0 \\ \sin \psi & \cos \psi & 0 \\ 0 & 0 & 1 \end{bmatrix} \quad (5.19)$$

The parameter values in the different terms in (5.18) are as in Table 5.2.

Table 5.2: CSAD rigid body and added mass parameters.

Rigid Body		Added mass	
Parameter	Value	Parameter	Value
m	127.92	$X_{\dot{u}}$	3.262
I_z	61.967	$Y_{\dot{v}}$	28.89
x_g	0	$Y_{\dot{r}}$	0.525
		$N_{\dot{v}}$	0.157
		$N_{\dot{r}}$	13.98

$$\mathbf{M} = \begin{bmatrix} m - X_{\dot{u}} & 0 & 0 \\ 0 & m - Y_{\dot{v}} & mx_g - Y_{\dot{r}} \\ 0 & mx_g - Y_{\dot{r}} & I_z - N_{\dot{r}} \end{bmatrix} = \mathbf{M}^\top > 0 \quad (5.20)$$

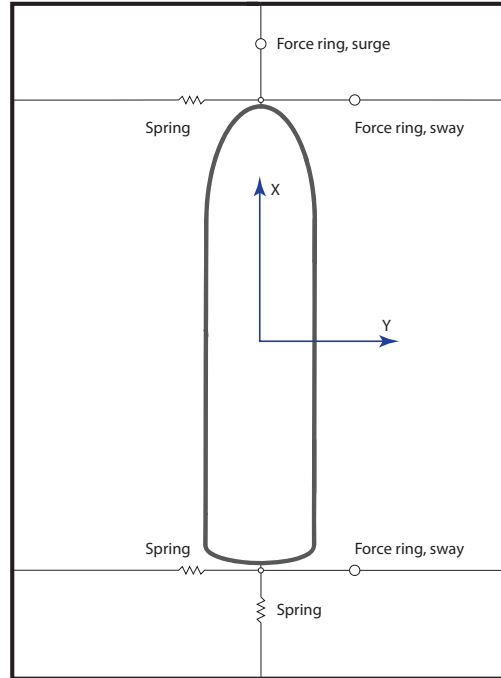


Figure 5.2: The towing setup for CSAD.

$$\mathbf{C}(\mathbf{v}) = \begin{bmatrix} 0 & -mr & Y_{\dot{v}}v + (Y_{\dot{r}} - mx_g)r \\ mr & 0 & -X_{\dot{u}}u \\ -Y_{\dot{v}}v - (Y_{\dot{r}} - mx_g)r & X_{\dot{u}}u & 0 \end{bmatrix} = -\mathbf{C}^T \quad (5.21)$$

5.3.1 Drag Coefficients

In order to estimate the vessel damping term in (5.16), for the 3 DOF model, several towing tests had to be performed in the MC Lab. The test setup is shown in Figure 5.2. Force rings are fitted in the stern and on the side to measure the force in different directions. The springs are there to keep the vessel straight and eliminate oscillations when forces are acting on the vessel in surge and sway. The test setup for finding the yaw moment has a minor change to it, the aft spring and force ring has switched places. The tests were performed by towing and rotating the vessel with different velocities. In order to obtain the resistance forces on the hull, all thrusters were directed along the x-axis backwards to reduce the resistance from thrusters.

The data series collected from the towing tests have been post processed in MATLAB, by using a modified version of the towing script for CSEI. By using a curve fitting tool in MATLAB, the damping terms as a function of velocity in surge, sway and yaw have been found. The results can be seen in Figure 5.3, 5.4 and 5.5.

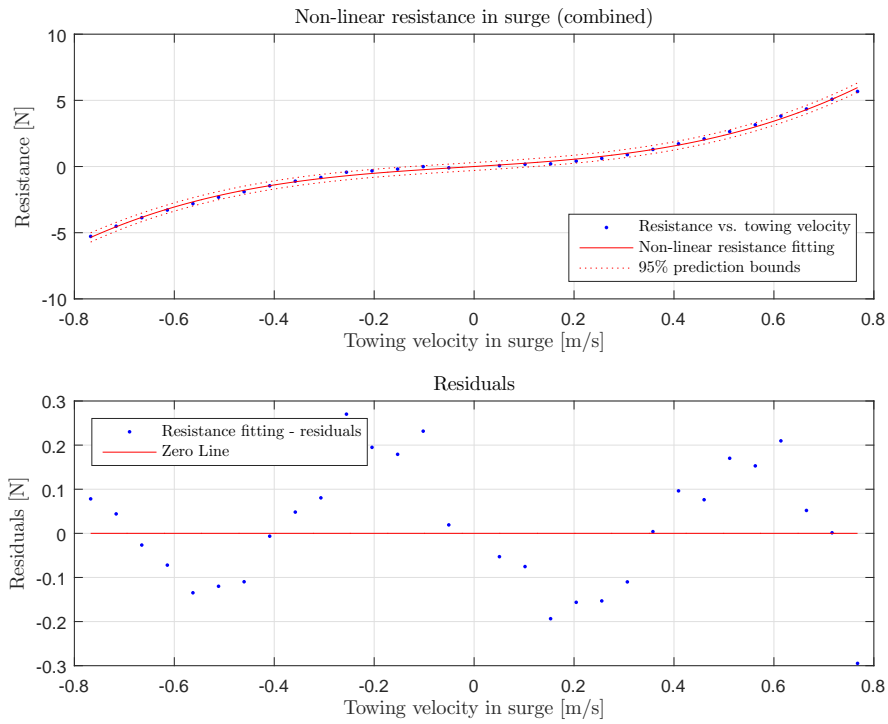


Figure 5.3: Drag forces acting on the hull in surge.

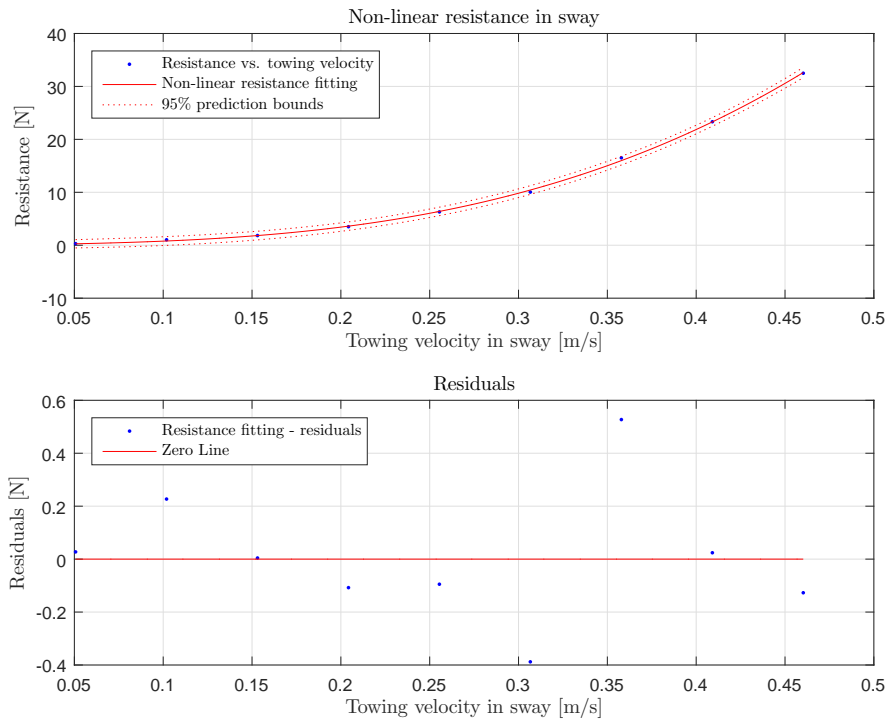


Figure 5.4: Drag forces acting on the hull in sway.

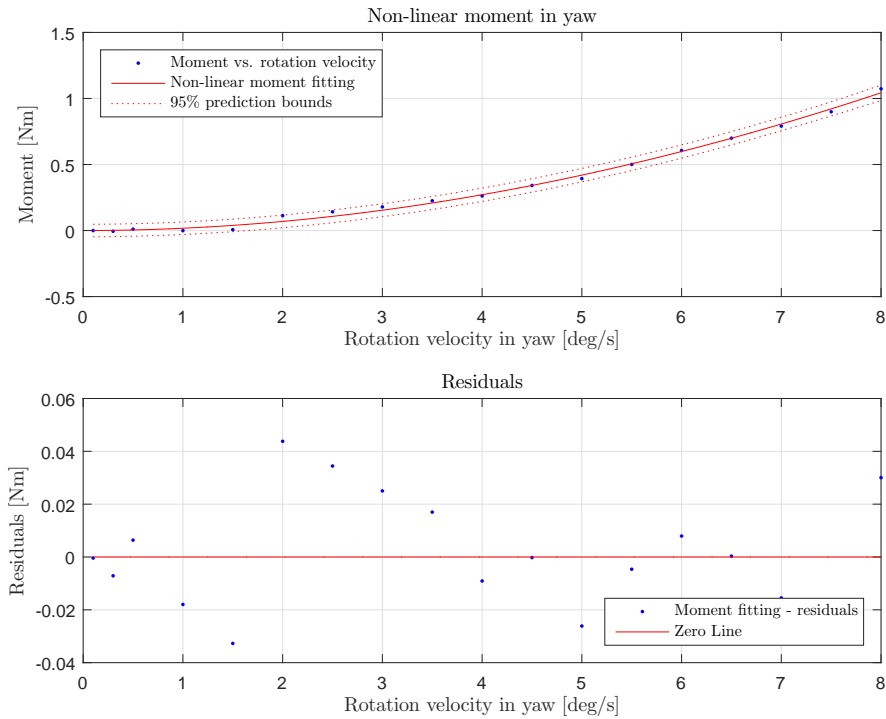


Figure 5.5: Drag forces acting on the hull in yaw.

From these results the linear and nonlinear drag coefficients for CSAD, in surge, sway and yaw, can be found. The results are based on a cubic function, with the form $y = ax^3 + bx^2 + cx$. Table 5.3 lists the resulting coefficients:

Table 5.3: Drag coefficients in surge, sway and yaw based on test result.

Surge		Sway		Yaw	
Parameter	Value	Parameter	Value	Parameter	Value
X_u	-2.332	Y_v	-4.673	N_r	-0.01675
X_{uu}	0	Y_{vv}	0.3976	N_{rr}	-0.01148
X_{uuu}	-8.557	Y_{vvv}	-313.3	N_{rrr}	-0.0003578

The coupling terms in sway and yaw were not obtained from these tests. In order to have an estimation of these values, the coupling terms from tests done on the CSIII were used.

Table 5.4: Drag coefficients in surge, sway and yaw with coupling terms.

Surge		Sway		Yaw	
Parameter	Value	Parameter	Value	Parameter	Value
X_u	-2.332	Y_v	-4.673	N_v	0
X_{uu}	0	Y_{vv}	0.3976	N_{vv}	-0.2088
X_{uuu}	-8.557	Y_{vvv}	-313.3	N_{vvv}	0
X_v	0	Y_r	-7.250	N_r	-0.01675
X_{vv}	0	Y_{rr}	-3.450	N_{rr}	-0.01148
X_{vvv}	0	Y_{rrr}	0	N_{rrr}	-0.0003578
		Y_{rv}	-0.805	N_{rv}	0.08
		Y_{vr}	-0.845	N_{vr}	0.08

$$\mathbf{D}(\mathbf{v}) = - \begin{bmatrix} d_{11}(u) & 0 & 0 \\ 0 & d_{22}(v, r) & d_{23}(v, r) \\ 0 & d_{32}(v, r) & d_{33}(v, r) \end{bmatrix}, \quad (5.22)$$

where the damping components are:

$$d_{11}(u) = X_u + X_{|u|u}|u| + X_{uuu}u^2, \quad (5.23)$$

$$d_{22}(v, r) = Y_v + Y_{|v|v}|v| + Y_{vvv}v^2 + Y_{|r|v}|r|, \quad (5.24)$$

$$d_{23}(v, r) = Y_r + Y_{|v|r}|v| + Y_{|r|r}|r| + Y_{rrr}r^2, \quad (5.25)$$

$$d_{32}(v, r) = N_v + N_{|v|v}|v| + N_{vvv}v^2 + N_{|r|v}|r|, \quad (5.26)$$

$$d_{33}(v, r) = N_r + N_{|v|r}|v| + N_{|r|r}|r| + N_{rrr}r^2. \quad (5.27)$$

Note: With this specific damping matrix, the model is only valid for low speed.

Chapter 6

Observer and Controller Design

6.1 Observer Design

Since most of the time the measurements are either noisy or can be incomplete, there is need for an observer. An observer is a system that provides an estimate of the internal state for a real system. There exists a lot of different types of observers, i.e. Luenberger, Kalman filter, etc., and in this thesis the nonlinear passive observer is used.

6.1.1 Nonlinear Passive Observer

The passive observer is based on Strand and Fossen (1999) where the main motivation was to reduce the tuning parameters in designing a Kalman filter. The non-linear passive observer gives these advantages during the tuning process and the Coriolis terms, $\mathbf{C}_{RB}\mathbf{v}$ and $\mathbf{C}_A\mathbf{v}_r$, and the non-linear damping term, $\mathbf{D}_{NL}|\mathbf{v}|\mathbf{v}$, are small due to low speed, so they can be neglected. The following assumptions are also necessary to prove passivity (Fossen, 2011):

Assumption 1. $\mathbf{w} = \mathbf{0}$ and $\mathbf{v} = \mathbf{0}$. *The zero-mean white Gaussian noise terms are omitted in the analysis of the observer. If they are included in the Lyapunov function analysis the error dynamics will be uniformly ultimate bounded (UUB) instead of uniform global asymptotical/exponential stable (UGAS/UGES).*

Assumption 2. $\mathbf{R}(y_3) = \mathbf{R}(\psi)$, *implying that $y_3 = \psi + \psi_w \approx \psi$. This is a good assumption since the magnitude of the wave-induced yaw disturbance ψ_w will normally be less than 5 degrees in extreme weather situations (sea state codes 5-9) and less than 1 degree during normal operation of the ship (sea state codes 0-4)*

Then by applying the assumptions to the resulting LF model we get the following non-linear passive observer equations:

$$\dot{\hat{\boldsymbol{\xi}}} = \mathbf{A}_w \hat{\boldsymbol{\xi}} + \mathbf{K}_1(\omega_0) \tilde{\mathbf{y}}, \quad (6.1)$$

$$\dot{\hat{\boldsymbol{\eta}}} = \mathbf{R}(\psi) \hat{\mathbf{v}} + \mathbf{K}_2 \tilde{\mathbf{y}}, \quad (6.2)$$

$$\dot{\hat{\mathbf{b}}} = -\mathbf{T}_b \hat{\mathbf{b}} + \mathbf{K}_3 \tilde{\mathbf{y}}, \quad (6.3)$$

$$\mathbf{M} \dot{\hat{\mathbf{v}}} = -\mathbf{D} \hat{\mathbf{v}} + \mathbf{R}(\psi)^\top \hat{\mathbf{b}} - \mathbf{R}(\psi)^\top \mathbf{G}_{m0} \hat{\boldsymbol{\eta}} + \boldsymbol{\tau}_{\text{thr}} + \mathbf{R}(\psi)^\top \mathbf{K}_4 \tilde{\mathbf{y}}, \quad (6.4)$$

$$\mathbf{y} = \hat{\boldsymbol{\eta}} + \mathbf{C}_w \hat{\boldsymbol{\xi}}, \quad (6.5)$$

where $\tilde{\mathbf{y}} = \mathbf{y} - \hat{\mathbf{y}}$ is the estimation error and $\mathbf{K}_1(\omega_0) \in \mathbb{R}^{6 \times 3}$, $\mathbf{K}_{2,3,4} \in \mathbb{R}^{3 \times 3}$ are the observer gains and $\mathbf{C}_w \in \mathbb{R}^{3 \times 6}$ are a constant matrix describing the sea state.

The matrix \mathbf{A}_w is assumed Hurwitz and describes the first-order WF-induced motion in a mass-damper spring system. The matrix is defined as the following:

$$\mathbf{A}_w = \begin{bmatrix} \mathbf{0}_{3 \times 3} & \mathbf{I}_{3 \times 3} \\ \boldsymbol{\Omega}^2 & -2\boldsymbol{\Gamma}\boldsymbol{\Omega} \end{bmatrix}, \quad (6.6)$$

where $\boldsymbol{\Gamma} = \text{diag}(\lambda_1, \lambda_2, \lambda_3)$ is a diagonal matrix of damping ratios and are often set between 0.05 and 0.2. The $\boldsymbol{\Omega} = \text{diag}(\omega_1, \omega_2, \omega_3)$ is a diagonal matrix containing the dominating wave response frequencies.

The gain matrices \mathbf{K}_i is calculated from the following equations:

$$K_{1i}(\omega_{oi}) = -2(\xi_{ni} - \lambda_i) \frac{\omega_{ci}}{\omega_{oi}}, \quad (6.7)$$

$$K_{1(i+3)}(\omega_{oi}) = 2\omega_{oi}(\xi_{ni} - \lambda_i), \quad (6.8)$$

$$K_{2i} = \omega_{ci}, \quad (6.9)$$

where $\xi_{ni} = 1.0$ and $\lambda = 0.1$ are typical values (Fossen, 2011).

Since there is a possibility that the mooring lines break, or the setup is non-symmetric, the resulting observer model needs to include the mooring forces that interact with the vessel. The mooring forces implemented into the observers are approximations of the catenary equations, due to the complexity of these equations.

There exists a function between the horizontal restoring component H_i and the horizontal distance X_i when the heave motion is zero, such that

$$H_i = f_{X_i}(X_i), \quad i = 1, \dots, M, \quad (6.10)$$

where $f_{X_i} : D_{X_i} \mapsto \mathbb{R}$ is a locally Lipschitz map from the feasible region $D_{X_i} \in \mathbb{R}$ into horizontal

restoring force.

6.2 Controller Design

The control objective is to bring the vessel to the desired position and keep it there. This can be expressed mathematically as

$$\text{Objective: } \lim_{t \rightarrow \infty} \boldsymbol{\eta}(t) = \boldsymbol{\eta}_d. \quad (6.11)$$

6.2.1 Heading Control

The heading controller adjusts the vessel heading towards the environmental forces to reduce the loads on the vessel and its mooring system. The heading controller can be described mathematically as PID-controller (Nguyen and Sørensen, 2009b):

$$\boldsymbol{\tau}_{pid}^\psi = -\mathbf{H}_\psi \mathbf{K}_i \mathbf{R}(\psi)^\top \boldsymbol{\xi} - \mathbf{H}_\psi \mathbf{K}_p \mathbf{R}(\psi)^\top (\boldsymbol{\eta} - \boldsymbol{\eta}_d) - \mathbf{H}_\psi \mathbf{K}_d (\mathbf{v} - \mathbf{v}_d), \quad (6.12)$$

where $\mathbf{H}_\psi = \text{diag}(0, 0, 1)$, since only the heading is subjected to control, $\mathbf{K}_{p,i,d}$ is the controller gains and $\boldsymbol{\xi} = \boldsymbol{\eta} - \boldsymbol{\eta}_d$.

6.2.2 Surge/Sway Damping and Restoring

The surge/sway controller dampens the unwanted large oscillatory motion in surge and sway, and reduces the stress on the mooring system. The surge/sway damping and restoring controller can be described mathematically as PD-controller (Nguyen and Sørensen, 2009b):

$$\boldsymbol{\tau}_{pd}^{xy} = -\mathbf{H}_{xy} \mathbf{K}_p \mathbf{R}(\psi)^\top (\boldsymbol{\eta} - \boldsymbol{\eta}_d) - \mathbf{H}_{xy} \mathbf{K}_d (\mathbf{v} - \mathbf{v}_d), \quad (6.13)$$

where $\mathbf{H}_{xy} = \text{diag}(1, 1, 0)$ and $\mathbf{K}_{p,d}$ are the controller gains.

6.2.3 Setpoint Chasing by Lowpass Filtering

The proposed setpoint chasing algorithm from Nguyen and Sørensen (2009a) is presented in (6.14). The objective of this controller is to keep the thrust at its minimum, but still reach the overall aim, $\boldsymbol{\eta} \rightarrow \boldsymbol{\eta}_d$.

$$\dot{\boldsymbol{\eta}}_d = -\boldsymbol{\Lambda} \boldsymbol{\eta}_d + \boldsymbol{\Lambda} \boldsymbol{\eta}_{xy}, \quad (6.14)$$

where $\dot{\boldsymbol{\eta}}_d \in \mathbb{R}^2$ is the system dynamics of the desired LF position of the vessel and $\boldsymbol{\Lambda} \in \mathbb{R}^{2 \times 2}$ is the first-order diagonal and non-negative filter gain matrix with the cutoff frequencies $1/T_{s_i}$ given by

$$\boldsymbol{\Lambda} = \text{diag}(1/T_{s_1}, 1/T_{s_2}). \quad (6.15)$$

This then continuously produces a new setpoint for the controller, so that the controller commands minimal force, until the maximum radius is reached. The controller is just a regular PID-controller that can be represented as:

$$\boldsymbol{\tau}_{pid} = -\mathbf{K}_p \mathbf{R}(\boldsymbol{\psi})^\top (\boldsymbol{\eta} - \boldsymbol{\eta}_d) - \mathbf{K}_i \mathbf{R}(\boldsymbol{\psi})^\top \boldsymbol{\xi} - \mathbf{K}_d (\mathbf{v} - \mathbf{v}_d), \quad (6.16)$$

where $\dot{\boldsymbol{\xi}} = \boldsymbol{\eta} - \boldsymbol{\eta}_d$ and $\mathbf{K}_{p,i,d}$ are the controller gains. To get a clearer view of how the setup for the setpoint generator is, a block diagram of this is shown in Figure 6.1.

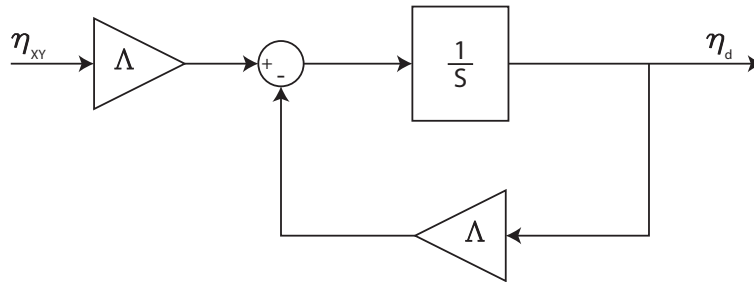


Figure 6.1: A block diagram of the setpoint generator.

6.2.4 Hybrid Control Concept

Nguyen and Sørensen (2009b) introduced a hybrid control concept that uses a supervisory switching algorithm to detect the sea state from the environmental load and wave peak frequency. The best controller for the specific sea state is determined automatically using the best-fit model and a hysteresis switching logic. They also proposed a set of control laws, some have been mentioned already, and they all can be seen in Table 6.1:

Table 6.1: Set of control laws [Adapted from: Nguyen and Sørensen (2009b)].

Control actions	Control laws
Integral action:	$\dot{\xi} = \eta - \eta_d$
1. Heading PID control:	$\tau_{pid}^\psi = -\mathbf{H}_\psi \mathbf{K}_i \mathbf{R}(\psi)^\top \xi - \mathbf{H}_\psi \mathbf{K}_p \mathbf{R}(\psi)^\top (\eta - \eta_d) - \mathbf{H}_\psi \mathbf{K}_d (\mathbf{v} - \mathbf{v}_d)$
2. Surge-sway damping:	$\tau_d^{xy} = -\mathbf{H}_{xy} \mathbf{K}_d (\mathbf{v} - \mathbf{v}_d)$
3. Surge-sway restoring:	$\tau_p^{xy} = -\mathbf{H}_{xy} \mathbf{K}_p \mathbf{R}(\psi)^\top (\eta - \eta_d)$
4. Surge-sway mean:	$\tau_i^{xy} = -\mathbf{H}_{xy} \mathbf{K}_i \mathbf{R}(\psi)^\top \xi$
Setpoint normal sea:	$\dot{\eta}_d = -\Lambda \eta_d + \Lambda \eta_{xy}, \quad \eta_{xy} = \mathbf{p}_{LF} \in \mathbb{R}^2$
Setpoint extreme sea:	$\eta_d = \mathbf{Pr}_{\text{safe}}\{\eta_{xy}\}$

where $\mathbf{H}_\psi = \text{diag}(0, 0, 1)$ and $\mathbf{H}_{xy} = \text{diag}(1, 1, 0)$ are the projections enabling the different controllers. $\mathbf{Pr}_{\text{safe}}\{\eta_{xy}\}$ is the projection of the LF position of the vessel into safe area to minimize the risk of mooring line breakage.

They also proposed this switching sequence:

Table 6.2: Switching sequence [Adapted from: Nguyen and Sørensen (2009b)].

Heading	Damping	Restoring	Mean	Control action	Setpoint	Sea state
✓				1		Calm
✓	✓			1+2		Normal
✓	✓	✓		1+2+3	Normal	Normal
✓	✓		✓	1+2+4	Extreme	Extreme
✓	✓	✓	✓	1+2+3+4	Extreme	Extreme

6.2.4.1 Supervisory Switching with Hysteresis Switching Logic

The developed switching algorithm customized for extreme loads are based on a safety circle. The radii of this circle is defined to be the area where the turret offset from the well is more than 10° (Wassink and List, 2013). By setting this radii to 0.11 meters, this criteria has been fulfilled. For each of the areas, inside and outside the circle, a controller has been developed and tune to keep the vessel at its desired position. Figure 6.2 shows what is meant by the safety circle.

To avoid chattering problem between the two controllers and make it unstable, a hysteresis-based switch logic is implemented. The proposed dwell-time switching logic from Hespanha (2002) is used to solve this problem. It is based on pre-specified amount of time before the controllers can be switched.

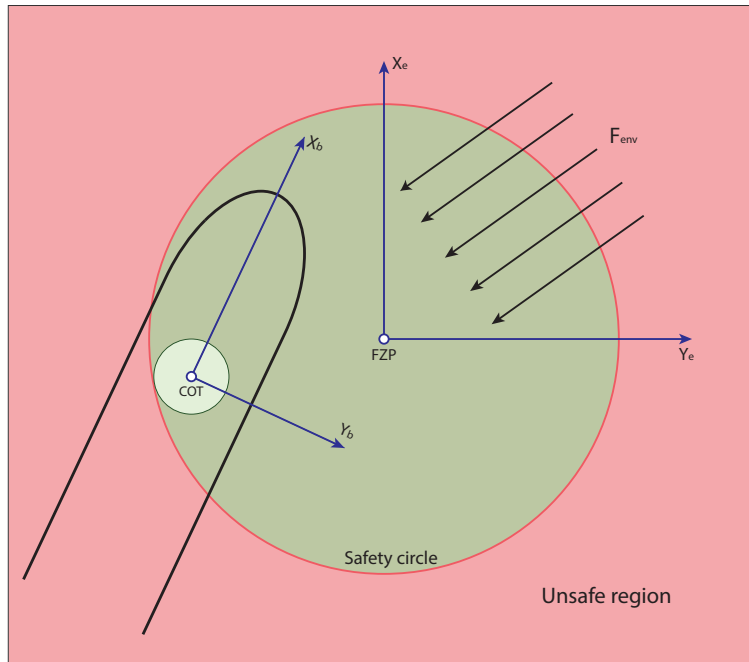


Figure 6.2: Explanation of the safety circle [Adapted from: Skjetne (2014)].

6.2.5 Additional Hybrid Switching Setup

In addition to the other hybrid switching controller, the author wanted to examine another method that estimates the sea states and select the corresponding controller. This controller will then be added to the original hybrid setup, but the controllers will now be more aggressive and tuned to their specific sea state.

This method is based on the work done by Aranovskii et al. (2007) on finding the frequency of a sinusoidal signal. Since a moored vessel can be perceived as a buoy in waves and these are a composition of sinusoidal waves, this method may work on estimating the sea state as well.

An unknown sinusoidal wave with a constant amplitude, frequency and phase is given by:

$$y(t) = A_y \sin(\omega_e t + \varepsilon), \quad (6.17)$$

and the objective is to estimate the frequency ω_e by measurements of only $y(t)$. The sinusoidal signal is the solution to the undamped harmonic oscillator:

$$\ddot{y} = -\omega_e^2 y = \varphi y, \quad (6.18)$$

where $\varphi = -\omega_e^2$ has to be estimated. Aranovskii et al. (2007) show that it is possible to track the measured sinusoidal signal by an auxiliary filter:

$$\dot{\xi}_1 = \xi_2, \quad (6.19)$$

$$\dot{\xi}_2 = -2\xi_2 - \xi_1 + y, \quad (6.20)$$

with a correcting second order transfer function:

$$\xi_1(s) = \frac{1}{(s+1)^2} y(s). \quad (6.21)$$

This tracks the sinusoidal signal until the cut-off frequency of 1 rad/s. By modifying this second order transfer function into:

$$\xi_1(s) = \frac{\omega_f^2}{(s + \omega_f)^2} y(s), \quad (6.22)$$

makes it possible to track higher frequencies waves. The cut-off frequency ω_f must be chosen such that $\omega_f > \omega_e$ to ensure that the filter tracks the correct frequency. Then the frequency estimator becomes:

$$\dot{\xi}_1 = \xi_2, \quad (6.23)$$

$$\dot{\xi}_2 = -2\omega_f \xi_2 - \omega_f^2 \xi_1 + \omega_f^2 y, \quad (6.24)$$

$$\dot{\varphi} = k_a \xi_1 (\dot{\xi}_2 - \hat{\varphi} \xi_1), \quad (6.25)$$

$$\hat{\omega}_e = \sqrt{|\hat{\varphi}|}. \quad (6.26)$$

By further investigation, this method was tested in sea state estimation by Nielsen et al. (2015). Thus, this work is a simulation verification on the area, performed on the CSAD model.

Chapter 7

Experiment Setup

In order to perform the experiments as accurate as possible, in scale 1:90. It is important to consider which factors that impact the model, when applying external forces to the vessel. The most critical factors are the scaling of the mooring system and the waves. These two contributions are explained more in detailed in Sections 7.1 and 7.2.

An illustration of how the vessel model is connected to the mooring system, the setup for the mooring system and wave direction can be seen in Figure 7.1.

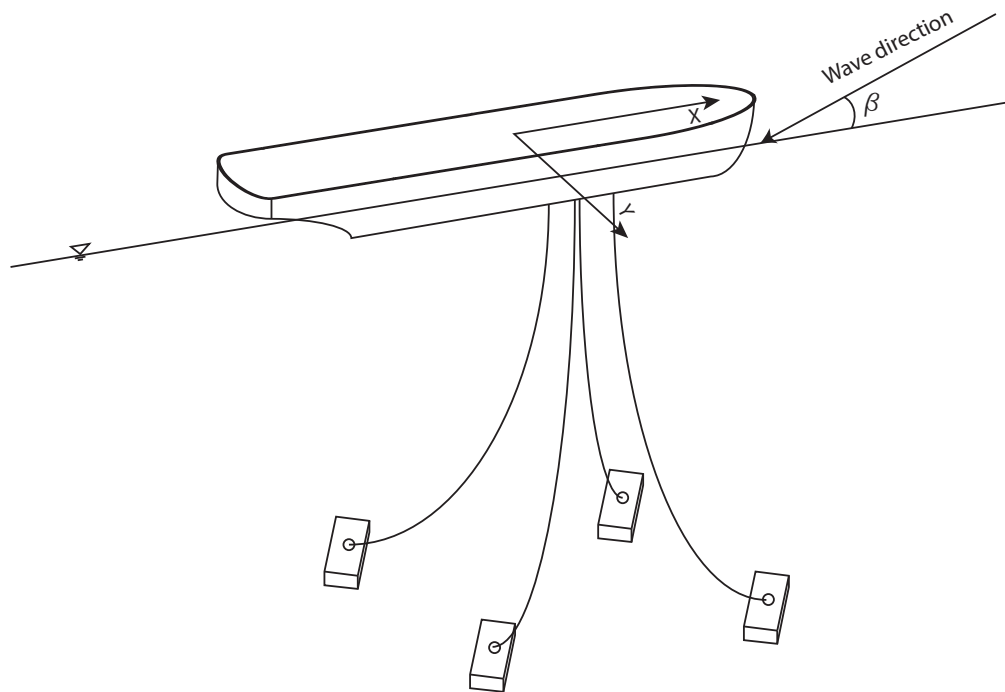


Figure 7.1: The experiment setup, with wave direction in an angle to the bow.

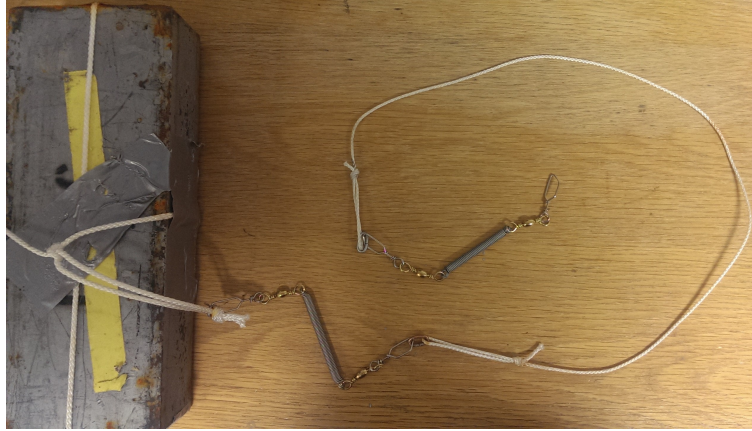


Figure 7.2: One of the mooring lines that are used in the experiments.

7.1 Mooring

To replicate the mooring system with the same damping and restoring characteristics as the simulation is difficult. By studying MARINTEK (2014) the author found a method that gives a good replica, but not the same as the simulation model. This replica consist of springs, ropes and swivels, see Figure 7.2. By attaching the end of the mooring lines to a 10 kg weight, it also gives the possibility to change the position and how tight the mooring lines should be. The vessel is fitted with 4 mooring lines in these experiments.

7.2 Waves

The waves need to be scaled according to the model scale; 1:90. By applying the method of Froude scaling, as presented in Section 5.2.2.1, the waves used in the experiment are as presented in Table 7.1. To determine what kind of waves that were necessary to check, Price and Bishop (1974) were used as a reference. They divided waves into different sea states according to frequency and wave height, see Table 7.2. Here the different sea states and their probability of occurrence in the northern North Atlantic is presented, where sea states 3, 4 and 5 occur most often. Sea states also depend on season, as rougher sea states occur more often in the winter.

Table 7.1: Scaled waves in the experiment.

Full scale		Model scale	
Significant wave height (H_s) [m]	Peak wave frequency (ω_p) [rad/sec]	Significant wave height (H_s) [m]	Peak wave frequency (ω_p) [rad/sec]
0.5	0.93	0.0055	8.823
2.5	0.68	0.0278	6.451
4	0.60	0.0444	5.692
9	0.46	0.1000	4.364

Table 7.2: Definition of sea states according to Price and Bishop (1974).

Sea State Code	Description of sea	Significant wave height (H_s) [m]	Peak wave frequency (ω_p) [rad/sec]	% probability Northern North Atlantic
0	Calm (glassy)	0	1.29	
1	Calm (rippled)	0-0.1	1.29-1.11	6.0616
2	Smooth (wavelets)	0.1-0.5	1.11-0.93	
3	Slight	0.5-1.25	0.93-0.79	21.5683
4	Moderate	1.25-2.5	0.79-0.68	40.9915
5	Rough	2.5-4.0	0.68-0.60	21.2383
6	Very rough	4.0-6.0	0.60-0.53	7.0101
7	High	6.0-9.0	0.53-0.46	2.6931
8	Very	9.0-14.0	0.46-0.39	0.4346
9	Phenomenal	Over 14	Less than 0.39	0.0035

Chapter 8

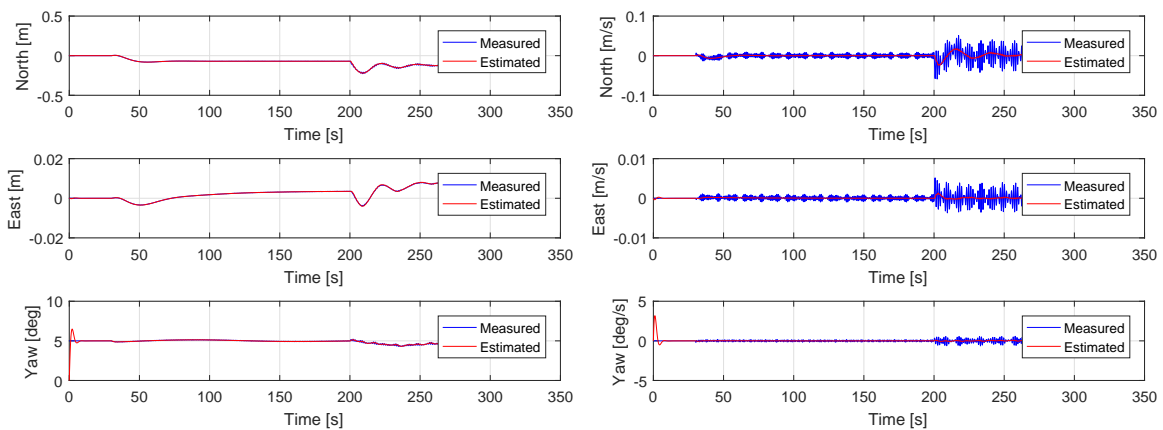
Results

8.1 Observer Verification

In order to have correct position and velocity, an observer verification has to be made. The measured position and velocity is compared to the estimated, and tuned so these are similar, just without the high frequent wave component.

8.1.1 Simulation

The results from Figure 8.1 show that the observer filters out the high frequent wave motion, for both position and velocity. Then the observer feeds the controller with the slowly varying motion from the vessel.



(a) Position over time in surge, sway and yaw. (b) Velocity over time in surge, sway and yaw.

Figure 8.1: Observer verification in simulations.

8.1.2 Experiment

The results in Figure 8.2 show that the observer filters out the high frequent wave motion for position. Regarding the velocity, it is estimated as in the simulations, but now there is no measured data to compare towards. Then the observer feeds the controller with the slowly varying motion from the vessel.

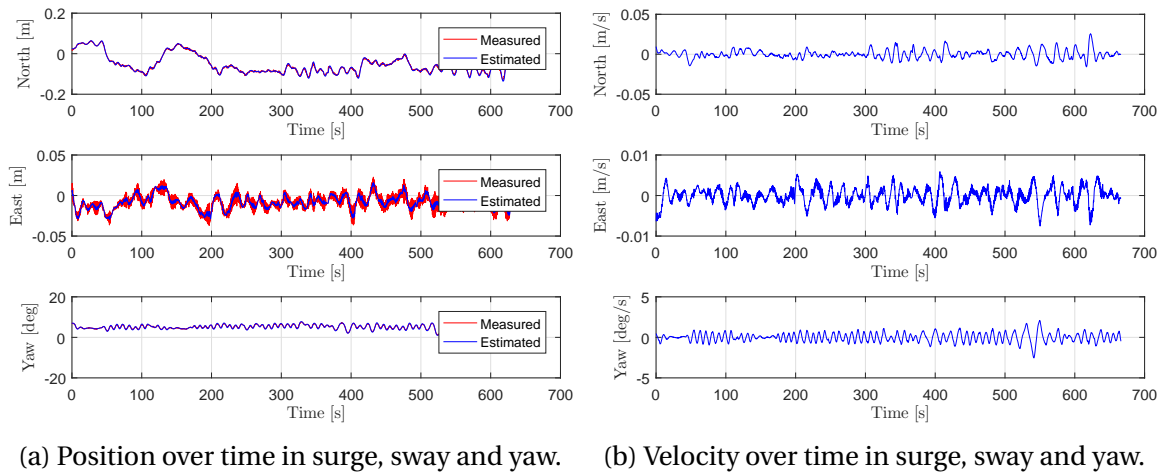


Figure 8.2: Observer verification in experiment.

8.2 Simulation

Results from the simulations are presented in this section. The results are presented through 2D-plots of the measured and desired positions, time plots of measured and desired position and heading. The results are divided into four subsections; heading controller, surge/sway damping and restoring controller, hybrid control with setpoint chasing and the additional hybrid switching setup. The wave height in the different cases varies, but they all have the same wave direction, at $\beta_w = 180^\circ$.

8.2.1 Heading Controller

The heading controller presented in Section 6.2.1 has been tested on the simulation model developed in Section 5. This controller is simulated in two different conditions; $H_s = 4$ meters and $H_s = 9$ meters, to evaluate the outcome of only having a heading controller.

8.2.1.1 $H_s = 4$ m

Figure 8.3 shows the behavior of the vessel in waves with $H_s = 4$ meters. The vessel is kept around the desired heading angle, $\psi = 5^\circ$, and the desired position in surge and sway are shifting according to the setpoint chasing algorithm. The thrust is kept to its minimum and the mooring dampen and restores the vessel to equilibrium, between the environmental forces and mooring forces.

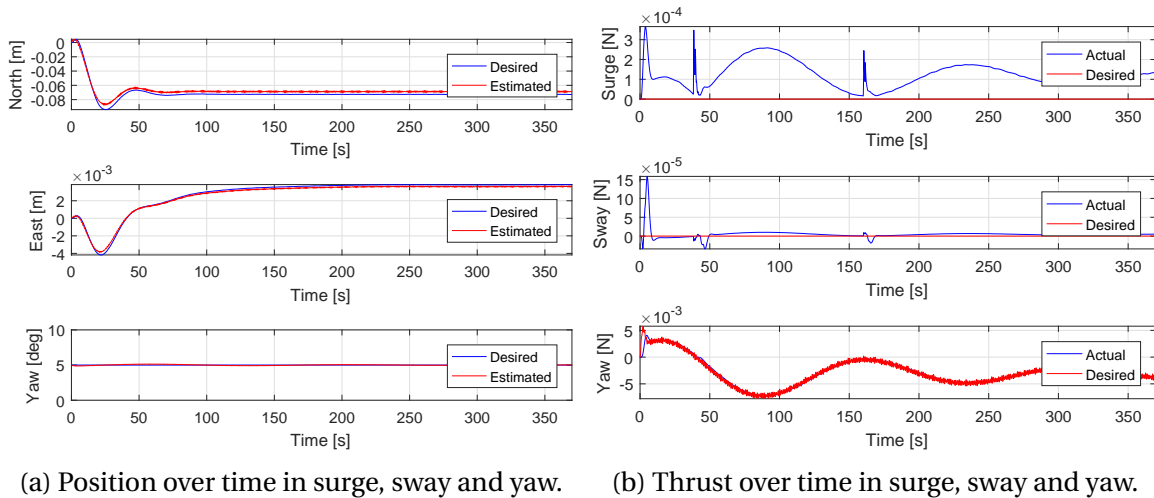
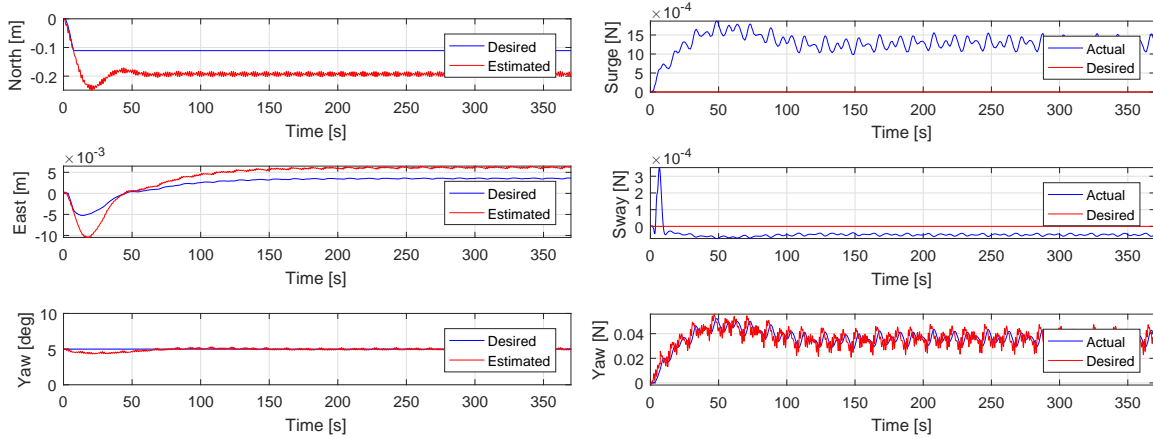


Figure 8.3: Results from heading controller simulations, with wave height $H_s = 4$ meters.

8.2.1.2 $H_s = 9$ m

Figure 8.4 shows the behavior of the vessel in waves with $H_s = 9$ meters. The vessel is kept around the desired heading angle, $\psi = 5^\circ$. The desired position in surge and sway cannot be fulfilled due the controller. Figure 8.4a shows that the position is outside the safety circle, this may cause more stress on the mooring system. Since the vessel is only regulated in yaw, the equilibrium between the mooring system and the environmental forces is approximate 0.2 meters.



(a) Position over time in surge, sway and yaw. (b) Thrust over time in surge, sway and yaw.

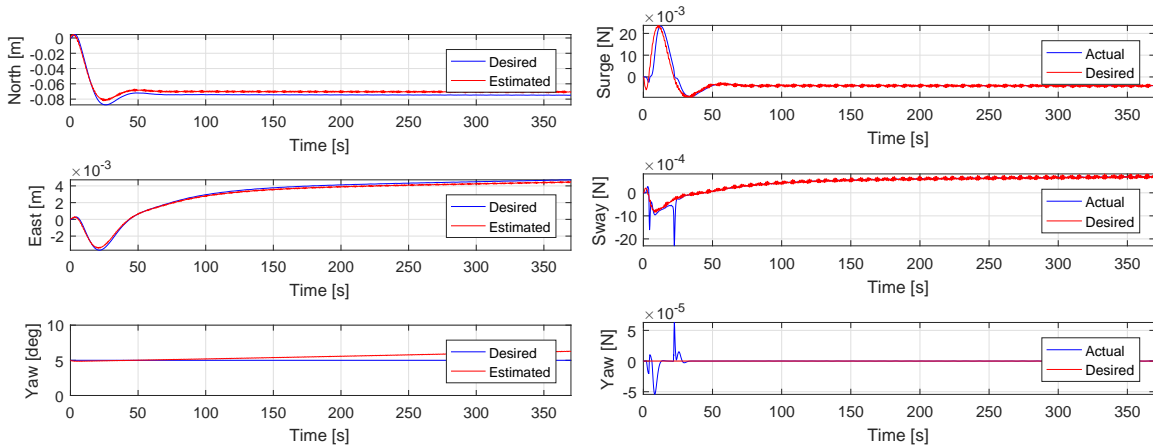
Figure 8.4: Results from heading controller simulations, with wave height $H_s = 9$ m.

8.2.2 Surge/Sway Damping and Restoring Controller

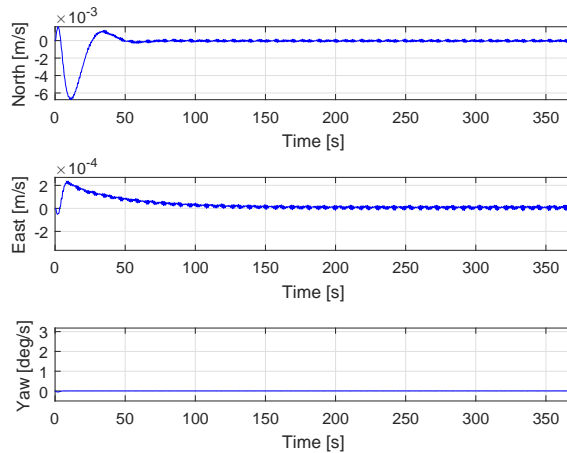
The same simulation model from Chapter 5 has been used to test the surge/sway damping and restoring controller in Section 6.2.2. This controller is simulated under the same conditions as the heading controller; $H_s = 4$ meters and $H_s = 9$ meters. This simulation is to evaluate the outcome of just having damping and restoring in surge and sway.

8.2.2.1 $H_s = 4$ m

Figure 8.5 shows the behavior of the vessel in waves with $H_s = 4$ meters. The controller manages to dampen and restore the vessel position in surge and sway. As the yaw plot in Figure 8.5a shows, the heading of the vessel starts to deviate from the desired heading. If the simulation had run for a longer time, the heading error probably would have increased. As Figure 8.5c shows, the velocity of the vessel decreases over time, which indicates that the vessel becomes more and more stationary.



(a) Position over time in surge, sway and yaw. (b) Thrust over time in surge, sway and yaw.



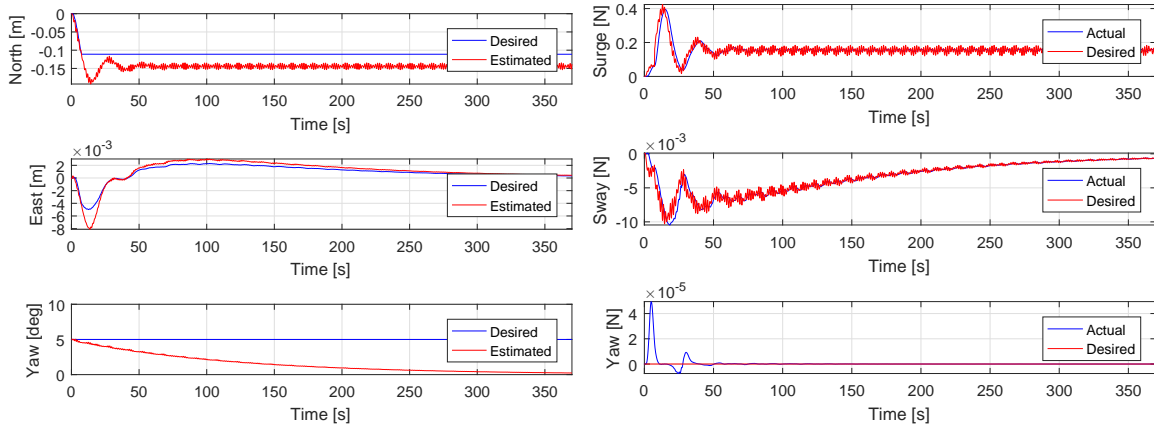
(c) Velocity over time in surge, sway and yaw.

Figure 8.5: Results from surge/sway damping and restoring controller simulations, with wave height $H_s = 4$ meters.

8.2.2.2 $H_s = 9$ m

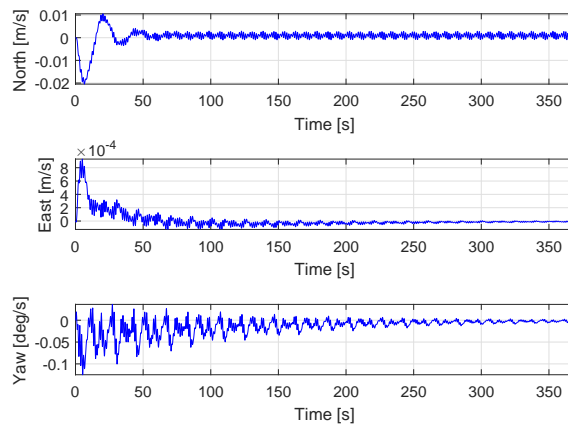
Figure 8.6 shows the behavior of the vessel in waves with $H_s = 9$ meters. From Figure 8.6a, we can see that the motion is being damped. As for the restoring of the position, the controller does not manage this. This was done intentionally, since the controller is not supposed to be aggressive inside the safety circle. As this The figure also shows that the vessel is outside this circle, but the switching between controllers was switched of in these simulations.

Now, if we look at the yaw plot in Figure 8.6a, it shows that the vessel is positioning itself against the waves and keeps this heading. As the velocity plot, Figure 8.6c, shows, the vessel becomes stationary as in the previous case.



(a) Position over time in surge, sway and yaw.

(b) Thrust over time in surge, sway and yaw.



(c) Velocity over time in surge, sway and yaw.

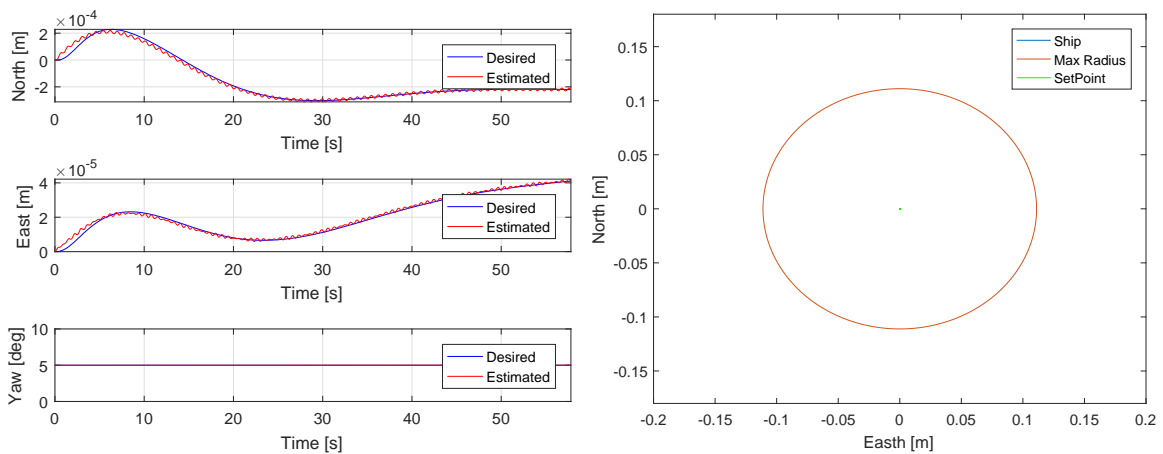
Figure 8.6: Results from surge/sway damping and restoring controller simulations, with wave height $H_s = 9$ meters.

8.2.3 Hybrid Control with Setpoint Chasing

The hybrid controller with setpoint chasing presented in Section 6.2.4 has been tested on the same simulation model. Two more sea states are added to see how the vessel behaves in them as well. The four different conditions are, $H_s = 0.5$ meters, $H_s = 2.5$ meters, $H_s = 4$ meters and $H_s = 9$ meters. The simulations are done to evaluate the outcome if combining different controllers is better than just one.

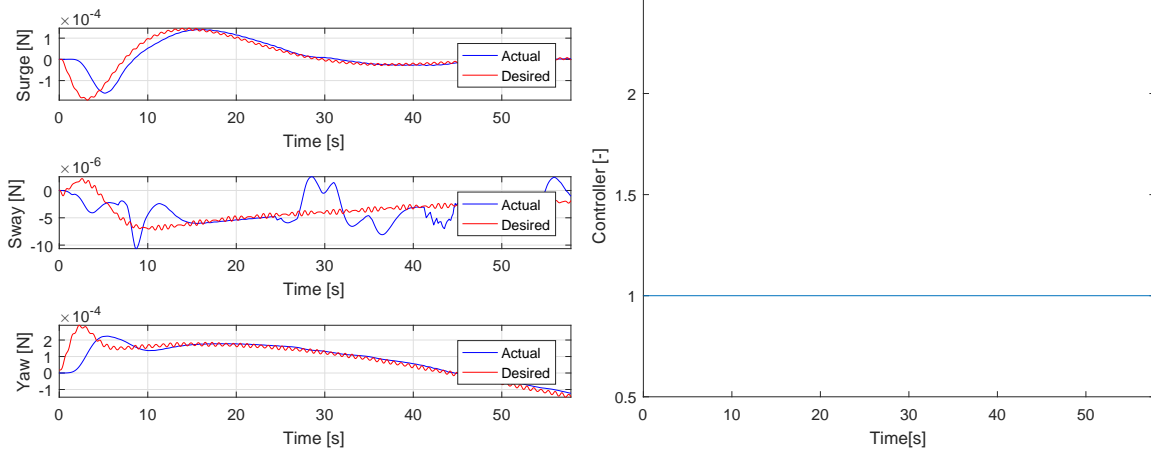
8.2.3.1 $H_s = 0.5$ m

Figure 8.7 shows the behavior of the vessel and the controller, in waves with $H_s = 0.5$ meters. As Figure 8.7a and 8.7b shows, the vessel does not move significantly. The results of this are that the vessel barely uses thrust, and there is only one active controller, seen in Figure 8.7d. As Figure 8.7a shows, the controller manage to keep a precise heading of 5° .



(a) Position over time in surge, sway and yaw.

(b) XY-plot over the position.



(c) Thrust over time in surge, sway and yaw.

(d) Active controller over time.

Figure 8.7: Results from hybrid controller with setpoint chasing simulation, with wave height $H_s = 0.5$ meters.

8.2.3.2 $H_s = 2.5$ m

Figure 8.8 shows the behavior of the vessel and the controller, in waves with $H_s = 2.5$ meters. Now, the vessel movement is slightly larger, compared to the previous case. As Figure 8.8a and 8.8b shows, this motion is less than 3 cm. The thrust, Figure 8.8c, helps dampen and restore the position of the vessel, until it becomes stationary. In this case, like the previous, there is only one active controller. This controller manages to keep the desired heading.

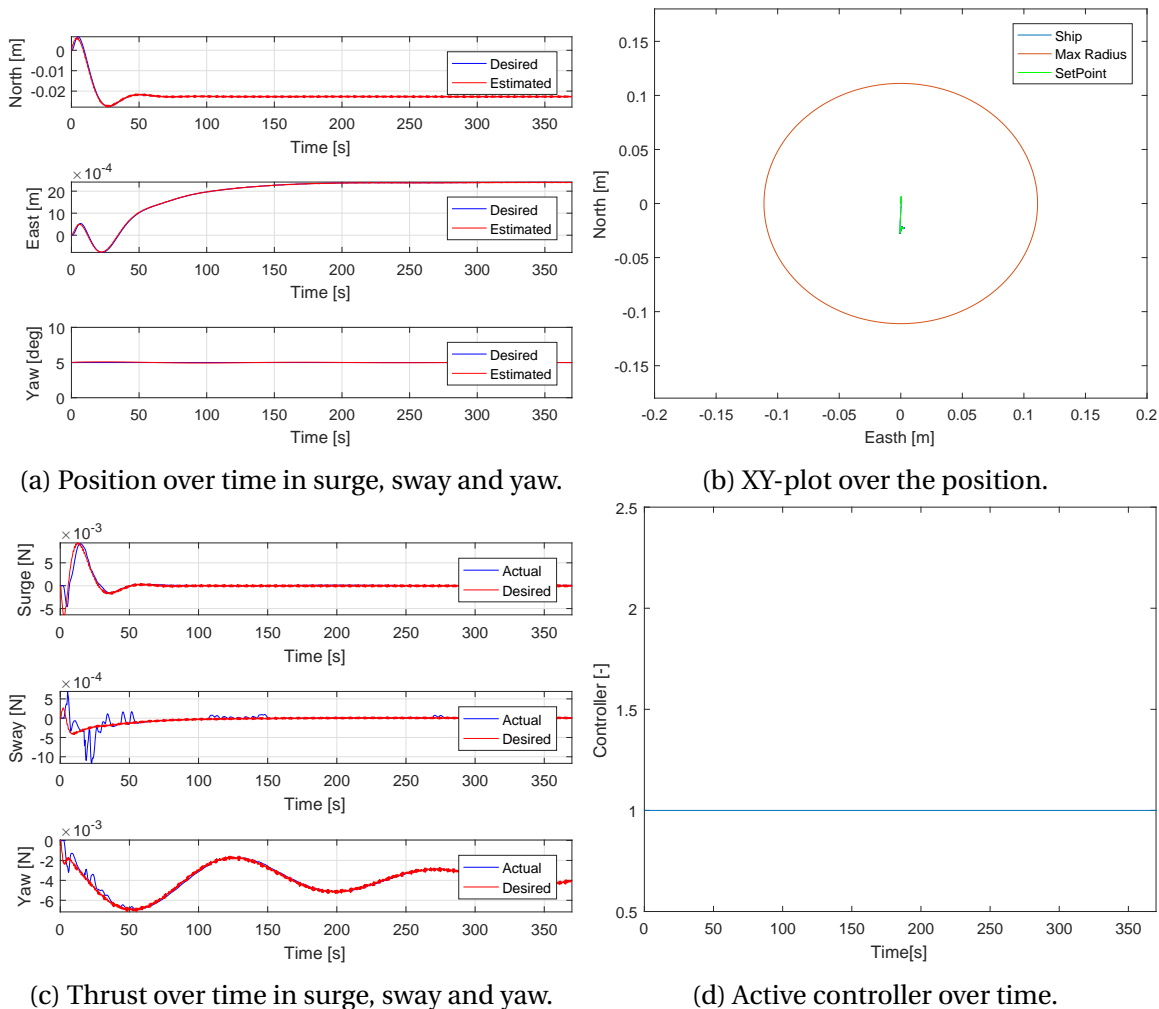


Figure 8.8: Results from hybrid controller with setpoint chasing simulation, with wave height $H_s = 2.5$ meters.

8.2.3.3 $H_s = 4$ m

Figure 8.9 shows the behavior of the vessel and the controller, in waves with $H_s = 4$ meters. As the previous cases, the results in Figure 8.9a and 8.9b shows that the vessel does not move outside the safety circle. So the vessel is positioning itself where the mooring force is equal to the wave force. This can be seen from Figure 8.9c, as the thrust becomes zero. The heading is also controlled to be 5° .

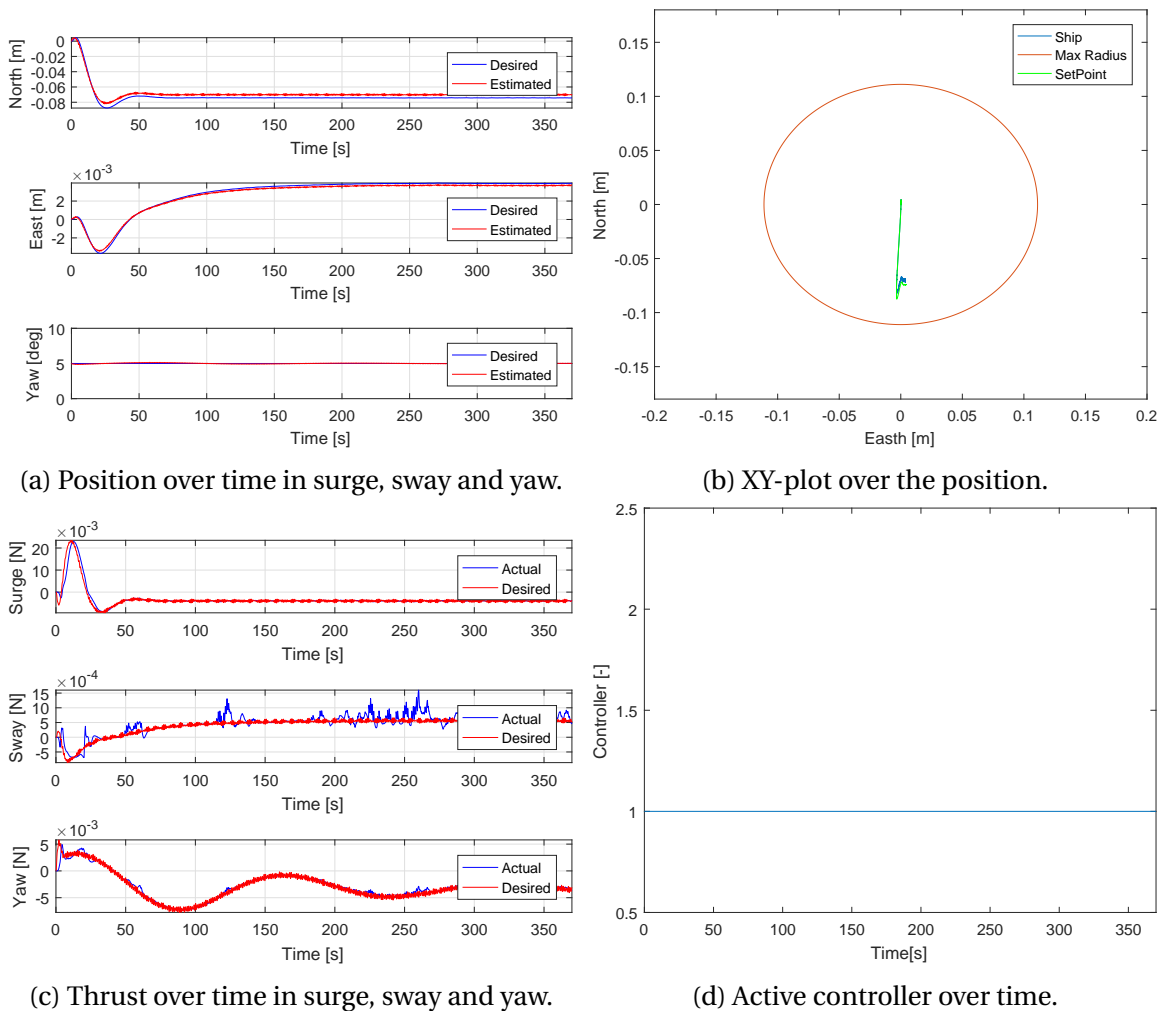
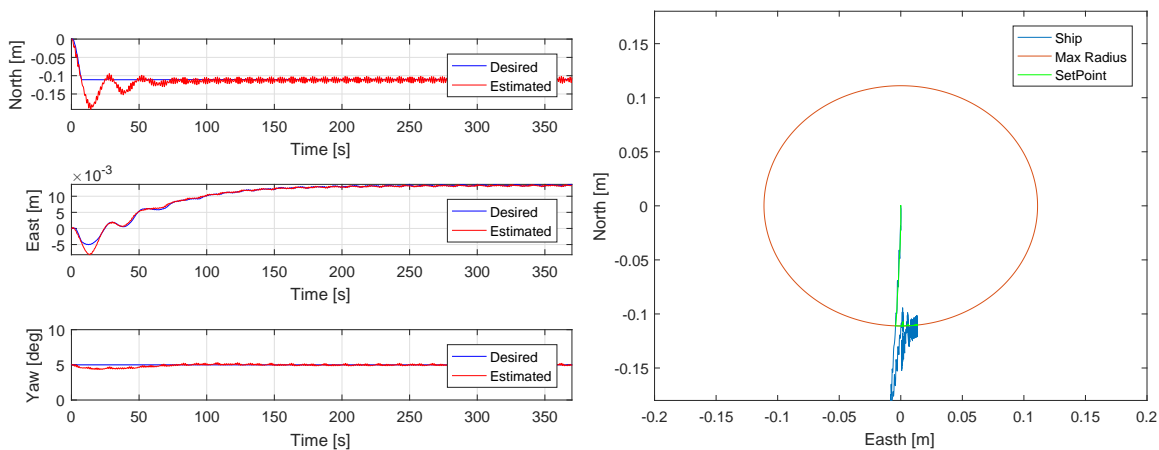


Figure 8.9: Results from hybrid controller with setpoint chasing simulation, with wave height $H_s = 4$ meters.

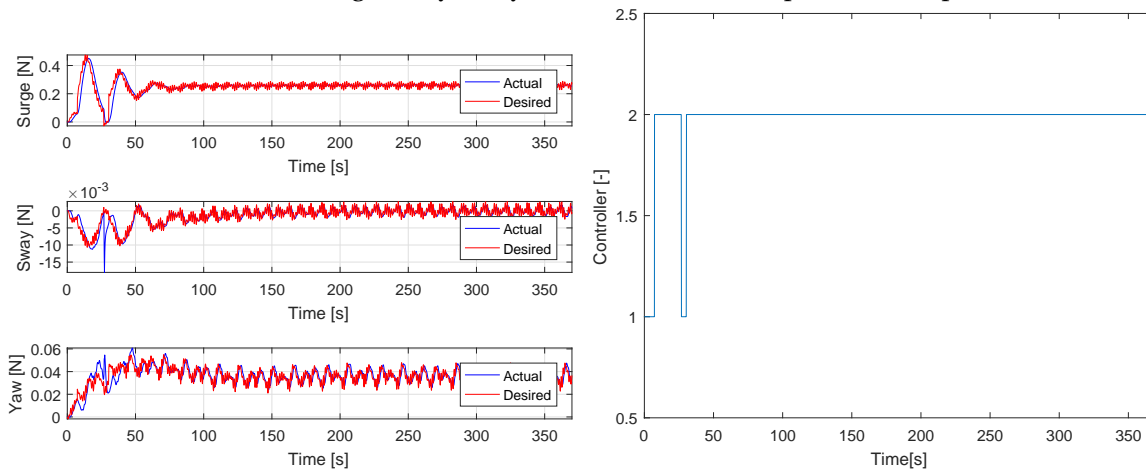
8.2.3.4 $H_s = 9$ m

Figure 8.10 shows the behavior of the vessel and the controller, in waves with $H_s = 9$ meters. Now, the results are different from the previous cases. With the exception of the first 40 seconds, Figure 8.10d shows that the controller is almost constant at controller two. From Figures 8.10a and 8.10b, it can be observed that the vessel now is positioning itself at the edge of the safety circle. Over time the thrust is minimized, as a result of this positioning. This can be observed in Figure 8.10c. As the previous cases, in this case the controller stabilizes the heading at 5° .



(a) Position over time in surge, sway and yaw.

(b) XY-plot over the position.



(c) Thrust over time in surge, sway and yaw.

(d) Active controller over time.

Figure 8.10: Results from hybrid controller with setpoint chasing simulation, with wave height $H_s = 9$ meters.

8.2.4 Additional Hybrid Switching Setup

The additional hybrid switching controller presented in Section 6.2.5, has been simulated in three different sea states; $H_s = 2.5$ meters, $H_s = 4$ meters and $H_s = 9$ meters. This is to check if the switching logic manage to identify the correct sea state, and switch to the corresponding controller.

Figure 8.11 shows that the switching setup manage to identify which wave frequency the vessel encounters. The results show that this have some error in the low frequency area. With higher frequencies, the filter is almost spot on. Then the corresponding controller is selected, with no shattering between controllers. In Figure 8.12, the results have been converted to normal wave height and frequency, for a better understanding.

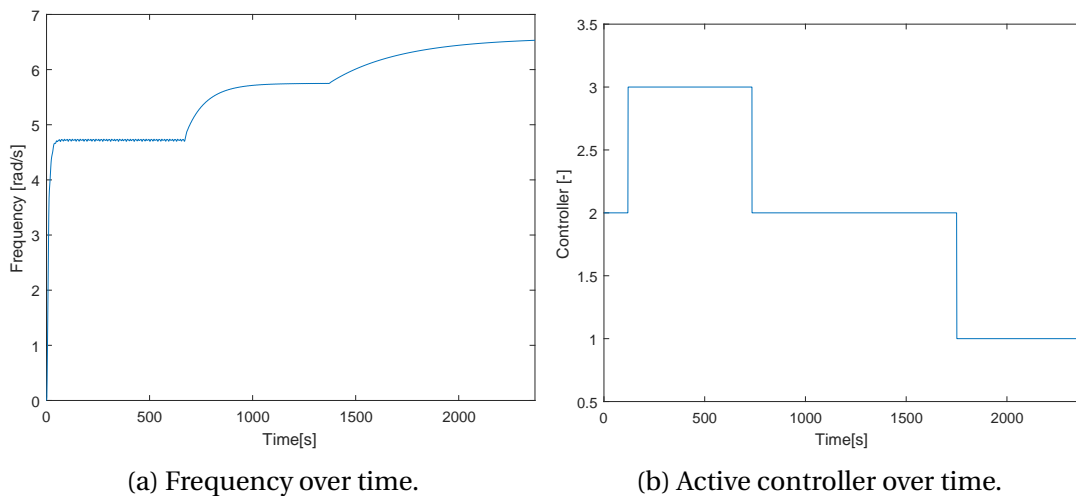


Figure 8.11: Results from the additional hybrid switching setup simulations, with wave heights $H_s = 2.5$ m, $H_s = 4$ m and $H_s = 9$ m.

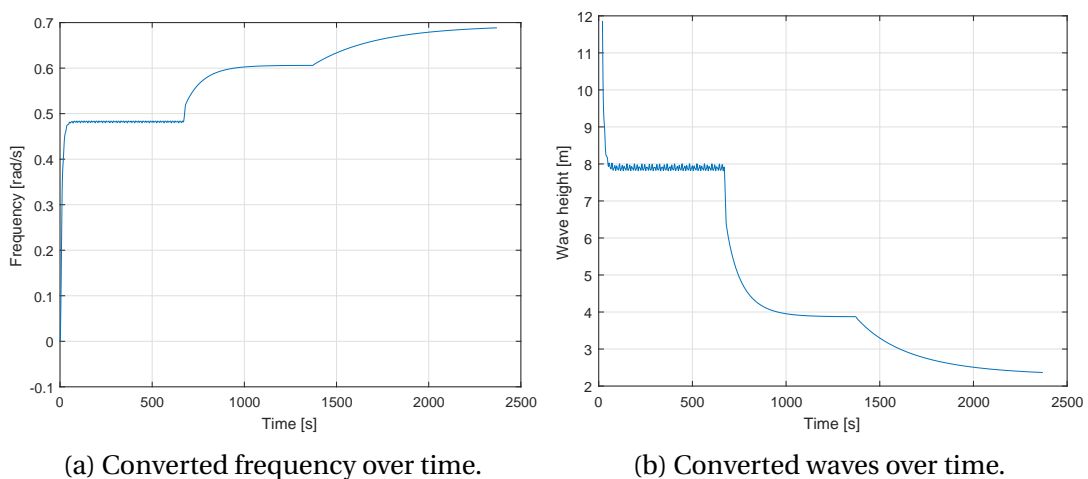


Figure 8.12: The converted wave frequency with corresponding wave height.

8.3 Experiment

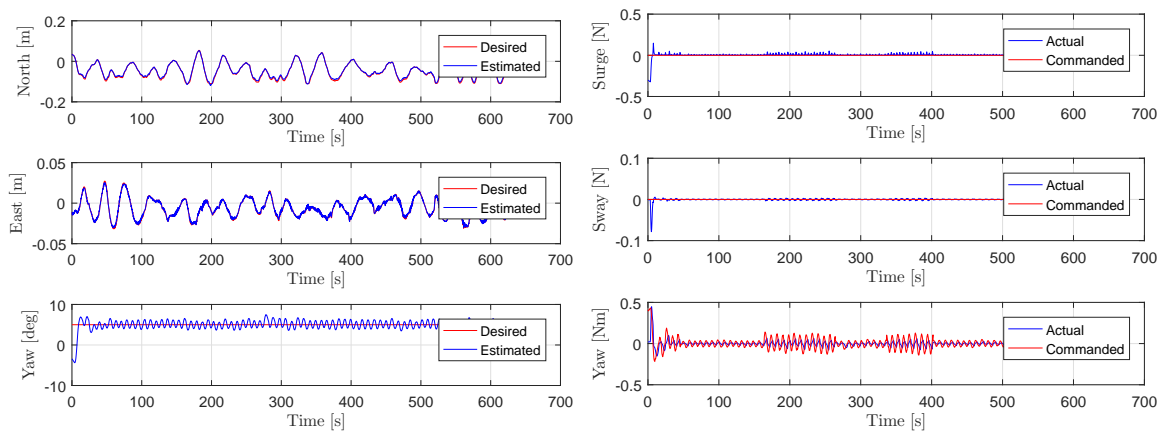
Results from the scale model experiments in the marine cybernetics laboratory are presented in this section. The results are presented in the same manner as the simulations. To recap, the results are presented through 2D-plots of the measured and desired positions, time plots of measured and desired position and heading. The results are divided into three subsections; heading controller, surge/sway damping and restoring controller and hybrid control with set-point chasing. The wave height in the different cases varies, but they all have the same wave direction, at $\beta_w = 180^\circ$.

8.3.1 Heading Controller

The heading controller from Section 6.2.1 is now implemented on the CSAD model. The controller has been tested with two different conditions; $H_s = 4$ meters and $H_s = 9$ meters. This is to evaluate the performance of the heading controller, and compare the results with the ones in Section 8.2.1.

8.3.1.1 $H_s = 4$ m

Figure 8.13 shows the behavior of the vessel in waves with $H_s = 4$ meters. The vessel is kept around the desired heading angle, $\psi = 5^\circ$, as Figure 8.13a shows. From this figure it can be observed that the heading is oscillating. The reason for this will be discussed later in Chapter 9. As Figure 8.13b shows, the thrust is varying. This variation in yaw thrust, is due to that it switches between two controllers. The latter one is more aggressive.



(a) Position over time in surge, sway and yaw. (b) Thrust over time in surge, sway and yaw.

Figure 8.13: Results from heading controller experiments, with wave height $H_s = 4$ meters.

8.3.1.2 $H_s = 9$ m

Figure 8.14 shows the behavior of the vessel in waves with $H_s = 9$ meters. From Figure 8.14a it can be observed that the controller is struggling more to keep the desired heading. The heading is fairly close to 5° , with some spikes occasionally. This is caused by a higher wave encounters the vessel. In this case the vessel is using the more aggressive controller, due to the high waves. As Figure 8.14a shows, the vessel does not manage to stay inside the safety circle. A consequence of this is that the mooring system must withstand all of the wave force.

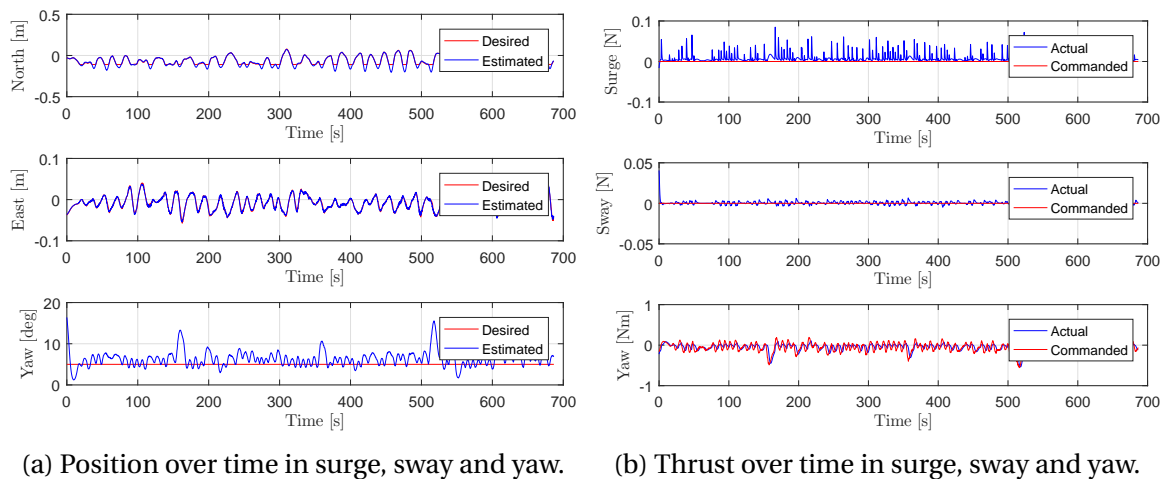


Figure 8.14: Results from heading controller experiments, with wave height $H_s = 9$ meters.

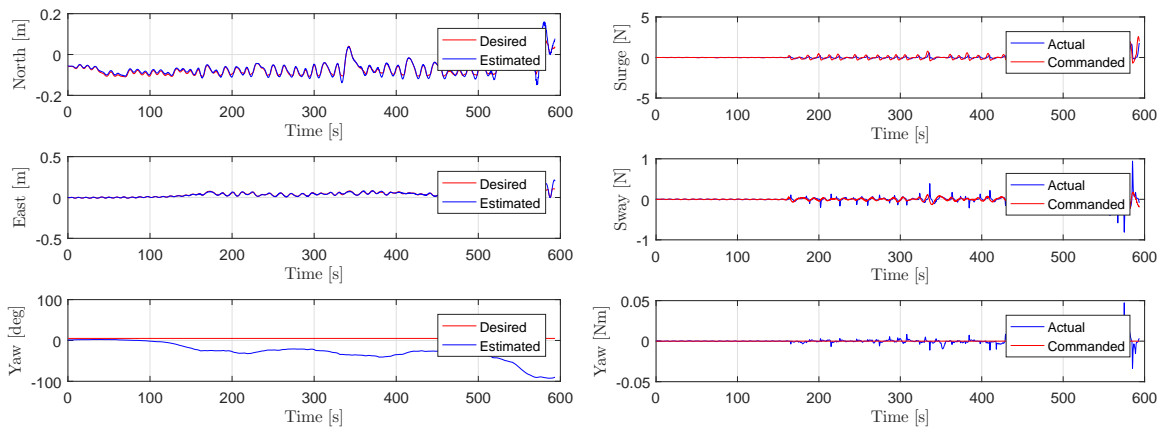
For both cases, the controller ensures that the vessel maintain the desired heading angle. As the position plots in surge shows, there is no other method than the mooring lines to keep the vessel in position.

8.3.2 Surge/Sway Damping and Restoring Controller

The surge/sway damping and restoring controller presented in Section 6.2.2 has been implemented on the CSAD model. The controller has been used in experiments with two different sea states; $H_s = 4$ meters and $H_s = 9$ meters. This is to evaluate the controller results, and compare them to the ones from the simulations.

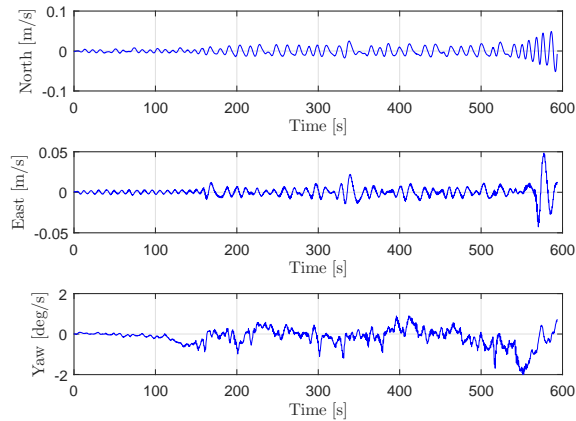
8.3.2.1 $H_s = 4$ m

Figure 8.15 shows the behavior of the vessel in waves with $H_s = 4$ meters. As Figures 8.15a and 8.15b shows, the controller tries to dampen and restore the vessel position. Since the heading is not controlled, the heading error becomes large very fast. This causes a dangerous situation, since the vessel has now the side against the waves.



(a) Position over time in surge, sway and yaw.

(b) Thrust over time in surge, sway and yaw.

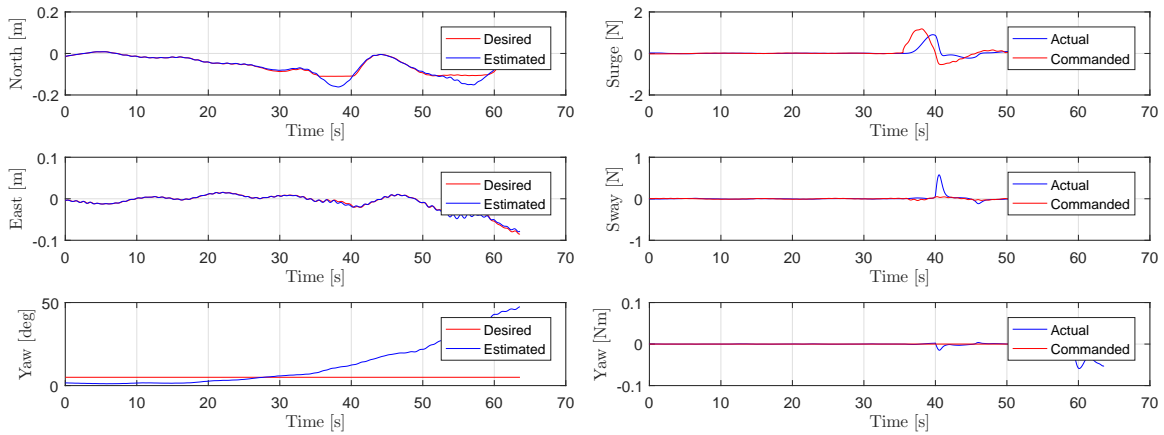


(c) Velocity over time in surge, sway and yaw.

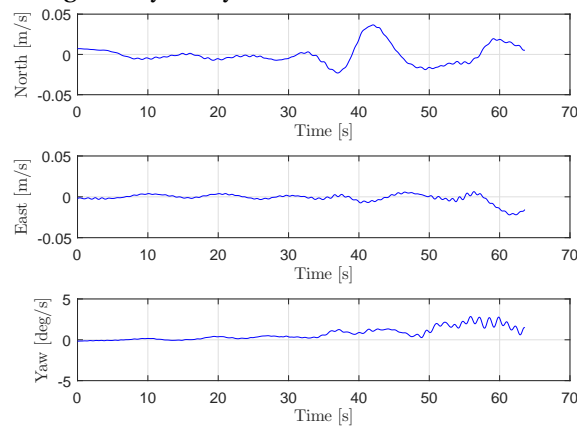
Figure 8.15: Results from surge/sway damping and restoring controller experiments, with wave height $H_s = 4$ meters.

8.3.2.2 $H_s = 9$ m

Figure 8.16 shows that this is a fairly short experiment, due to the heading error becomes large too fast. The same tendencies that were observed for $H_s = 4$ meters are presents for this sea state as well. The only difference is that now; the heading error becomes large in a shorter time-frame as a direct consequence of higher waves.



(a) Position over time in surge, sway and yaw. (b) Thrust over time in surge, sway and yaw.



(c) Velocity over time in surge, sway and yaw.

Figure 8.16: Results from surge/sway damping and restoring controller experiments, with wave height $H_s = 9$ meters.

For both cases the controller dampens the vessel motion and tries to restore the position, but as the heading error becomes large the vessel struggles. This causes the vessel to get its side against the waves, which can cause a dangerous situation.

8.3.3 Hybrid Control with Setpoint Chasing

The hybrid controller with setpoint chasing from Section 6.2.4, has been tested in four different sea states; $H_s = 0.5$ meters, $H_s = 2.5$ meters, $H_s = 4$ meters and $H_s = 9$ meters. Now, the experiments are done to evaluate the performance of having a combination of different controllers. This can then be compared to the results from the simulations in Section 8.2.3.

8.3.3.1 $H_s = 0.5$ m

Figure 8.17 shows the behavior of the vessel and the controller, in waves with $H_s = 0.5$ meters. From Figure 8.17a and 8.17b, it can be observed that the vessel moves more compared to the simulations. As Figure 8.17a and 8.17c shows, the controller is struggling to stabilize the heading. The reason for this will be discussed later in Chapter 9.

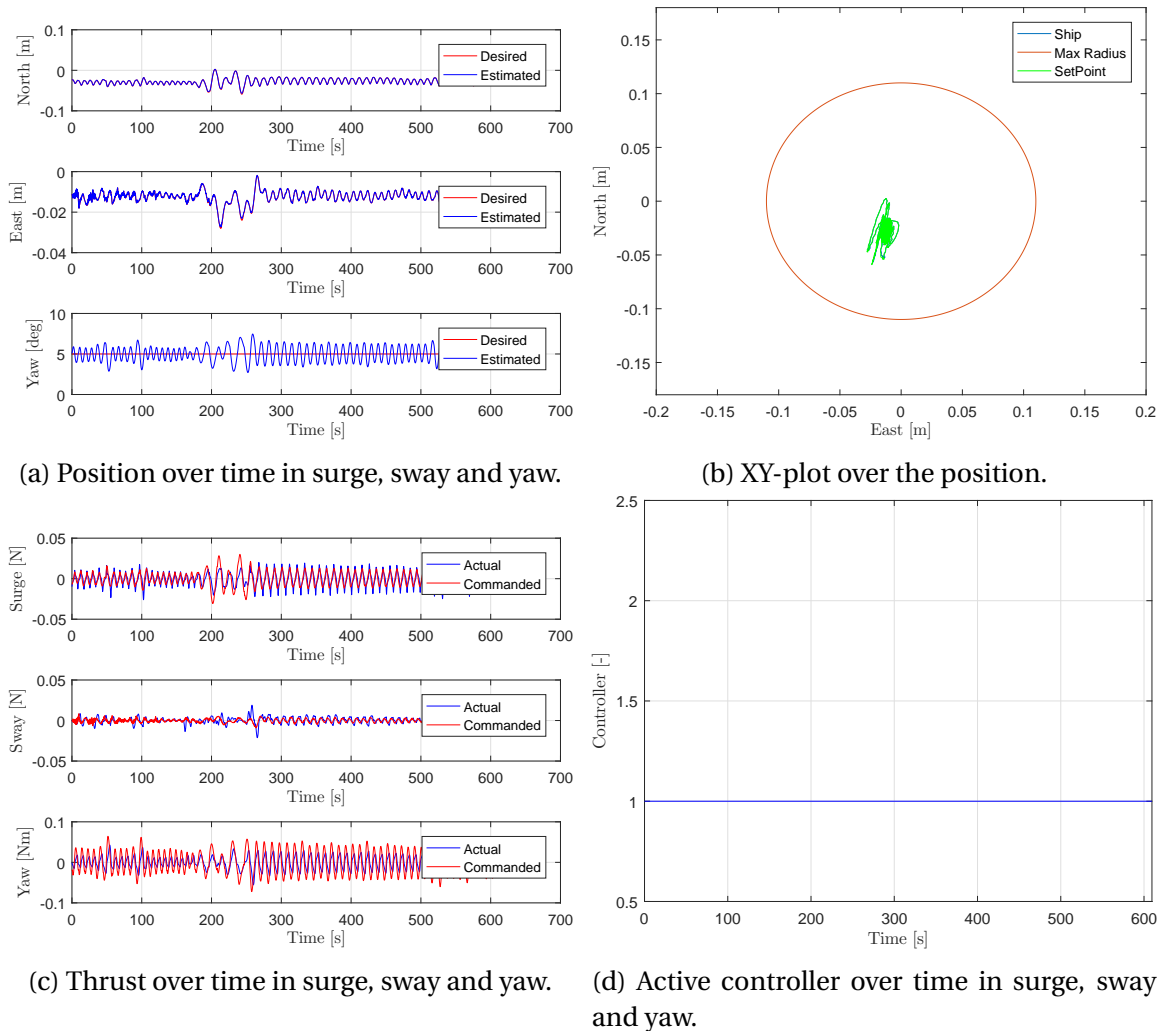


Figure 8.17: Results from hybrid controller with setpoint chasing experiments, with wave height $H_s = 0.5$ meters.

8.3.3.2 $H_s = 2.5$ m

Figure 8.18 shows the behavior of the vessel and the controller, in waves with $H_s = 2.5$ meters. Like in the previous case, the vessel motion is larger than the simulation. This can be seen in Figure 8.18a and 8.18b. Since the vessel stays inside the safety circle, controller one is the only controller used, see Figure 8.18d. As seen in Figure 8.18a and 8.18c, the problem with the heading is also present here.

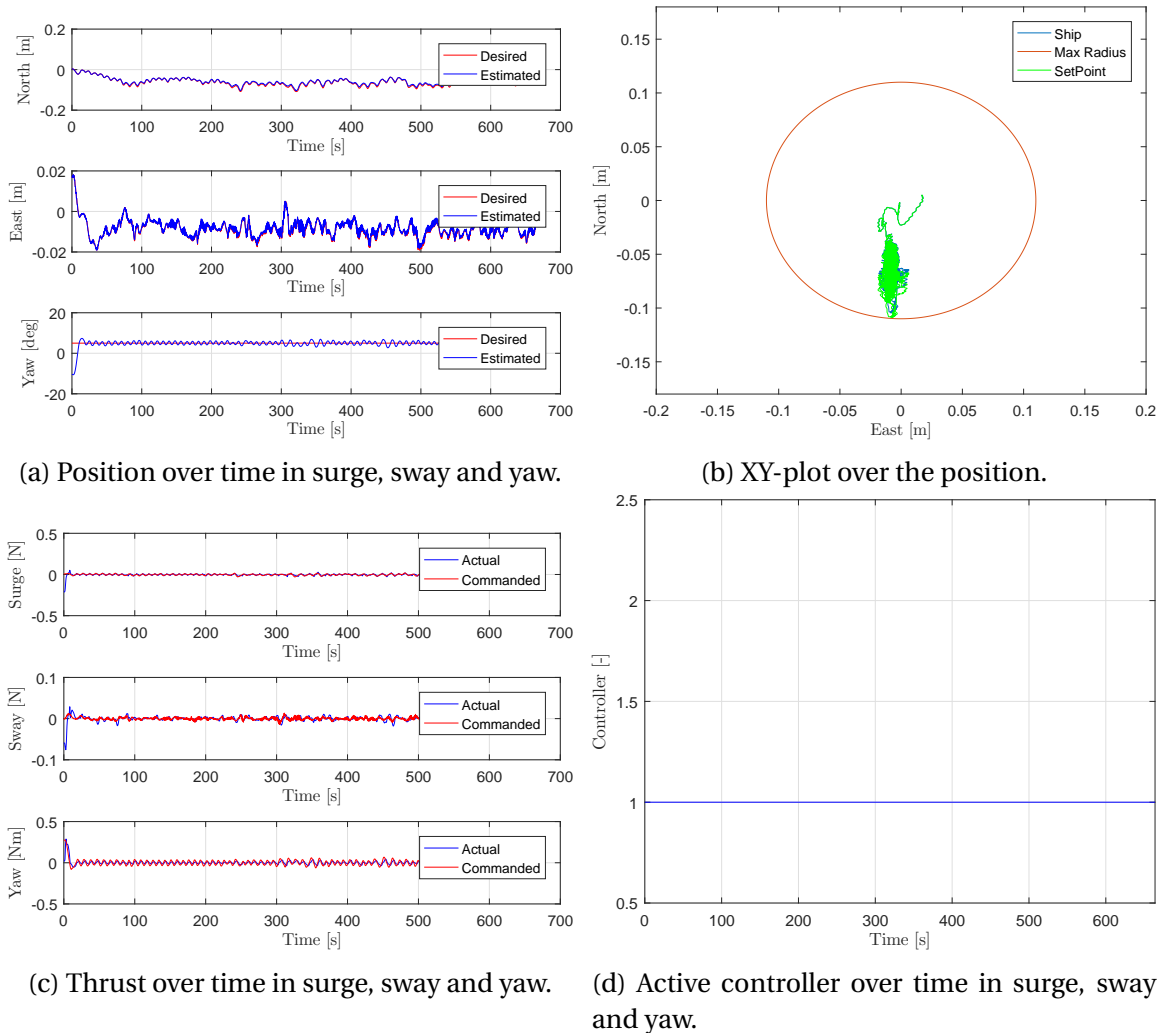
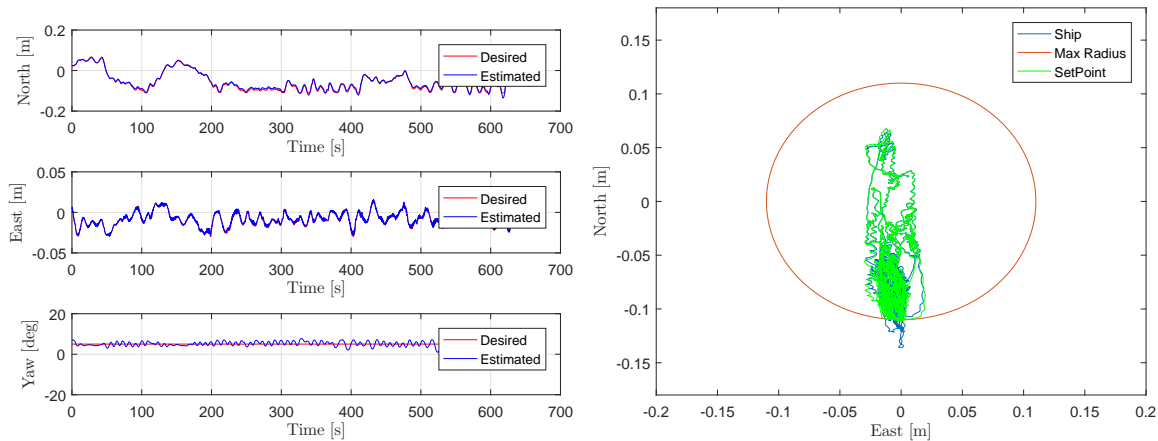


Figure 8.18: Results from hybrid controller with setpoint chasing experiments with wave height $H_s = 2.5$ meters.

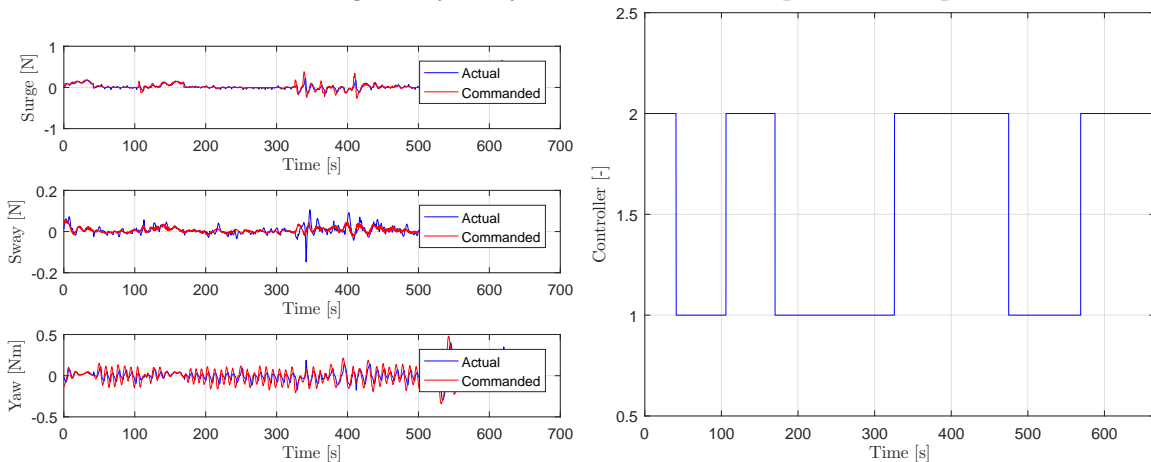
8.3.3.3 $H_s = 4$ m

Figure 8.19 shows the behavior of the vessel and the controller, in waves with $H_s = 4$ meters. From Figure 8.19d, it can be seen that the controllers now switch, according to the switching criteria in Section 6.2.4.1. As a direct consequence of the vessel moving outside the safety circle, Figure 8.19a and 8.19b. The same problem with stabilizing the heading is present in this case as well.



(a) Position over time in surge, sway and yaw.

(b) XY-plot over the position.



(c) Thrust over time in surge, sway and yaw.

(d) Active controller over time in surge, sway and yaw.

Figure 8.19: Results from hybrid controller with setpoint chasing experiments, with wave height $H_s = 4$ meters.

8.3.3.4 $H_s = 9$ m

Figure 8.20 shows the behavior of the vessel and the controller, in waves with $H_s = 9$ meters. From Figure 8.20a and 8.20b, it can be seen that the vessel is centering itself at the edge of the safety circle. Of course, with some variations in all directions. A consequence of this is that controller two is used all the time. This is to keep this position, as controller one is not so aggressive. From Figure 8.20a and 8.20c, the same problem with the heading error can be seen.

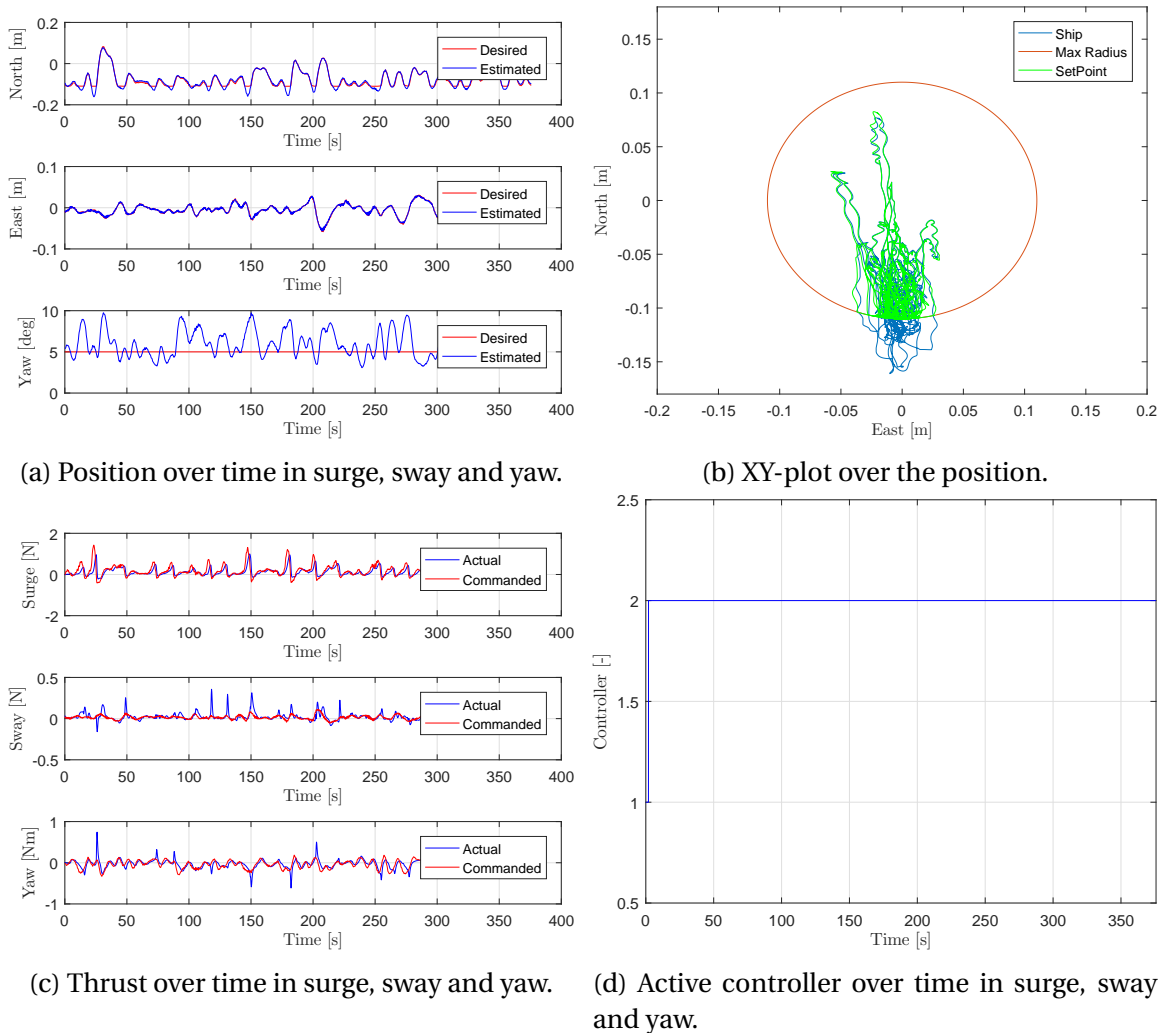


Figure 8.20: Results from hybrid controller with setpoint chasing experiments, with wave height $H_s = 9$ m.

Chapter 9

Discussion

The intention of this thesis was to make a mathematical model corresponding to CSAD, and develop some TAPM control laws to compare towards both the mathematical model and CSAD. The mathematical model was first derived from equations and a parameter identification was performed. Further, the mathematical model was implemented into Simulink, and simulations with the different controllers were performed. Finally, the controllers were implemented on CSAD for scale model testing in the Marine Cybernetics Laboratory. The results from these simulations and experiments are discussed further in this chapter.

9.1 Heading Controller

As presented in Figures 8.3a, 8.4a, 8.13a and 8.14a, the vessel followed the desired heading quite accurately both during simulations and scale model experiments. The deviations between the measured and desired position are small for all simulations for the first case, $H_s = 4$ m. For the $H_s = 9$ m case, there will be a deviation due to that the vessel is outside the safety circle. Regarding the heading error, this is small considering the uncertainties in the simulation model and the laboratory. This will be elaborated in this chapter.

In simulations with the heading controller, the vessel has a very small deviation in heading, 0.5° at most. This occurs when the vessel first encounters the waves, and is normal. Despite some spikes in the heading in the last experiment case, the heading errors have been small for both simulations and experiments. Overall, an exact and accurate control of the vessel's heading has been achieved, and the results is very promising. The heading controller in the scale model tests might be improved by further tuning of the controller. The proposed improvement has not been included, as the results are satisfying, with deviation at a maximum of 5° .

9.2 Surge/Sway Damping and Restoring Controller

The surge/sway damping and restoring controller performs as expected, in both the simulations and the experiments. From Figures 8.5b, 8.6b, 8.15b and 8.16b, the thrust force in surge, sway follows the velocity plots in Figures 8.5c, 8.6c, 8.15c and 8.16c. In addition, Figures 8.5a, 8.6a, 8.15a and 8.16a show that the vessel is trying restore the position in surge and sway.

Comparison of the results from the simulations and the experiments reveals a huge difference in their behavior. As Figures 8.5a, 8.6a, 8.15a and 8.16a show, the heading is drifting way off in the experiments. In the simulation the vessel positions itself against the waves and keeps this heading. This problem is addressed in Section 9.5. As a remark to these results, the vessel is in need of a heading controller to keep its heading, or the vessel will turn as the yaw plots in Figures 8.15a and 8.16a show.

9.3 Hybrid Controller with Setpoint Chasing

As presented in Figures 8.7a, 8.8a, 8.9a, 8.10a, 8.17a, 8.18a, 8.19a and 8.20a, the setpoint generated path for the vessel works very well. The vessel is controlled accordingly to the setpoint, and the thrust is kept to its minimum inside the safety circle. There may be some improvements to the setpoint chasing algorithm, by tuning the non-negative filter gain matrix better, but improvements would be infinitesimal. From Figures 8.10b, 8.19b and 8.20b, it can be seen that the setpoint exceeds the safety circle. If the vessel exits, Figures 8.10d, 8.19d and 8.20d, show that the switching between the controllers works perfectly, and does not make the controlled system unstable.

As seen in the yaw plot in Figures 8.17a, 8.18a, 8.19a and 8.20a, the same problem with the heading occurs here also. As mentioned earlier, reasons for this is discussed later in Section 9.6.

Since the controllers are reactive, which means that the incident has to happen before the controller react, there will be a deviation from the desired position. This is caused by the varying wave height that encounters the vessel. A system that may remove the deviation, are proactive controllers. These controllers have inputs on how the environmental forces will act, and responds with the correct thrust to withstand these forces at impact. More on this topic and more effective stationkeeping in ice, are presented by Skjetne et al. (2014).

9.4 Additional Hybrid Switching Setup

From Figures 8.12a and 8.12b, the switching logic is able to determine what wave frequency the vessel encounters. As the figures show, it is more precise when the vessel encounters a higher wave frequency. This has to do with that the acceleration motion of the model is more distinct at higher frequencies, so the Aranovskii filter manages to find the frequency more efficiently. There are also some uncertainties to this method of finding the wave frequency, since this is simulated with no noise input on the acceleration measurements. With noise present the filter may not manage to find the correct frequency. This problem on the other hand can be solved by using a lowpass filter to remove some of the noise.

9.5 Simulation Uncertainties

In the simulations there can be some uncertainties that leads to wrong results. First of all, the method to identify the system parameters for the vessel may not have given the correct values, if we compare the behavior from the simulations and the experiments. The reason for this may come from the vessel drawing in ShipX, since this was missing the cylindrical hole where the turret is mounted. The outcome of this is that the simulation model's mass is larger than the scale model. Other errors may lead from this, for example the damping and restoring terms will be different. In addition to this, the vessel RAOs, generated to get the correct response from the vessel when it encounters waves, may be wrong. The difference in vessel response can especially be seen, if the heading in Figures 8.4a and 8.14a are compared.

When it comes to the 3 DOF simulations, there are uncertainties due to some coupling terms have been copied from CSIII. The rest of the damping terms may also be questioned, since drag test results contained a significant amount of noise. All in all, this will give a good estimation on how the vessel will behave. Like any simulations, the transition from a simulation model to a scale model requires tuning of the controllers.

Finally, the full scale mooring model, developed by Ren (2015), may not have been scaled correctly to fit the simulation model. This scaling was done by Froude scaling, which should give an accurate scaling.

9.6 Experiment Uncertainties

There are several uncertainties in this kind of experiments with a scale model. There are probably many uncertainties that the author has not recognized, but the ones identified will be presented in this section.

First of all, the positioning system in the Marine Cybernetics laboratory is extremely sensitive regarding the vessel position, and the connection can easily be lost while running the experiments. This can create deviations in the position, or may require new simulations due to loss of signal.

Second, the mooring system used may not be correct according to scale and the mooring model from Ren (2015). The springs used may have been too stiff or too loose, and the mooring lines may not have been tightened enough. All in all, this setup gave damping and restoring forces, just like a mooring system does, but it may not be in desired scale as mentioned.

Another uncertainty can be the thrust allocation implemented in the model, in order to account for the mappings between thrust output and hardware on the model. This may be the reason for the heading deviation in the results, and different thrust allocation, with fixed thrusters, could reduce these deviations.

There are overall many uncertainties causing the deviations in the results, which is why the achieved results should be considered satisfactory, despite of these uncertainties.

As general remarks to both the simulations and experiments, it may be hard to tune the different controllers and observer. During the simulation and experiments, this has been done manual by using trial and error method, until the best and most stable response was achieved.

Chapter 10

Concluding Remarks

10.1 Conclusion

This thesis has focused on developing a scale model of an arctic drillship, the C/S Inocean Cat I Drillship. A literature review was conducted, with focus on a general approach to TAPM systems, to learn the basic functions that are different from traditional DP and mooring systems. In addition to this, a study on the equipment and other cyberships were performed, to get familiar with the different aspects in the C/S Inocean Cat I Drillship.

The C/S Inocean Cat I Drillship has been designed, constructed and assembled, according to plans from Bjørnø (2015) with minor modifications. This has now given NTNU a new research platform in MC Lab. However, work still remains to improve the C/S Inocean Cat I Drillship even better. The model is easy to operate and control, and the combination with cRIO, VeriStand and Simulink are simple to use. There are some limitations from Simulink to VeriStand model, but these may be solved in different ways.

A simulation model has been derived, based on the model scale C/S Inocean Cat I Drillship. This model has been implemented in Simulink. The moored vessel is under impact from environmental loads, and different control algorithms are used. The controlled system is stable under given conditions, but the results are different if compared to the experiments. These differences need to be solved, so a more precise simulation model has to be developed. All in all, the simulation model gives a good prediction how the results will be in the experiments.

A functioning TAPM system was demonstrated, but the performance was not perfect. This could have been improved by making a more sophisticated mooring system, that enhance the possibilities of damping and restoring. The time spent on tuning the different controllers may have also improved the performance. Other functions were also implemented, but not demonstrated in this thesis, since these are basic functions. The HMI created gives the user the necessary infor-

mation to operate the vessel. This HMI can easily be modified by the user to fit their needs.

The topic of this master thesis has been interesting and challenging. It is hoped that this thesis, with the following master thesis' will stimulate further development in the field of thruster-assisted position mooring systems.

10.2 Further Work

Based on the conclusion, there are still parts that need to be sorted out on C/S Inocean Cat I Drillship. Both the simulation model and the scale model need improvements, to make this research foundation even better.

The simulation model needs improvements, to make this model more equal to the scale model. Some of the differences that have been found and need to be sorted out are:

1. The 6 DOF model is based on simplified work drawings, since this drawing is missing the hole for the turret in the hull. Sorting this out will probably fix some differences, but not all.
2. Another thing for the 6 DOF model is that the mooring model needs to be more similar to the one used in the experiments.
3. Sort out how the vessel responses are by making the RAOs from experiments, such that the simulation model will behave similarly.
4. For the 3 DOF, more tests have to be performed to replace the values copied from CSIII.

For the scale model there is also improvements to be done. The following list is improvement that are discovered, but there may be more.

1. Fit the model with IMU, as intended, to measure the acceleration. This will open up for more complex control algorithms, by using acceleration feedback among other.
2. The lid on the model is made out of Plexiglas, which will easily fracture if the screws are tighten too hard. To sort this out, another material has to be used. The easiest solution is to fit a metal edge on the existing lid, so that this takes the stress away from the holes in the Plexiglas where the screws are, and distributes it over a wider area.
3. Another improvement that is desired, is the ability to force the turret to turn. This solution needs a replacement of the turret, such that a servo can turn it around. This servo is already bought, and are the same as the ones that turn the thrusters.
4. As a last item on the improvement list, the mooring system needs to be made in scale with the correct restoring and damping ability.
5. An error message comes up during the first minutes, when the file are deployed onto the vessel. If possible, this error message needs to be sorted out, such that there is no need for restarts.

Bibliography

- Aalbers, A., Janse, S., and Boom, W. D. (1995). DP Assisted and Passive Mooring for FPSO's. *Offshore Technology Conference*.
- aero naut (2015). Precision Schottel drive unit 30mm. Retrieved 14th of November 2015, from <http://www.aero-naut.de/typo3temp/pics/fe12866e10.jpg>.
- Aranovskii, S. V., Bobtsov, A. A., Kremlev, A. S., and Luk'Yanova, G. V. (2007). A robust algorithm for identification of the frequency of a sinusoidal signal. *J. Comput. Syst. Sci. Int. Journal of Computer and Systems Sciences International*, 46(3):371–376.
- Berntsen, P. I. B., Aamo, O. M., and Leira, B. J. (2006). Dynamic positioning of moored vessels based on structural reliability. *Proceedings of the 45th IEEE Conference on Decision and Control*.
- Bjørnø, J. (2015). Development of the “C/S Inocean Cat I Drillship” Model. Unpublished project thesis, Norwegian University of Science and Technology, Trondheim, Norway.
- Fossen, T. (2001). Nonlinear passive weather optimal positioning control (WOPC) system for ships and rigs: experimental results. *Automatica*, 37(5):701–715.
- Fossen, T. I. (2008). Description of MSS Vessel Models: Configuration Guidelines for Hydrodynamic Codes. http://www.marinecontrol.org/pdf/2008_06_19_MSS_vessel_models.pdf.
- Fossen, T. I. (2011). *Handbook of Marine Craft Hydrodynamics and Motion Control*. John Wiley & Sons, Ltd.
- Fossen, T. I. and Perez, T. (2004). Marine Systems Simulator (MSS). <http://www.marinecontrol.org>.
- Frederich, P. (2016). Constrained Optimal Thrust Allocation for C/S Inocean Cat I Drillship. Unpublished master thesis, Norwegian University of Science and Technology, Trondheim, Norway.

- Hespanha, J. P. (2002). Tutorial on Supervisory Control. *Lecture Notes for the workshop Control using Logic and Switching for the 40th Conf. on Decision and Contr., Orlando, Florida.*
- International Maritime Organization (IMO) (1994). Guidelines for vessels with dynamic positioning systems. <http://www.uscg.mil/hq/cg5/ocsncoe/docs/DP%20Guidance/IMO%20MSC%20Circ.645.pdf>.
- ISO (2013). Petroleum and natural gas industries - specific requirements for offshore structures, part 7: Stationkeeping systems for floating offshore structures and mobile offshore units. ISO ISO/TC 67/SC 7, Under development.
- Jorde, J. (2014). Design & Engineering Innovation of Statoil's CAT I Arctic Drillship. Presented at the IBC 3rd Annual Drillships, Singapore.
- Kjerstad, O. K. and Breivik, M. (2010). Weather Optimal Positioning Control for Marine Surface Vessels. *IFAC Proceedings Volumes*, 43(20):114–119.
- Leira, B. J., Berntsen, P. I., and Aamo, O. M. (2008). Station-keeping of moored vessels by reliability-based optimization. *Probabilistic Engineering Mechanics*, 23(2-3):246–253.
- MARINTEK (2014). Model testing of offshore structures. Retrieved 25th of January 2016, from http://www.ivt.ntnu.no/imt/courses/tmr7/lecture/Offshore_testing-cmu-v1-2014_small.pdf.
- National Instruments (2015). What is the CompactRIO Platform? Retrieved 10th of October 2015, from <http://www.ni.com/compactrio/whatis/>.
- Nguyen, D. T., Blanke, M., and Sørensen, A. J. (2007). Diagnosis and Fault-Tolerant Control for Thruster-Assisted Position Mooring. *IFAC Proceedings Volumes*, 40(17):287–292.
- Nguyen, D. T. and Sørensen, A. J. (2009a). Setpoint Chasing for Thruster-Assisted Position Mooring. *IEEE Journal of Oceanic Engineering IEEE J. Oceanic Eng.*, 34(4):548–558.
- Nguyen, D. T. and Sørensen, A. J. (2009b). Switching control for thruster-assisted position mooring. *Control Engineering Practice*, 17(9):985–994.
- Nielsen, U. D., Bjerregård, M., Galeazzi, R., and Fossen, T. I. (2015). New Concepts for Shipboard Sea State Estimation. In *OCEANS 2015 - MTS/IEEE Washington*, pages 1–10.
- Nilsen, T. (2003). *Development of Cybership III*. Master thesis, Norwegian University of Science and Technology.
- NTNU (2015a). Handbook of Marine HIL simulation and Marine cybernetics laboratories. Retrieved 5th of September 2015, from https://github.com/NTNU-MCS/MC_Lab_Handbook.

- NTNU (2015b). Marine cybernetics laboratory (mc-lab). Retrieved 10th of October 2015, from <http://www.ntnu.edu/imt/lab/cybernetics>.
- Price, W. G. and Bishop, R. E. D. (1974). *Probabilistic Theory of Ship Dynamics*. Chapman and Hall.
- Ren, Z. (2015). *Fault-Tolerant Control of Thruster-Assisted Position Mooring System*. Master thesis, Norwegian University of Science and Technology.
- Sørensen, A., Strand, J., and Fossen, T. (1999). Thruster assisted position mooring system for turret-anchored FPSOs. *Proceedings of the 1999 IEEE International Conference on Control Applications (Cat. No.99CH36328)*, 2:1110–1117.
- Sørensen, A. J., Leira, B., Strand, J. P., and Larsen, C. M. (2001). Optimal setpoint chasing in dynamic positioning of deep-water drilling and intervention vessels. *International Journal of Robust and Nonlinear Control Int. J. Robust Nonlinear Control*, 11(13):1187–1205.
- Sørensen, A. J. and Strand, J. P. (2000). Positioning of small-waterplane-area marine constructions with roll and pitch damping. *Control Engineering Practice*, 8(2):205–213.
- Skjetne, R. (2014). Report: Literature Survey on Position Mooring Control Systems. Unpublished work, Norwegian University of Science and Technology, Trondheim, Norway.
- Skjetne, R. (2015). Work Note: ROV control modes. Unpublished work, Norwegian University of Science and Technology, Trondheim, Norway.
- Skjetne, R., Imsland, L., and Løset, S. (2014). The Arctic DP Research Project: Effective Station-keeping in Ice. *MIC Modeling, Identification and Control: A Norwegian Research Bulletin*, 35(4):191–210.
- Statoil (2012). Rig strategy. Retrieved 25th of May 2016, from <http://www.statoil.com/en/TechnologyInnovation/TechnologyManagement/Pages/Statoils%20riggstrategi.aspx>.
- Strand, J. P. and Fossen, T. I. (1999). Nonlinear passive observer design for ships with adaptive wave filtering. *New Directions in nonlinear observer design Lecture Notes in Control and Information Sciences*, page 113–134.
- Strand, J. P., Sørensen, A. J., and Fossen, T. I. (1998). Design of automatic thruster assisted mooring systems for ships. *MIC Modeling, Identification and Control: A Norwegian Research Bulletin*, 19(2):61–75.
- Wassink, A. and List, R. V. D. (2013). Development of Solutions for Arctic Offshore Drilling. *SPE Arctic and Extreme Environments Technical Conference and Exhibition*.

Appendix A

Instruction Manuals for C/S Inocean Cat I Drillship

These manuals provides the necessary information to operate the C/S Inocean Cat I Drillship. It is assumed that the same equipment used during this thesis is available, and can be used. If more help is needed, check the Marine Cybernetics Laboratory handbook (NTNU, 2015a).

A.1 OCA-150 Manual

O.S. ENGINE

IMPORTANT: It is of vital importance, before attempting to operate your OCA-150 to read through this instruction manual.

BRUSHLESS MOTOR ESC FOR HELICOPTERS/AIRPLANES OCA-150



INSTRUCTION MANUAL

● Corresponding motors

For airplanes: Check the specifications of the motor and relationship with the propeller (Dia. and pitch) and select propellers with which more than 45A current may not flow.

※ O.S. brushless motors OMA-3810-1050, OMA-3815-1000, OMA-3820-1200 and OMA-3825-750 are recommended. Even with these motors, carefully select Propellers with which more than 45A current may not flow.

For helicopters (suitable for 450 class helicopters): Select motors of 3500~4400 KV values. (400~550W class)

※ The motor of more than 45A maximum current cannot be used, otherwise the ESC may be failed.

The OCA-150 is ECS installed with the latest FET for brushless motors. By using an optional extra ESC Programmer OCP-1, settings of ESC can be programmed quickly and securely to meet model's specific requirements.

● Before operating OCA-150

※ **Misuse or abuse of LiPo batteries is very dangerous. Be sure to follow the instruction manual supplied with the batteries.**

※ **Be sure to install the connectors which match the batteries, securely soldering to the battery connecting wires of the ESC. Never use the ESC with the connectors temporarily connected.**

※ **Batteries can be used: LiPo 2~6 cells (7.4~22.2V), NiCd/NiMH 6~18 cells (7.2~21.6V)**

※ **OCA-150 is equipped with BEC output as power output for receiver. Do not connect the battery for receiver when connecting the OCA-150. If both the ESC**

■ Notes on installation

⚠ WARNINGS

⚠ **Never use the OCA-150 beyond the working conditions listed in the specifications listing.**

⚠ **Do not mistake the polarity of the batteries.**

※ Reverse connection may cause fire and ESC will be damaged or be burnt instantly.

⚠ **Never short out any place of the ESC, batteries, motor, receiver and connectors.**

※ Short circuit may cause fire and ESC will be damaged or be burnt instantly.

※ Be sure to install the ESC so that the soldering connection of the input/output wires may not touch conductive part.

⚠ **Be sure to install the receiver and receiver antenna away from the place where high current flows such as ESC, motor wires, battery wires, power batteries.**

※ Malfunction of the receiver due to noise will cause to lose model control which is very dangerous.

⚠ **Be sure to insert connectors all the way securely.**

※ Disconnection due to vibration may cause to lose model control which is very dangerous.

⚠ **Be sure to install the ESC so that oil, grease and water may not come in contact with the ESC.**

⚠ **Be sure to install the ESC at the place where there is plenty of air flow for cooling.**

⚠ **Do not wrap the ESC with aluminum foil, etc.**

※ Wrapping may spoil cooling effect and the ESC may not develop its original performance.

⚠ **Be sure to install the motor securely and fix all the wires.**

⚠ NOTE

⚠ **Do not disassemble. Do not open the ESC case.**

※ Opening of the case may cause damage inside components and render it irreparable.

■ Notes on operation

⚠ WARNINGS

⚠ **Never touch or allow any part of the body to come into contact with any rotating part while operating.**

※ Sudden rotating may cause serious injury.

※ Be careful with some receivers the motor may rotate for a moment when the power puts on.

⚠ **Do not fly when rainy.**

※ Entry of water drops into the ESC may cause malfunction and out of model control which is very dangerous. Also, it will cause failure. If malfunction is detected due to entry of water drops, send the ESC to the manufacturer or its distributor in each country for inspection and repair.

⚠ **Be sure to follow the procedures mentioned below as to ON and OFF of the power switch.**

● **ON:** Hold the throttle stick at stop position. Switch on the transmitter then receiver power.

● **OFF:** Hold the throttle stick at stop position. Switch off the receiver then transmitter power.

※ With reverse procedure propeller may rotate suddenly, which is very dangerous.

⚠ **Be sure to remove the batteries when not in use.**

※ Accidental switching on may cause sudden rotating of propeller or cause fire, which is very dangerous.

⚠ **Be sure to check the ESC and all the movements of model controls before attempting flight.**

※ Incorrect settings or using of unsuitable model may cause to lose model control which is very dangerous.

⚠ NOTE

⚠ **Do not touch the motor nor ESC right after flight.**

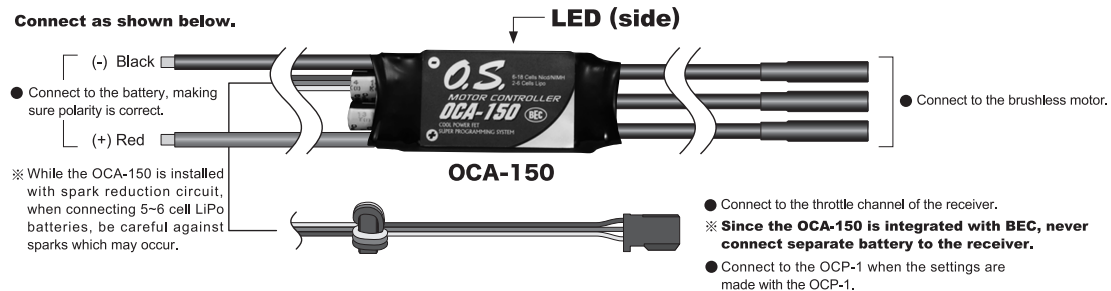
※ Touching them may cause burn.

HOW TO CONNECT THE OCA-150

(PREPARATION)

Solder the corresponding battery connector to the battery connection wires of the ESC. Also, use a heat-shrink tube to isolate the connection. Solder the corresponding connectors (female) to the motor connection wires of the ESC. Also, use a heat-shrink tube to isolate the connection.

Connect as shown below.



SETTING OF THROTTLE POSITIONS



Set the high point and the slowest point as follows.
(In case of model type AIR/HELI)

Preparation

As explained before, connect the ESC, receiver and motor. **Do not connect power battery at this time.**

Preparation

Set the throw angle of the throttle channel on the transmitter 100%. **In case of Futaba, set the reverse function of the throttle channel to the reverse.**

Procedure	Stick	LED
① Power the transmitter on and hold the throttle stick at full high.		---
② Connect the power battery. ● 10 seconds after a short beep, a double beep is emitted.		Lights up
③ Within 3 seconds after the step ②, fully pull down the throttle stick. ● After a short beep, a double beep is transmitted.		
④ Disconnect the power battery.		

※ When the LED on the ESC flashes, reverse the throttle channel using the servo reverse function on the transmitter. Disconnect the power battery and repeat the procedure from the beginning.

※ In case of model type CAR or BOAT and reverse function ON, step ③ should be replaced with the following.

Set the throttle stick neutral (a short beep)→reverse(a short beep)→(a double beep)→disconnect power battery to set high point, neutral point and reverse point.

SETTING OF PARAMETERS

Five parameters can be set without using the programmer in the following manner.

No.	Parameter type	When selecting the parameter	When checking and changing the parameter	
		LED/Beep	LED Lights up/ Beep (every 2 seconds)	LED flashes/ Beep (every 0.5 seconds)
1	Battery type	One flash/Beep (continues)	LiPo	NiCD/NiMH
2	Direction of motor rotation	Two flashes/Beeps (continues)	Normal	Reverse
3	Governor ON/OFF (HELI) Brake ON/OFF (AIR) Reverse ON/OFF (CAR/BOAT)	Three flashes/ Beeps (continues)	OFF	ON
4	Model type	Four flashes/Beeps (continues)	AIR	HELI
5	Model type	Five flashes/Beeps (continues)	BOAT	CAR



(IMPORTANT) After setting model type at No.4 or No.5, do not check the setting, or the different model type will be overwritten.

How to select parameter type (number).

Select the parameter type (number) with the following procedure.

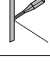


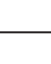
Preparation

As explained before, connect the ESC, receiver and motor. **Do not connect power battery at this time.**

Procedure	Stick	LED
① Switch the receiver on and hold the throttle stick at full high position.		---
② Connect the power battery. ● 10 seconds after a short beep, a double beep is emitted and after 3 seconds a long double beep is emitted. ● Then, very short beep continues. (This confirms the parameter No.1 is selected.)		Lights up
③ Move the throttle stick quickly high→slow→high. ● Very short double beep continues. (This confirms the parameter No.2 is selected.)		
By repeating step③, parameter No.3 (to be confirmed by very short triple beep) through parameter No.5 (to be confirmed by very short quintuple beep) can be selected.		

How to change parameter.

After selecting the parameter No. as explained above, change the parameter with the following procedure.

Procedure	Stick	LED
(Parameter to check or change is being selected.)		Flashes
① Hold the throttle stick at the slowest position. ● After 3 seconds, a beep is emitted. ● Then, LED and beep show the current setting.		Lights up or Flashes
(to change the current setting) Move the throttle stick quickly slow→high→slow. ● LED indication and beep change to confirm setting changed.		
② (to return to parameter No. selection) Move the throttle stick to full high position. ● A double beep is emitted to confirm returned to parameter selection.		Flashes
③ Disconnect the power battery ● Setting is saved.		

INITIAL SETTING

The following example explains how to set initial setting to use governor (in case of HELI) or air brake (in case of AIR).

SETTING OF THROTTLE POSITIONS

Store full high and slowest positions of the throttle stick in the ESC.

※ Follow the SETTING OF THROTTLE POSITIONS procedure explained before.

SETTING OF PARAMETERS

Set each parameter of the ESC according to the using conditions.

(IMPORTANT)

With the OCA-150, model type AIR is stored as default. First select model type AIR or HELI and make each setting.

SELECTION OF BATTERY TYPE (Parameter No.1)

Select according to the type of power battery to use.

LiPo: LiPo battery

NiCD/NiMH: NiCd battery or Nickel-metal hydride battery

ON/OFF OF GOVERNOR (Parameter No.3) (In case of HELI)

To use governor function, set ON.

ON/OFF OF AIR BRAKE (Parameter No.3) (In case of AIR)

To use air brake function, set ON.

※ Set each parameter following the SETTING OF PARAMETERS explained before.

※ Detailed setting of parameter can be set using the optional extra ESC Programmer OCP-1.

After completing the initial setting, disconnect the power battery.

NORMAL OPERATION

WARNINGS

- ⚠ **Be sure to set the parameters according to the throttle positions and using conditions before using the OCA-150.**
- ⚠ **When normal operation is ready, check the direction of motor rotation. If the rotation is reverse, correct it by re-setting of the parameter or changing connection of the motor.**

※ Wrong setting may cause sudden rotation of the motor or out of model control which is very dangerous.

● In normal operation, connect the power battery with the throttle stick at the slowest position. After hearing a set of very short and short beep, you can operate the ESC. At this time, LED lights up.

- ※ If the power battery is connected with the throttle stick not at the slowest position, LED flashes. In this case, move the throttle stick to the slowest position and a set of very short and short beep is emitted to confirm ready to operate.
- ※ If the power battery is connected with the throttle stick at high and entered into the setting mode, disconnect the power battery and repeat from the beginning.

SETTINGS USING ESC PROGRAMMER OCP-1

By using an optional extra ESC Programmer OCP-1, settings of ESC can be programmed quickly and securely to meet model's specific requirements.



Editing Buttons

● Connection of the programmer

Connect the OCP-1, power battery and motor to OCA-150 as explained before.

● Operation of editing buttons

Selection of setting item	Select setting parameter with outer arrow buttons(↓ or ↑).
Change of setting	Use inner INC(+) and DEC(-) buttons to select setting or change setting.
Change of model type	You can change model type by pressing both arrow buttons at the same time.

● Setting items

Items can be programmed with the OCP-1 are listed below.

Setting Item (Model type: HELI/AIR)	
① Selection of battery type	⑩ Selection of air brake type (only AIR)
② Setting of cut off voltage	⑪ Air brake ON/OFF (only AIR)
③ Selection of cut off type	⑫ Setting of motor pole number
④ Selection of motor rotating direction	⑬ Setting of gear ratio
⑤ Setting of advance timing	⑭ Indication of maximum RPM
⑥ Setting of acceleration	⑮ Indication of average RPM
⑦ Setting of start power	⑯ Down load the set data to the ESC
⑧ Response setting of governor function (only HELI)	⑰ Access to the stored data in the programmer
⑨ Governor function ON/OFF (only HELI)	⑱ Storing the set data in the programmer's memory

● How to set

When the OCP-1 and power battery are connected to the ESC, current settings of the ESC are automatically stored in the OCP-1.

Select the item to change with the arrow buttons (↓ or ↑) and change the setting with INC(+) and DEC(-) buttons.

(IMPORTANT)

When the parameter setting of the ESC with the OCP-1 is completed, write the set data to the ESC with "⑰ Down load the set data to the ESC" function. Set data cannot be written to the ESC with only parameter setting.

① Selection of battery type



Setting range: LiPo, NiCd
Default: LiPo

Select power battery type to use with INC(+) and DEC(-) buttons.

- ※ When the battery type is changed, "CUT OFF VOLTAGE" and "CUT OFF TYPE" parameters are changed.

② Setting of cut off voltage



Setting range: Auto, 4.5-50V
Default: Auto

Set the cut off voltage according to the battery to use with INC(+) and DEC(-) buttons.

- ※ With LiPo in Auto mode, the ESC cuts off at 3V per cell. In case of NiCd, the ESC cuts off at total 12V.

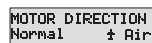
③ Selection of cut off type



Setting range: Soft off, Hard off
Default: Soft off

Select the cut-off method when battery voltage drops to the set cut-off voltage.

④ Selection of motor rotating direction

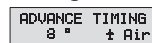


Setting range: Normal, Reverse
Default: Normal

Select motor rotating direction.

- ※ If the direction is reverse, change the mode.
- ※ Direction can be changed by changing connection of the motor.

⑤ Setting of advance timing



Setting range: 0-25°
Default: 8°

The following range of values is recommended.

- 0-10° for in-runner motors
- 14-25° for out-runner motors

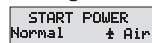
⑥ Setting of acceleration



Setting range: Lowest/Low/Normal/High/Highest
Default: Normal
Slow ⇄ Fast

Set how fast the ESC runs up to maximum speed using INC(+) and DEC(-) buttons. (Delay function) Usually this function is set when ON/OFF is done with switch.

⑦ Setting of start power

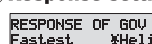


Setting range: Lowest/Low/Normal/High/Highest
Default: Normal
(Power small) ⇄ (Power large)

Set the power (torque) level of the motor starting up.

- ※ When used in a helicopter model, the value should be small to avoid premature gear wear.

⑧ Response setting of governor function (only HELI mode)



Setting range: Slowest/Slow/Normal/Fast/Fastest
Default: Slowest
Slow ⇄ Fast

To set the governor working response characteristics.

Note: The faster, the higher current is consumed.

- ※ To avoid shortening ESC and power battery life, it is suggested to set slower.

⑨ Governor function ON/OFF (only HELI)



Setting range: On/Off
Default: Off

Select governor function ON or OFF.

- ※ Governor function works to keep the RPM corresponding to throttle position (throttle curve) against load changes due to pitch operation or voltage changes of the power batteries. Note that higher current of the power batteries is consumed.

⑩ Selection of air brake type (only AIR mode)



Setting range: Slow/Normal/Fast or Value 5-100%
Default: Normal
Slow ⇄ Fast

With model type AIR, adjust the air brake effect. Select to stop the motor gradually or suddenly with INC(+) and DEC(-) buttons.

- ※ With 100% motor stops suddenly.

⑪ Air brake ON/OFF (only AIR mode)

ABRAKE ON/OFF
OFF Pole Air

Setting range: On/Off
Default: Off

Select air brake ON or OFF.

⑫ Setting of motor pole number

MOTOR POLE NUM
2 Pole Air

Setting range: 2~36 poles
Default: 2

Change the value according to the motor to use.

※ This setting is required to indicate actual RPM.

⑬ Setting of gear ratio

GEAR RATIO
1.0 : 1 Air

Setting range: 1.0:1 ~ 25.0:1
Default: 1.0:1

Input the gear ratio (motor RPM : rotor RPM).

※ RPM to indicate is calculated by motor pole number and gear ratio.

⑭ Indication of maximum RPM

MAXIMUM RPM
000000 RPM Air

The maximum RPM during the last flight is indicated.

※ RPM to indicate is calculated by motor pole number and gear ratio. Default is test value when the ESC leaves the factory. It changes when the motor is run.

⑮ Indication of average RPM

AVERAGE RPM
000000 RPM Air

The average RPM during the last flight is indicated.

※ RPM to indicate is calculated by motor pole number and gear ratio. Default is test value when the ESC leaves the factory. It changes when the motor is run.

⑯ Down load the set data to the ESC

DOWN LOAD
Really? No Air

This is to write (transfer) the set values to the ESC. Press INC(+) to start writing.

※ Beep once every second continues until the writing is completed. If you want to quit in the middle, press DEC(-).

⑰ Access to the stored data in the programmer

RESTORE MEMORY
Really? No Air

This is to access the stored data in the programmer. Press INC(+) to start the process.

※ Beep once every second continues until the process is completed. If you want to quit in the middle, press DEC(-).

⑱ Storing the set data in the programmer' s memory

BACKUP MEMORY
Really? No Air

This is to store the set date in the programmer' s memory. Press INC(+) to start the process.

※ Beep once every second continues until the process is completed. If you want to quit in the middle, press DEC(-).

SPECIFICATIONS

OCA-150	
Function	Forward-Stop-Brake-Reverse
Working voltage range	6~25V
Load current (Peak)	50A (60A 5 seconds)
BEC output	5.5V, 3A (Peak 5A)
Size	50x25x10mm
Weight	52g
Cell number	6-18 NiCd/NiMH, 2-6 LiPo
Parameter setting	ESC/ESC Programmer OCP-1 (Optional extra)
Protective function	Start protection/Low voltage cut-off/No signal cut-off/Overheat protection
PWM Frequency	32kHz

- ※ Cool Power FET: Latest generation power FET
- ※ ESC Programmer OPC-1: By connecting to OCA-150, detailed setting can be done easily.
- ※ Start protection: Stops involuntary starting of the motor.
- ※ Low voltage cut-off: Stops the motor before the voltage reaches the level where control is lost and potential over-discharge damage to the cells occurs.
- ※ No signal cut-off: Switches the ESC OFF when signal from the transmitter is not received.
- ※ Overheat protection: When the temperature rises extraordinary due to overload, restrict output to protect the ESC.
- ※ Battery cell number auto recognition: Function to recognize automatically cell number of the battery to connect.
- ※ BEC output: Power to receiver is supplied from the ESC.

● Pay careful attention to the advices with the following headings.**⚠ DANGER**

This covers the possibility which might involve death and serious injury.

⚠ WARNINGS

These cover the possibilities which might involve death and serious injury and also may cause damage or injury.

⚠ NOTES

These cover the many other possibilities, generally less obvious source of danger, but which, under certain circumstances, may also cause danger or injury.

Graphic symbols:  : Prohibited items  : Items never fail to take action

O.S. ENGINES MFG.CO.LTD.
URL : <http://www.os-engines.co.jp>

6-15 3-Chome Imagawa Higashisumiyoshi-ku
Osaka 546-0003, Japan TEL. (06) 6702-0225
FAX. (06) 6704-2722

© Copyright 2011 by O.S.Engines Mfg. Co., Ltd. All rights reserved.

A.2 Operating Manual

This operation manual is customized from the CSEI manual, found in NTNU (2015a). If more help is needed to make the CSAD operating, see NTNU (2015a).

A.2.1 Controller Implementation

1. Download the control system from GitHub: https://github.com/NTNU-MCS/CS_Drillship_cRIO.
2. Unzip the control system. The preferred path is C:\CS_Drillship_cRIO\. Other paths require updating paths in the project definition.
3. Simulink implementation and compilation.
 - (a) Update `ctrl_student.slx` according to your controller design. Additional input and output, resets and data logging may be added.
 - (b) Do not alter the predefined input and output: `x_m`, `y_m`, `psi_m`, `pwm_1`, `pwm_2`, `pwm_3`, `pwm_4`, `pwm_5`, `pwm_6`, `alpha_1`, `alpha_2`, `alpha_3`, `alpha_4`, `alpha_5` and `alpha_6`.
 - (c) Select a suitable solver, as described in NTNU (2015a). The remaining configuration, such as target selection is preselected in the file.
 - (d) Compile the model as described in NTNU (2015a). If using the preferred path, the MATLAB current folder should be C:\CS_Drillship_cRIO\02 Simulink source\, in order to ensure that the resulting .out file is created in C:\CS_Drillship_cRIO\02 Simulink source\ctrl_student_VxWorks_rtw.
4. CSAD VeriStand Project configuration
 - (a) Open `CSAD.nivproj` to access the project.
 - (b) Update `ctrl_student.out`
 - i. Browse the left pane tree and select `ctrl_student`, then refresh.
 - ii. If necessary, add mappings. Do not change the existing mappings.
 - iii. Save and close to return to the Project Explorer.
5. Implement a suitable workspace for your controller in control screen 4: `ctrl_student`.

A.2.2 Ship Launching Procedure - Before Sailing

A.2.2.1 Power Up and Connection

1. Place the vessel onto the water.
2. Place the batteries at their respective positions, 6 in total.
3. Place ballast weight into the hull to get the right draft, 20 kg in the aft and 27 kg in the fore.
4. Connect batteries:
first the red wire to the red/positive pole, then the black wire to the black/negative pole. Then switch the system on with the button on the back of the watertight box.
5. Wait for cRIO and RPi start up. When complete, the Bluetooth dongle blue LED blinks evenly at approximately 1 Hz.
6. Turn on Sixaxis by pushing the PS3 button. When successfully connected, the Bluetooth dongle blue LED is almost constantly lit and one of the Sixaxis' red LEDs (1, 2, 3, or 4) is lit.
7. Wait for WiFi connection to HIL lab network. When connected, the WiFi bridge's blue LED is constantly lit.
8. Verify laptop access: ping the CSAD IP (192.168.0.55) in the command prompt. While the round trip times may vary, it is essential to have 0% loss.
9. Then press deploy in the VeriStand Project.

A.2.2.2 Positioning System

If the positioning system is not initialized for CSAD, follow the procedures in (NTNU, 2015a, Chap. 4).

A.2.3 Known Errors

In the startup face of the vessel there is one error that has reviled itself, the reason for this error is unknown and may be an easy fix. After approximately 3-6 minutes of operating time, i.e. used in either manual mode or automatic mode, Veristand gets an error. This error is shown in Figure A.1. The solution to this, is to restart the vessel by switching it on and off again button on the back of the watertight box. Then it can run until the batteries run out.

Another error appears, if there have been changes in the FPGA. Then the tick for each of the PWM signals have reset to 100 000. The solution to this is just setting them back to 800 000.

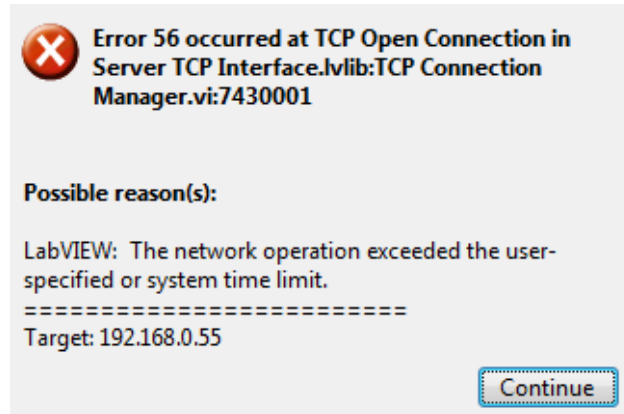


Figure A.1: Error code 56 in the startup phase.

A.2.4 Ship Docking Procedure - After Sailing

If the experiments are finished, see 1. If not, see 2.

1. Maneuver the vessel to the side of the basin.
 - (a) Undeploy the running project to disable all actuators.
 - (b) Take out the ballast weights and batteries.
 - (c) Take CSAD out of the water and place in its stand.
 - (d) Connect batteries again, and connect the charger. Remember to disconnect the power supply for the WiFi bridge, before connecting the charger.
 - (e) Connect the Sixaxis gamepad to the laptop for charging.
2. Maneuver the vessel to the side of the basin.
 - (a) Undeploy the running project to disable all actuators.
 - (b) Connect the charger. Remember to disconnect the power supply for the WiFi bridge, before connecting the charger.
 - (c) Connect the Sixaxis gamepad to the laptop for charging.

Appendix B

Content in Attached Zip-file

The following files are included in the attached zip-file:

- Digital version of the thesis.
- Digital version of the poster.
- Video of a experiment with $H_s = 9$ meters.
- Results from towing tests.
- Results from all the runs in MC Lab.
- MATLAB and Simulink files for the simulation model, both unedited and the ones used with controllers.